Title
Interleukin-10 Deficiency Drives the Development of Mouse B cell Leukemia/Lymphoma

Author
Fitch, Briana

Publication Date
2020

Peer reviewed|Thesis/dissertation

Interleukin-10 Deficiency Drives the Development of Mouse B cell Leukemia/Lymphoma

by

Briana Fitch

DISSERTATION

Submitted in partial satisfaction of the requirements for degree of

DOCTOR OF PHILOSOPHY

in

Biomedical Sciences

in the

GRADUATE DIVISION

of the

UNIVERSITY OF CALIFORNIA, SAN FRANCISCO

Approved:

DocuSigned by:
Ben Braun
0A719FCB14E648A...

Ben Braun

Chair

DocuSigned by:
Scott Kogan

Scott Kogan

DocuSigned by:
Michelle Hermiston

Michelle Hermiston

DocuSigned by:
James Rubenstein
01FD168D0BC147B...

James Rubenstein

Committee Members

This dissertation is dedicated to my mom,

and in loving memory of my cousin, Aurelia Price.

We did it!

ACKNOWLEDGEMENTS

I would first like to thank my thesis advisor Scott Kogan, who has been a phenomenal mentor throughout my entire time as a PhD student in his lab. I am incredibly fortunate to have received training from an advisor who is both a talented scientist and kindhearted person. I appreciate the immense amount of time and energy that Scott has devoted to helping me design experiments, interpret data, review presentations, and revise grant proposals. I am inspired by his enthusiasm for research and teaching, and strive to approach my future scientific endeavors with the same level of excitement. I would also like to thank my co-mentor, Michelle Hermiston, for advocating for me at every stage of my graduate training. Michelle's guidance and insight on the clinical relevance of my project gave me to confidence to pursue training in clinical research for the next stage of my career. To my committee members, James Rubenstein and Ben Braun, thank you for providing critical feedback that helped to drive my thesis project forward.

I would also like all of the past and present members of the Kogan lab as well as the members of our neighbor labs in S-577. I am especially thankful to Mi Zhou for reminding me to take breaks for lunch, tea, and pleasant conversation. Mi's willingness to help me plan and execute experiments was essential to the completion of my dissertation work. I'd also like to thank my mentee Jamilla Situ for sharing her limitless curiosity, which motivated me to be a better mentor and scientist. Special thanks to my best friends and past roommates, Christina Abundis and Ferras Bashqoy, for being reliable sources of hope and optimism. To Ferras, thank you for helping me lead a balanced life by making time for "life over lab!"

Finally, I would like to thank all members of my family, but especially my mom, grandma, and cousin Donavan for nurturing my love of science from a young age and supporting me through all of the ups and downs of my academic journey. I would not be the person that I am today without their support.

CONTRIBUTIONS TO THE CURRENT WORK

The work in this dissertation was prepared as a manuscript entitled, “Interleukin-10 Deficiency Drives the Development of Mouse B cell Leukemia/Lymphoma.” This work was performed under the supervision of Dr. Scott Kogan, M.D. Additional guidance and insights were provided by Dr. Joseph Wiemels, Ph.D., Dr. Melissa Reeves, Ph.D., Dr. Mi Zhou, M.D., Ph.D., and thesis committee members Dr. Michelle Hermiston, M.D., Ph.D., Dr. James Rubenstein, M.D., and Dr. Ben Braun, M.D., Ph.D.

Interleukin-10 Deficiency Drives the Development of Mouse B cell Leukemia/Lymphoma

Briana Fitch

ABSTRACT

Excessive inflammatory responses to common childhood infections are associated with an increased risk of pediatric B-cell Acute Lymphoblastic Leukemia (B-ALL). Despite the identification of several neonatal inflammatory markers as B-ALL risk factors, the mechanism(s) by which these markers stimulate an excessive immune response leading B-ALL remain largely unknown. Here, we demonstrate that IL-10 deficiency, a neonatal risk factor for B-ALL, indirectly impairs B lymphopoiesis and increases B cell DNA damage through induction of inflammation in mice. Altered B cell number and DNA damage in *Il10*$^{-/-}$ mice were associated with a module of 6 pro-inflammatory/myeloid-associated cytokines (IL-1α, IL-6, IL-12p40, IL-13, CCL4/MIP-1β, and G-CSF). Importantly, inflammation and defects in bone marrow B cells were attenuated by treating pre-leukemic *Il10*$^{-/-}$ *Ckdn2a*$^{-/-}$ mice with antibiotics that target *Helicobacter* species. In the TEL-AML1 *Ckdn2a*$^{-/-}$ mouse model of B-ALL, decreased levels of IL-10 accelerated B cell neoplasms in a dose dependent manner, and altered the mutational profile of B cell neoplasm to favor C>T and T>C mutations. Infection of *Cdkn2a*$^{-/-}$ mice to *Aspiculuris*, a parasite that induces IL-10 production, delayed the development of B cell neoplasms in *Cdkn2a*$^{-/-}$ mice, demonstrating a novel protective effect of microbial exposure. Our results identify commensal bacteria as modulators of bone marrow B cell responses to IL-10 deficiency, and suggest that microbial dysbiosis underlies the infectious etiology of pediatric B-ALL.

TABLE OF CONTENTS

LIST OF FIGURES

LIST OF TABLES

CHAPTER 1: INTRODUCTION

1.1 INFECTIOUS ETIOLOGY OF PEDIATRIC B-ALL

Although excessive inflammation in response to infection is a risk factor for pediatric B-cell Acute Lymphoblastic Leukemia (B-ALL), the underlying genetic and environmental causes of abnormal immune response have yet to be confirmed[1–3]. The trend toward decreasing opportunities for microbial exposures in modern societies is commonly proposed as an underlying cause of abnormal inflammatory responses in the pathogenesis of ALL, as well as other childhood diseases including lymphoma, allergies, and asthma[4,5]. Severe inflammation may provide pre-leukemic clones with the necessary environmental stimulation to acquire secondary driver mutations[6]. One of the most common chromosomal translocations in pediatric ALL, *ETV6-RUNX1* (also referred to as TEL-AML1), coordinates with infections to redirect the recombinase activity of RAG[7]. The resulting RAG activity generates large deletions at off-target sites, ultimately aiding in the development of ALL[7]. Mouse models have been paramount in identifying infectious stimuli that are capable of triggering this response in progenitor B cells. The list of infectious stimuli with this capacity ranges from lipopolysaccharide (LPS) to a host of infectious pathogens[8,9]. It is now critically important to further understand whether this mechanism is relevant to the specific states of microbial and immune dysfunction that are risk factors in human pediatric B-ALL, as this may confirm targets for early interventions to prevent the development of this disease in children.

1.2 ROLE OF IL-10 DEFICIENCY IN CANCER

Neonatal deficiency in interleukin-10 (IL-10), a key cytokine in establishing early microbial homeostasis and immune tolerance to infection, is a strong predictor of childhood B cell malignancies[10]. Children born with low levels of IL-10 have a 25-fold increased risk for developing ALL, whereas children with inherited *IL10R* deficiency have a high risk of developing

B-cell non-Hodgkin Lymphoma[11,12]. IL-10 is a potent anti-inflammatory cytokine that suppresses myeloid cell activation, migration, and cytokine production by triggering downstream JAK/STAT signaling pathways[13]. Very early onset of severe inflammatory bowel disorder (IBD) is observed in children born with IL-10 and IL-10R deficiency[14]. Additionally, *Il10*$^{-/-}$ mice have been consistently used as a model system for IBD and colitis-associated colon cancer, in which bacterial infection and tumor promoting inflammation drive double stranded DNA breaks in intestinal cells[15–17]. Although the gut is the primary site of inflammation in IL-10 deficient humans and mice, gut dysbiosis and inflammation can have distal genotoxic effects on peripheral blood lymphocytes that may contribute to extraintestinal hematological malignancies[18]. Therefore, low IL-10 levels may be a source of excessive inflammation that drives B cell DNA damage during the development of childhood B cell leukemia/lymphoma.

IL-10 also has B cell stimulatory properties, which may impact the development of childhood B cell malignancies in a cell-intrinsic manner that is independent of inflammation suppression. B cell stress conditions that are induced by limited growth factors may have the capacity to exert a selective pressure on B cells that drives the acquisition of *de novo* mutations or provides a competitive advantage to pre-leukemic clones. IL-10 is a B cell growth factor that enhances the survival and proliferation of B cell progenitors and mature B cells[19,20]. Since B cells alternate between mutually exclusive stages of proliferation and recombination, decreased IL-10 levels may halt B cell proliferation and, as a result, prolong recombination and DNA damage[21]. Alternatively, cytokine mediated B cell suppression may allow for the selection of pre-leukemic clones, as TGF-β has been demonstrated to disproportionately impair normal B cells relative to B cells expressing TEL-AML1[22]. The multiple cell-intrinsic and cell-extrinsic pathways in which IL-10 deficiency may impact B cell DNA damage have not been fully explored.

1.3 AIMS OF THIS STUDY

We sought to identify what role IL-10 deficiency has, if any, in the development of childhood B cell malignancies. Based on the epidemiological evidence linking low IL-10 levels and infections to childhood leukemia, we proposed that IL-10 deficiency increases the risk of childhood B cell leukemia/lymphoma by driving aberrant inflammatory responses to infectious stimuli. To address this hypothesis, we crossed *Il10*$^{-/-}$ mice to our previously described TEL-AML1 *Cdkn2a*$^{-/-}$ model of pediatric B-ALL[23]. In addition to developing B-ALL, this model is also susceptible to B cell lymphomas and is responsive to environmental cues such as radiation[23]. We report that IL-10 deficiency leads to increased DNA damage in bone marrow B cells as a result of inflammation. Given the association between inflammation and microbial dysbiosis in *Il10*$^{-/-}$ mice[24], these data are compatible with such dysbiosis being a source of DNA damage. Survival studies demonstrate that IL-10 deficiency increases the aggressiveness of B cell disease, whereas pinworm exposure, known to elicit host IL-10 production[25], is protective for leukemia/lymphoma.

CHAPTER 2: INFLAMMATION IS ASSOCIATED WITH DISRUPTION OF B LYMPHOPOIESIS IN *Il10*$^{-/-}$ MICE

2.1 INTRODUCTION

The role of IL-10 in *in vivo* B cell development is controversial. Although some studies suggest that *Il10*$^{-/-}$ mice have a deficit of B cells in the bone marrow[26], others report normal B cell development[24] in these mice. This dilemma is furthered by the lack of investigations on B cell development in mice with IL-10 receptor (IL-10R) gene mutations. A goal of the current study was to determine why *in vivo* IL-10 deficiency suppresses B cell development in particular circumstances.

IL-10 can impact proliferation[20,27] and differentiation[28] of B cells, but these responses are influenced by the developmental stage and activation state of the B cells in culture. In the case of B cell progenitors that have been isolated from murine bone marrow, early CD19^{-} B cells have a proliferative response to recombinant murine IL-10 (rmIL-10), whereas the growth of slightly more differentiated CD19^{+} B cell progenitors is suppressed by rmIL-10[19]. Another bi-directional effect of IL-10 is observed in mature B cells with different activation states. During early activation, mature human IgM^{+} B cells are impaired by IL-10, however during late activation, these cells proliferate in response to IL-10[20]. Therefore, *in vivo* studies that combine B cell subsets for analysis instead of resolving distinct B cell populations may not detect an effect of IL-10 deficiency on B cell development.

In addition to the B-cell intrinsic properties of IL-10 described above, IL-10 also has B-cell extrinsic properties that may play a role in B cell development. The only reports of altered B cell dynamics in *Il10*$^{-/-}$ mice have been conducted in the presence of spontaneous gut inflammation or colitis[26]. Gut dysbiosis in *Il10*$^{-/-}$ mice and loss of IL-10 responsiveness in myeloid cells are each capable of driving the unregulated differentiation of splenic transitional B cells into marginal zone B cells[24]. The myeloid response that occurs in *Il10*$^{-/-}$ mice is typically characterized by an

increased presence of granulocytes, and pro-inflammatory cytokines[24,29]. Increased myeloid cell activation and/or production may contribute to the inflammatory state of *Il10*$^{-/-}$ mice. Interestingly, both inflammation and myeloid cell production are associated with suppression of B cell development[30]. Whether myeloid growth factors or pro-inflammatory cytokines actively suppress B cell development in *Il10*$^{-/-}$ mice remains largely unknown.

The question that we aimed to address is whether the impairment of B cell development in *Il10*$^{-/-}$ mice is influenced by a B-cell intrinsic or B-cell extrinsic mechanism. Given that B-cell extrinsic myeloid responses drive B cell loss and are prominent in *Il10*$^{-/-}$ mice, we hypothesized that the loss of B cells in *Il10*$^{-/-}$ mice is correlated with increased abundance of myeloid cells and myeloid-associated cytokines. Our approach to defining the relationship between B cell development and myeloid inflammation in *Il10*$^{-/-}$ mice was to perform a comprehensive analysis of different B cell subsets across the lymphoid tissues of *Il10*$^{-/-}$ mice displaying variable levels of inflammation and wild-type mice with no inflammation. Our results indicate that B cell loss in *Il10*$^{-/-}$ mice is most profound in the pre-B cell population and that the cytokines G-CSF and IL-12p40 may play a role in this B cell deficit.

2.2 RESULTS

2.2.i Hematopoiesis is altered in Il10$^{-/-}$ *mice*

We first sought to determine whether *Il10*$^{-/-}$ mice in our colony had reduced levels of bone marrow B cells relative to wild-type controls. *Il10*$^{-/-}$ mice that have been housed under SPF conditions can spontaneously develop an inflammatory response that is characterized by an early expansion of cytokine-producing macrophages and CD4+ Th1 cells in the gut[29]. The severity of inflammation in *Il10*$^{-/-}$ mice is influenced by mouse husbandry conditions within an animal facility and genetic background. In regard to genetic background, the strongest inflammatory responses have been observed on the C3H/HeJBir and 129/Sv backgrounds. *Il10*$^{-/-}$ mice on the 129/SvEv

develop enterocolitis and have been used to model Crohn's Disease[31]. Intermediate inflammatory responses are present in BALB/cJ and NOD/Lt mice and mild inflammation has been reported on the C57BL/10 and C57BL/6J genetic bakcgrounds[32,33].

We had a particular interest in examining patterns of inflammation on the FVB/N background because it is commonly used in genetically engineered cancer models, including our model of TEL-AML1 B-cell Acute Lymphoblastic Leukemia (B-ALL)[23]. Inflammation in *Il10*$^{-/-}$ mice on the FVB/n background had not been previously described and the genetic variants that promote inflammation in *Il10*$^{-/-}$ mice have yet to be reported. Therefore, it was unclear whether the FVB/n genetic background would be permissive for the development of spontaneous inflammatory responses in *Il10*$^{-/-}$ mice that were housed in our SPF facility. We observed indications of IL-10 deficiency induced colitic lesions, including diarrhea and rectal prolapse, in a subset of 8-week-old *Il10*$^{-/-}$ mice on the FVB/n background, herein referred to as *Il10*$^{-/-}$ mice. We therefore selected an age range of 8-12 weeks-old to determine whether there was additional evidence of inflammation or B cell disruption in *Il10*$^{-/-}$ mice. To this end, myeloid and lymphoid lineages were enumerated in the bone marrow, spleen, and peripheral blood of age- and sex-matched wild-type and *Il10*$^{-/-}$ mice. We observed that *Il10*$^{-/-}$ mice had an increased count of CD11b+ CD19- myeloid cells across each of the three lymphoid tissues that were surveyed, but had decreased counts of CD19+ B cells in the bone marrow and blood (**Figure 2.1A**). This loss of B cells did not extend to the spleen, suggesting that *Il10*$^{-/-}$ mice may have a compensatory mechanism of B cell expansion in secondary lymphoid organs. The numbers of CD3+ T cells were not significantly altered by IL-10 loss. These results indicate that myeloid and B cell lineages are specifically impacted by IL-10 loss in mice on the FVB/n background.

To investigate the impact of IL-10 loss on B lymphopoiesis, we used flow cytometry to identify the following subsets of CD19+ B220+ B cells in the bone marrow of adult mice: pro-B cells (CD43+ IgD- IgM-), pre-B cells (CD43- IgD- IgM-), IgM+ Immature B cells (IgM+ IgD-), and mature recirculating (MR) B cells (IgD+ IgM+). Strikingly, the decrease in B cells in *Il10*$^{-/-}$ mice

was almost exclusively in the pre-B cell population, which was abundant in control FVB/n mice (**Figure 2.1B**). MR B cells were also significantly decreased in the bone marrow *Il10*$^{-/-}$ mice. The drastic reduction in pre-B cells resulted in a relative increase in the percent of pro-B and IgM+ B cells within the CD19+ B220+ bone marrow B cell population (**Figure 2.1C**). We did not detect a decrease in pro-B or IgM+ B cells in *Il10*$^{-/-}$ mice; however, these B cell populations are far less abundant in adult mice than pre-B cells. We also performed parallel analyses in young 4-6-week-old mice and found that young *Il10*$^{-/-}$ mice had a significant decrease in the percent of B1 progenitors, pre-pro B (B2 progenitors), pro-B, pre-B, IgM+ Immature B, transitional B, and MR B cells compared to FVB/n controls (**Figure 2.2A**). Therefore, IL-10 deficiency in mice on the FVB/n background can result a loss of the major B cell subsets in pups and a less expansive loss in pre-B and MR B cells in adult mice.

Inflammation has a well described capacity for directing the hematopoietic output of the bone marrow to favor neutrophil production at the expense of B cell development[30,34]. We hypothesized that neutrophils would be the predominant myeloid population that was expanded in *Il10*$^{-/-}$ mice. Gr1+ neutrophil and Gr1- monocyte subpopulations of CD11b+ CD19- myeloid cells were measured by flow cytometry and the absolute count was calculated based on the CBC white blood cell count. We observed increased neutrophil and monocyte counts in the bone marrow, blood, and spleen of *Il10*$^{-/-}$ mice relative to controls (**Figure 2.1D**). Together, these data show that myeloid cell expansion occurs concurrently with B cell deficiency in our colony of *Il10*$^{-/-}$ mice.

2.2.ii Myeloid-derived cytokines in Il10$^{-/-}$ *mice are associated with B cell loss*

We next investigated the potential impact of inflammation on B cell numbers in *Il10*$^{-/-}$ mice. IL-10 has an important role in promoting Th2 immunity[35–37] and suppressing Th1 and myeloid-related immune responses[38–40]. In previous work, *Il10*$^{-/-}$ mice with inflammation demonstrated a

bias toward Th1 immunity, as demonstrated by increased levels of IL-1α, IL-6, TNF-α, and IFN-γ in the colon[29]. To determine whether a similar immune response was present in the blood of *Il10*$^{-/-}$ mice, we measured the concentration of 32 cytokines that are involved in Th1, Th2, Th17, and innate immune responses. Of the 32 cytokines profiled, 6 were significantly increased in *Il10*$^{-/-}$ mice (adjusted p-value < 0.05), whereas significant decreases in cytokine levels were not detected (**Table 2.1**). Surprisingly, *Il10*$^{-/-}$ plasma did not have increased expression of the Th1-related cytokines IFN-γ and TNF-α. Notably, G-CSF levels in *Il10*$^{-/-}$ mice showed a 46-fold increase in median concentration relative to control mice (**Table 2.1**). Additional myeloid growth factors, including IL-3 and M-CSF[41], were elevated in the blood of *Il10*$^{-/-}$ mice, as well as the pro-inflammatory cytokines IL-1α, IL-6, and MIP-1β (CCL4) (**Figure 2.1E**). Cytokines that bridge the innate and adaptive immune responses, such as IL-12p40, IL-13, and IL-17A[42–45], were also expressed at higher levels in *Il10*$^{-/-}$ mice (**Figure 2.1E**). These data demonstrate that myeloid growth factors and pro-inflammatory cytokines predominated the peripheral blood inflammatory response in *Il10*$^{-/-}$ mice.

To identify which inflammatory cytokines may contribute to the reduction of bone marrow B cells in *Il10*$^{-/-}$ mice, we first used Pearson correlation to determine the association between selected cytokines and the abundance of different B cell populations. Of the cytokines that were elevated in *Il10*$^{-/-}$ mice, G-CSF and IL-3 have been reported to suppress murine B cell progenitors[46–49]. Increased levels of IL-3, but not G-CSF, were significantly correlated with decreased pre-B cell numbers in *Il10*$^{-/-}$ mice (**Figure 2.1F**). Of note, the increased percent of neutrophils within the bone marrow of *Il10*$^{-/-}$ mice was also associated with reduced pre-B cell numbers (**Figure 2.1G**), supporting a role of myelopoiesis in the disruption of B cell development.

Linear regression was then used to further examine whether increased cytokine production was predictive of B cell or myeloid findings in *Il10*$^{-/-}$ mice. Regression analyses was first performed on flow cytometry data and absolute levels of all 32 measured cytokines. P-values

were adjusted using the Bonferroni-Holm method to obtain the family-wise error rate (FWER). The cutoff for significance was FWER < 0.05. G-CSF and IL-12p40 were both significantly correlated with decreased counts of pre-B and MR B cells (**Table 2.2**). In contrast, G-CSF correlated with increased peripheral blood neutrophils and IL-12p40 correlated with increased bone marrow monocytes. These results are consistent with previous reports in which G-CSF treatment shifted the hematopoietic output of murine bone marrow to favor neutrophil production by depleting pre-B cells[34]. These data also suggest that IL-12 may be involved in an analogous mechanism in which monocyte production is favored at the expense of pre-B cells and MR B cells. Taken together, our analyses of cytokines revealed that the pro-inflammatory cytokines IL-3, G-CSF, and IL-12p40 were associated with the loss of B cells in the bone marrow of *Il10*$^{-/-}$ mice.

A limitation of using absolute cytokine concentrations for analysis is that information on relative changes in cytokine levels is missed. This is of particular importance when analyzing samples with inflammation, a process that could increase the concentration of several cytokines. We found that, in regard to absolute concentration, most cytokines in our dataset were positively correlated with each other (**Figure 2.3A**) and with the mean cytokine concentration in each sample (**Figure 2.3B**). We therefore decided to use a previously described approach for calculating an adjusted cytokine concentration that takes into account the overall cytokine concentration within each sample[50]. Although some cytokine correlations differed after cytokine adjustment, G-CSF and IL-12p40 were correlated with each other before and after adjustment (**Figure 2.3C**). We then repeated our linear regression analysis, this time substituting adjusted cytokine levels for absolute cytokine concentrations. We observed that, after adjustment, G-CSF and IL-12p40 were still the only cytokines that had a significant association with decreased numbers of bone marrow pre-B cells and MR B cells (**Table 2.3**). This analysis further strengthens our conclusion that inflammation is associated with B cell loss in *Il10*$^{-/-}$ mice.

We then evaluated potential mechanisms by which myeloid growth factors and pro-inflammatory cytokines may mediate a reduction of bone marrow B cells in *Il10*$^{-/-}$ mice, starting

with extramedullary hematopoiesis. G-CSF treatment can displace hematopoietic progenitors and B cells from their local niche in the bone marrow to the periphery[51]. We assessed whether the site of B lymphopoiesis was relocated from the bone marrow to the periphery in *Il10*$^{-/-}$ mice by measuring the total cellularity and number of hematopoietic progenitors in the bone marrow, blood, and spleen. Despite observing an increase in the spleen/body weight ratio (**Figure 2.2B**) and spleen cellularity (**Figure 2.2C**), only a modest displacement of LSKs and CLPs was observed in *Il10*$^{-/-}$ mice (**Figure 2.2D**). The myeloid expansion that we observed in the spleen likely accounts for increased cellularity and weight of the spleen in *Il10*$^{-/-}$ mice. A greater percent of HSCs and CLPs were proliferating in *Il10*$^{-/-}$ mice, but the level of proliferation was similar between tissues (data not shown), suggesting that bone marrow progenitors in *Il10*$^{-/-}$ mice do not have a lower proliferative capacity than progenitors in other lymphoid tissues. It is possible that extramedullary niches may be more permissive for the development or survival of B cells than the inflamed bone marrow. If this were the case, then peripheral lymphoid tissues in *Il10*$^{-/-}$ mice would be expected to have more B cells than FVB/N mice. However, we found a decreased number of B cells in the blood and spleen of *Il10*$^{-/-}$ mice (**Figure 2.1B**). These data are not consistent with a role of extramedullary hematopoiesis or B cell mobilization in reducing the presence of B cells in *Il10*$^{-/-}$ bone marrow.

2.2.iii IL-10 deficiency contributes to pathways of B cell transformation

To investigate the role of IL-10 deficiency in pathways of B cell transformation, we focused on DNA damage, as others have described an increased presence of RAG-mediated mutations in models of B-ALL that are driven by infectious stimuli[8,52]. Inflammation-associated DNA damage is also induced in small intestinal cells and peripheral blood T cells of *Il10*$^{-/-}$ mice. There is limited characterization of peripheral blood B cell DNA damage in *Il10*$^{-/-}$ mice and these studies have not reported DNA damage in the bone marrow B cell compartment. We asked whether B cells carry a higher level of DNA damage in *Il10*$^{-/-}$ mice than in FVB/n controls. Given that RAG activity and

inflammatory factors in mice can induce double stranded DNA breaks (DSBs) in immunoglobulin (Ig) and non-Ig genes[8], we proposed that IL-10 deficiency-induced inflammation might increase the percent of bone marrow B cells with DSBs. To identify B cells with DSBs we used flow cytometry to measure γH2AX, a DNA repair protein which responds rapidly to DSBs. In *Il10*$^{-/-}$ mice, the percent of γH2AX^{+} cells was significantly increased in bone marrow B cells relative to FVB/n controls (**Figure 2.4A**). We expected pre-B cells to have the highest percent of DNA damage among bone marrow B cell populations because pre-B cells have high intrinsic levels of RAG and experience more suppression in our *Il10*$^{-/-}$ mice than other B cell populations. In two independent experiments using at least 5 mice per group, analysis of γH2AX expression among B cell subsets revealed that an increased percent of pro-B cells and IgM^{+} immature B cells expressed γH2AX in *Il10*$^{-/-}$ mice (**Figure 2.4B**). This result was not representative of a third replicated experiment; however it is feasible that pro-B and IgM+ B cells would have the capacity for increased RAG-mediated mutagenesis, as endogenous RAG regulates VDJ recombination and receptor editing in these populations. Taken together, our results demonstrate that IL-10 loss severely restricts B cell development in the bone marrow and promotes DNA DSBs in the few remaining B cells.

To directly assess the impact of IL-10 loss on *in vivo* B cell proliferation, we injected BrdU into *Il10*$^{-/-}$ and FVB/n mice, then collected bone marrow for analysis 1 hour later. Inflammation in aged mice has been associated with reduced pro-B cell proliferation[53], therefore we expected B cell progenitors in *Il10*$^{-/-}$ mice to have decreased levels of proliferation. Surprisingly, loss of IL-10 resulted in increased proliferation in bone marrow B cells (**Figure 2.4C**) with no detectable proliferative advantage in any particular B cell subset (**Figure 2.4D**). This suggests that the absence of IL-10 provides some B cells with a proliferative advantage, possibly by exerting a selective pressure that drives the acquisition of favorable mutations. Overall, our results provide evidence that IL-10 deficiency negatively selects against B cells and drives a subset of B cells to acquire DNA damage and proliferate.

2.2.iv Myeloid inflammation in Il10$^{-/-}$ mice is associated with B cell DNA damage

Given the association between inflammatory markers and human pediatric ALL, we were interested in testing whether properties of B cell transformation, such as DNA damage and hyperproliferation, were correlated with cytokine levels in *Il10*$^{-/-}$ mice. Linear regression analysis did not reveal any significant associations between individual cytokines and B cell DNA damage or proliferation. However, during complex immune responses such as inflammation, cytokines may change in groups. Clustering analysis is an appropriate approach for identifying patterns of cytokine expression that are associated with disease symptoms or outcomes. We therefore decided to apply clustering analysis to our cytokine dataset to determine whether cytokine clusters were more significantly associated with B cell DNA damage and proliferation than individual cytokines. To this end we used CytoMod[50], an unsupervised approach to clustering absolute and adjusted levels of cytokines across individuals. We then used linear regression to determine whether there was an association between cytokine modules and altered B cell DNA damage or proliferation. Of the 3 absolute cytokine modules that were identified in our cohort of FVB/n and *Il10*$^{-/-}$ mice (**Figure 2.5A**), none were associated with changes in B cell number, DNA damage, or proliferation. However, of the 5 adjusted cytokine modules (**Figure 2.5B**), plasma module 5 (PM5) was associated with an increased percent of DNA damage in bone marrow B cells and decreased numbers of pre-B and MR B cells (**Table 2.5**). The adjusted module PM5 contained the following cytokines: IL-1α, IL-6, IL-12p40, IL-13, G-CSF, and MIP-1β (**Figure 2.5B**). Multiple KEGG pathways were significantly associated with PM5 including cytokine-cytokine receptor interaction, IBD, and the Jak-STAT signaling pathway (data not shown). However, none of these pathways were unique to the PM5 module. These data ultimately demonstrate that the combination of cytokines in the PM5 module is more strongly associated with B cell DNA damage in *Il10*$^{-/-}$ mice than any individual cytokine that was measured. These results provide further evidence that inflammation in *Il10*$^{-/-}$ mice is associated with B cell deficiency and DNA damage. A valuable

question for future studies is whether identifying cytokine modules in newborns would be a useful approach for predicting levels of B cell DNA damage or B-ALL risk in humans.

2.3 DISCUSSION

Our data demonstrate that IL-10 deficiency can increase neutrophil and monocyte output while also decreasing the number of B cells in the bone marrow. Therefore, it is possible that IL-10 plays opposing roles in myelopoiesis and B lymphopoiesis. We aimed to understand whether the role of IL-10 in hematopoiesis was mediated directly through a loss of IL-10 production in myeloid and B cells or indirectly through a change in the bone marrow microenvironment. We found evidence for an indirect mechanism, as the drastic changes in myeloid and B cell abundance in *Il10*$^{-/-}$ mice were associated with the myeloid-derived pro-inflammatory cytokines G-CSF and IL-12p40. G-CSF has a well-established function in neutrophil production and pre-B cell suppression; therefore, it was not surprising that we found high G-CSF levels to be associated with myeloid expansion and B cell deficiency. Our results imply that B cell loss in *Il10*$^{-/-}$ mice was driven by pro-inflammatory cytokines. It is therefore possible that the impact of IL-10 loss on B cell development may have been missed in studies that analyzed *Il10*$^{-/-}$ mice in the absence of inflammation.

In contrast to numerous *in vitro* studies which show that recombinant IL-10 can function as a growth factor that directly stimulates or suppresses isolated B cells, our findings suggest that endogenous IL-10 may not be required for the maintenance of *in vivo* B cell homeostasis. This does not rule out the possibility that bone marrow B cells may become dependent on IL-10 signaling during an inflammatory response. IL-10 can stimulate B cell survival by activating the Bcl-2 anti-apoptotic pathway[54], thus B cell apoptosis could be a consequence of decreased IL-10 signaling in the context of inflammation. Interestingly, dysregulation of splenic marginal zone B cells in *Il10*$^{-/-}$ mice has been attributed to a loss of IL-10 signaling in myeloid cells, but not B cells[24].

It would be useful to determine whether a loss of IL-10 signaling in B cells is responsible for B cell suppression in *Il10*$^{-/-}$ mice. One approach to directly addressing this question would be to investigate B cell development in mice with a tissue-specific knockout of IL-10R in B cells. Alternatively, comparative analysis of wild-type and *Il10ra*$^{-/-}$ B cells after transplantation into *Il10*$^{-/-}$ mice with inflammation could also provide insight into the role of IL-10 signaling in B cell development.

Our work also revealed that the earliest B cell subset that is decreased in *Il10*$^{-/-}$ mice varies by age. Pre-B cells were the only B cell progenitor population that was decreased in adult *Il10*$^{-/-}$ mice, whereas pre-pro B, pro-B, and pre-B cells were each reduced in young *Il10*$^{-/-}$ mice. This difference may reflect the relatively low number of pre-pro and pro-B cells in the bone marrow of adult wild-type mice. Notably, IL-10 loss in young and adult mice did not decrease the number of common lymphoid progenitors (CLPs), which possess T and B cell differentiation potential under physiologic conditions. Since CLPs can differentiate into dendritic cells under inflammatory conditions[55], it is possible that inflammation in *Il10*$^{-/-}$ mice biased the differentiation potential of CLPs away from the B cell lineage in favor of dendritic cell production. *In vitro* analysis of the multilineage differentiation capacity of CLPs isolated from wild-type and *Il10*$^{-/-}$ mice could be useful in determining the effect of IL-10 deficiency on the capacity of CLPs to differentiate into committed B cell progenitors.

The slight increase in HSCs and CLPs that we observed in the spleen of *Il10*$^{-/-}$ mice raises the possibility that extramedullary B lymphopoiesis compensates for the profound loss of B cell progenitors in the bone marrow. One approach for demonstrating increased B lymphopoiesis outside of the bone marrow of *Il10*$^{-/-}$ mice would be to find evidence for an increased number of B cell progenitors in the periphery. However, we did not detect an increase in pro-B or pre-B cells in the blood or spleen of *Il10*$^{-/-}$ mice. When attempting to detect pre-B cells in the periphery, we looked to identify B cells with an IgK^{-} immunophenotype. In the bone marrow, the IgK^{-} population is largely composed of two B cell subsets: CD43^{+} pro-B cells and CD43^{-} pre-B cells. In contrast,

peripheral lymphoid organs house additional subsets of IgK$^-$ B cells, including mature B cells that that have lost surface immunoglobulin expression during differentiation into plasma cells. The increased number of IgK- B cell populations can present a challenge to detecting pre-B cells in the periphery. Based on the antibody panel that was used in this study, we cannot distinguish pre-B cells from mature IgK$^-$ B cell populations. That being said, there was no expansion in IgK$^-$ B cells in the periphery, suggesting that the pre-B cells that were lost from the bone marrow did not move into other tissues.

Our analysis of DNA damage across different B cells populations in Il10-/- mice revealed that, in particular experiments, pro-B cells and IgM+ B cells carried elevated levels of DNA damage. Notably, this pattern was not present in pre-B-cells. This may reflect the massive loss of pre-B cells in the bone marrow of *Il10*$^{-/-}$ mice, an acquisition of non-DSB DNA damage in pre-B cells, or different susceptibilities to DSBs among B cell populations during inflammation. The latter mechanism is supported by our observation that IgM+ B cells had the highest level of DNA damage and were the only B cell population to display increased proliferation in *Il10*$^{-/-}$ mice. It is interesting to consider that the increased proliferation of IgM+ B cells could be a compensatory response that is triggered by the loss of pre-B cells. Error-prone DNA replication is a possible consequence of such lymphocyte hyperproliferation in the context of inflammation. Additionally, human B cell subsets differ in endogenous expression of RAG and AID enzymes[56,57], which are capable of driving B cells mutagenesis when concurrently expressed. Exome sequencing or targeted V_H region sequencing could be useful in determining whether the mutagenic processes in *Il10*$^{-/-}$ mice differ between pro-B cells and IgM+ B cells.

In regard to disease relevance, our work presents a feasible mechanism for the epidemiological findings that decreased levels of IL-10 in newborns are associated with an increased risk of pediatric B-ALL[11]. Common infections, as opposed to a specific pathogen, are believed to contribute to pediatric B-ALL. To elucidate the paradigm of how common infectious exposures impact B cell mutagenesis, previous studies have stimulated B cells or the murine

immune system with TLR agonists[8] or a set of pathogenic exposures[9,58]. Our approach is distinguished by perturbing the mouse immune system in mice to reflect a specific immune defect that has been observed in humans with high ALL risk. Here, we report that B cell DNA damage in *Il10*$^{-/-}$ mice coincides with a set of pro-inflammatory cytokines that are associated with inflammatory bowel disease (IBD). Given that microbial dysbiosis is associated with the dysregulated immune response of IBD, our finding suggests that microbial dysbiosis may mediate B cell DNA damage, and possibly leukemogenesis, in the absence of IL-10. This interpretation is supported by numerous studies correlating newborn gut dysbiosis to childhood ALL risk[59]. It may be useful to classify the bacterial species that are associated with B cell DNA damage and ALL risk in future studies.

Another advantage of our approach was crossing the IL-10 deletion onto the FVB/n strain, which is a genetic background that has been commonly used to engineer mouse models of cancer. Previous studies have used *Il10*$^{-/-}$ FVB/n mice to understand the protective role of IL-10 in solid tumors[60,61]. Propagation of tumor promoting inflammation and impairment of tumor immune surveillance are cancer pathways that have been attributed to the loss of IL-10 in solid tumor mouse models. Few studies have used *Il10*$^{-/-}$ FVB/n mice to explore the role of IL-10 in hematological malignancies. Here, we identified pathways of B cell disease in the bone marrow of *Il10*$^{-/-}$ mice with inflammation. Altered B cell abundance, proliferation, and DNA damage were all heightened in *Il10*$^{-/-}$ mice that were not genetically engineered to express leukemic mutations. Overall, our data suggest that IL-10 protects the bone marrow microenvironment from giving rise to B cells with pre-leukemic properties. IL-10 therapy or treatment with immunosuppressive agents may therefore be beneficial approaches for decreasing ALL risk in children prone to aberrant immune responses to infection.

2.4 FIGURES

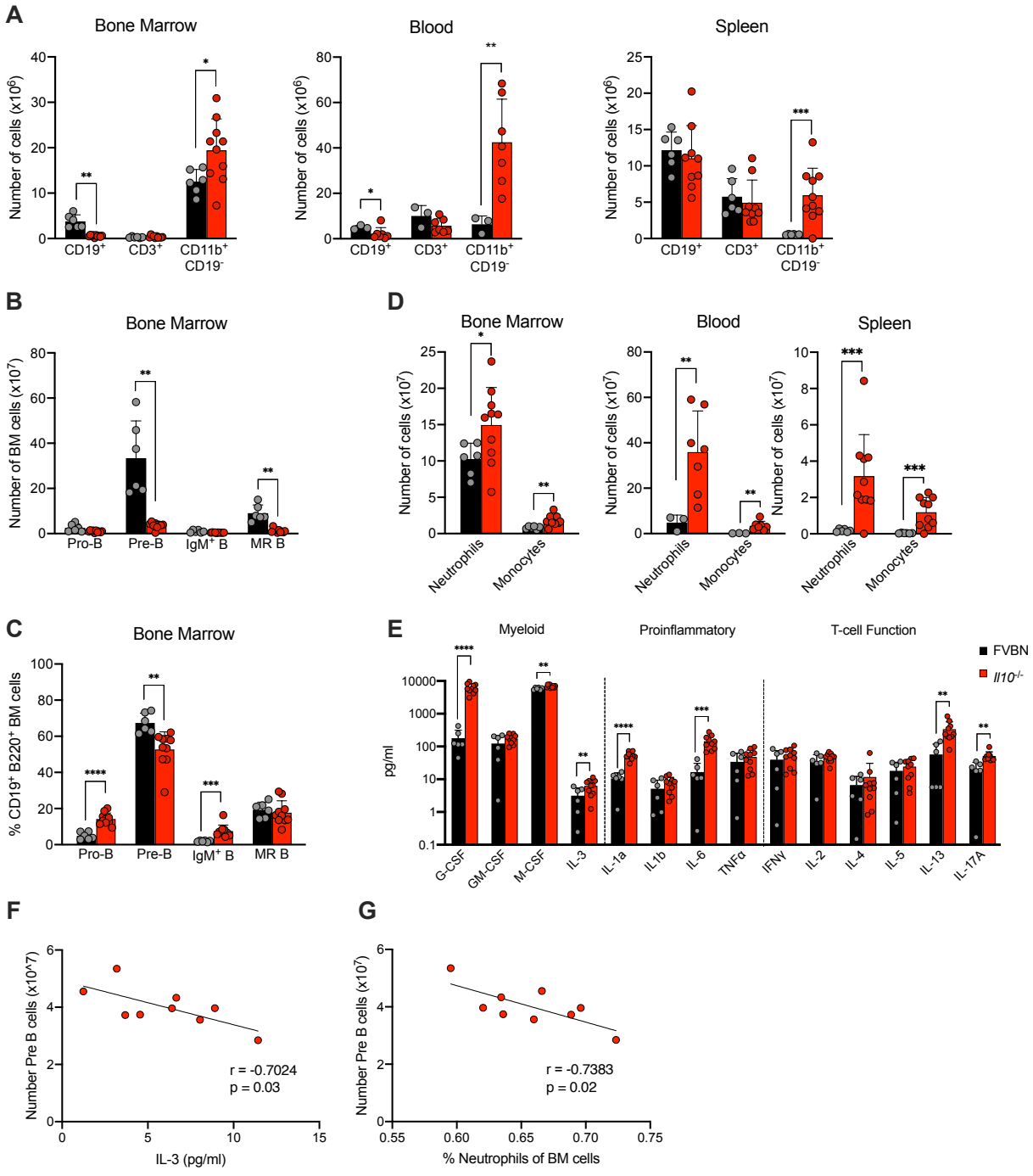

Figure 2.1. Disruption of hematopoiesis in *Il10*$^{-/-}$ mice is correlated with neutrophilic inflammation.

Analysis immune cell lineages and cytokines in 8-12 week-old FVB/n and *Il10*$^{-/-}$ mice. **(A)** Number of CD19^{+} B, CD3^{+} T, and CD11b^{+} CD19^{-} myeloid cells in the bone marrow, blood, and spleen. **(B)** Number of pro-B cells (B220^{+} CD19^{+} IgM^{-} IgD^{-} CD43^{+}), pre-B cells (B220^{+} CD19^{+}

IgM^- IgD^- $CD43^-$), IgM^+ immature B cells ($B220^+$ $CD19^+$ IgM^+ IgD^-), and mature recirculating (MR) B cells ($B220^+$ $CD19^+$ IgM^+ IgD^+) in the bone marrow. **(C)** Percent of B cell subsets in $B220^+$ $CD19^+$ bone marrow. **(D)** Number of neutrophils ($CD11b^+$ $CD19^-$ $Gr1^{hi}$ $Ly6C^{lo}$) and monocytes ($CD11b^+$ $CD19^-$ $Gr1^{lo}$ $Ly6C^{hi}$) in the bone marrow, blood, and spleen. **(E)** Absolute plasma concentrations of a selected panel of myeloid, pro-inflammatory, and T-cell regulatory cytokines detected by a bead-based multiplex Luminex assay. **(F)** Correlation between number of pre-B cells in the bone marrow and plasma concentration of IL-3 or **(G)** percent of neutrophils in the bone marrow of *Il10*$^{-/-}$ mice. Bar graph data show mean ± SD. Nominal p-values are represented. *$p \leq 0.05$, **$p \leq 0.01$, ***$p \leq 0.001$, ****$p \leq 0.001$.

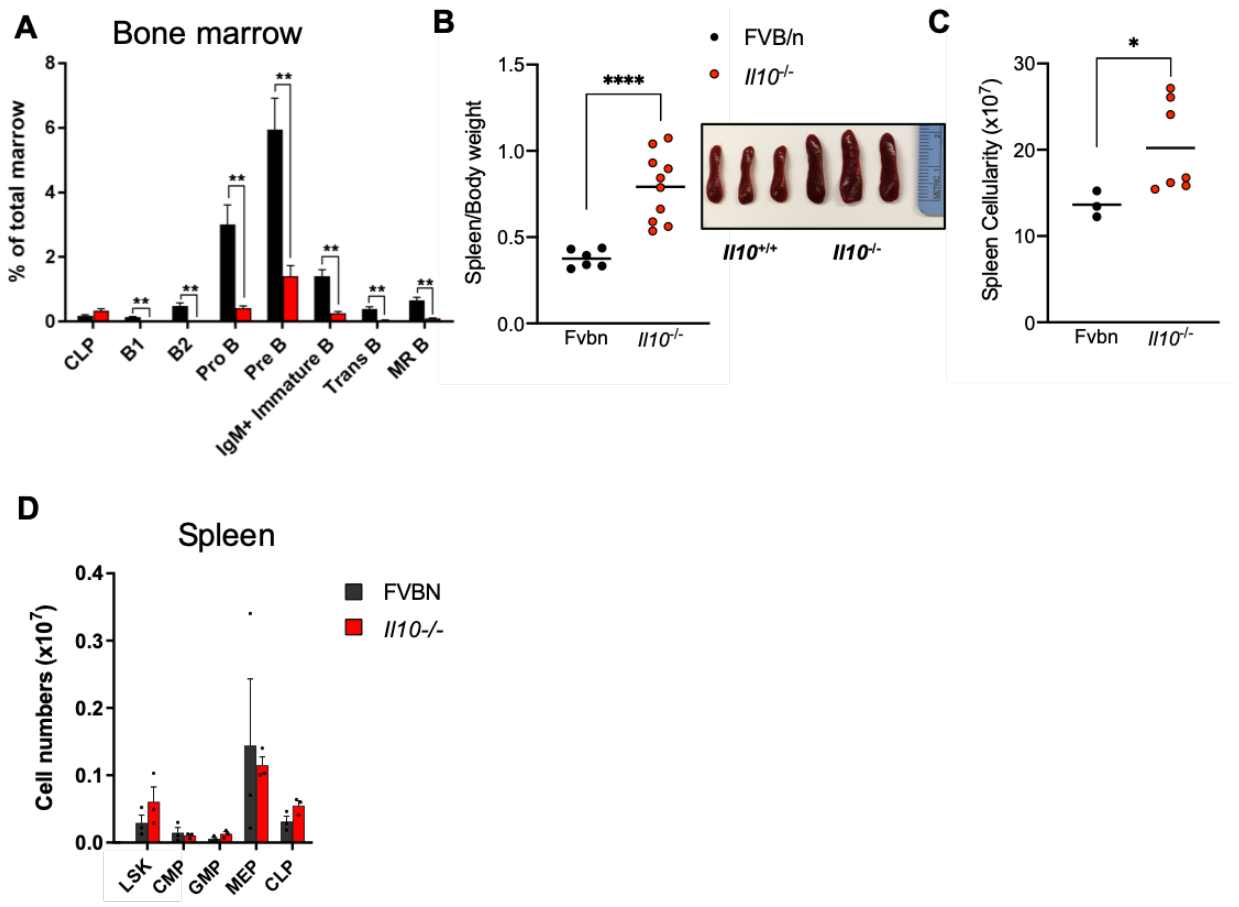

Figure 2.2. Distribution of hematopoietic stem and progenitor cells is altered in young *Il10*$^{-/-}$ mice.

Analysis of 4-6 week-old FVB/n and *Il10*$^{-/-}$ mice. **(A)** Percent of CLP (Lin^{-}, IL7-R^{+} , C-kit^{lo}, Sca-1^{lo}), B1 progenitors "B1" (Lin^{-}, CD93^{+} B220^{-} CD19^{+}), pre-pro B cells/B2 progenitors "B2" (Lin^{-}, CD93^{+} B220^{+} CD19^{-} CD43^{+}), pro-B cells (B220^{+} CD19^{+} IgM^{-} IgD^{-} CD43^{+}), pre-B cells (B220^{+} CD19^{+} IgM^{-} IgD^{-} CD43^{-}), IgM^{+} immature B cells (B220^{+} CD19^{+} IgM^{+} IgD^{-}), transitional B cells (B220^{+} CD19^{+} IgM^{+} IgD^{lo}), and mature recirculating (MR) B cells (B220^{+} CD19^{+} IgM^{+} IgD^{+}) of total live bone marrow cells. **(B)** Ratio of spleen to body weight and gross morphology of spleen. **(C)** Spleen cellularity. **(D)** Number Lin- LSK (Lin^{-} C-kit^{+} Sca-1^{+}) CMP (Lin^{-}, C-kit^{+} , Sca-1^{-}, CD34^{+} , FcgR^{-}), GMP (Lin^{-}, C-kit^{+} , Sca-1^{-}, CD34^{+} , FcgR^{+}), MEP (Lin^{-}, C-kit^{+} , Sca-1^{-}, CD34^{-}, FcgR^{-}), CLP (markers listed under **A**) in the bone marrow. Bar graph data show mean ± SD. *p ≤ 0.05, **p ≤ 0.01, ***p ≤ 0.001, ****p ≤ 0.001.

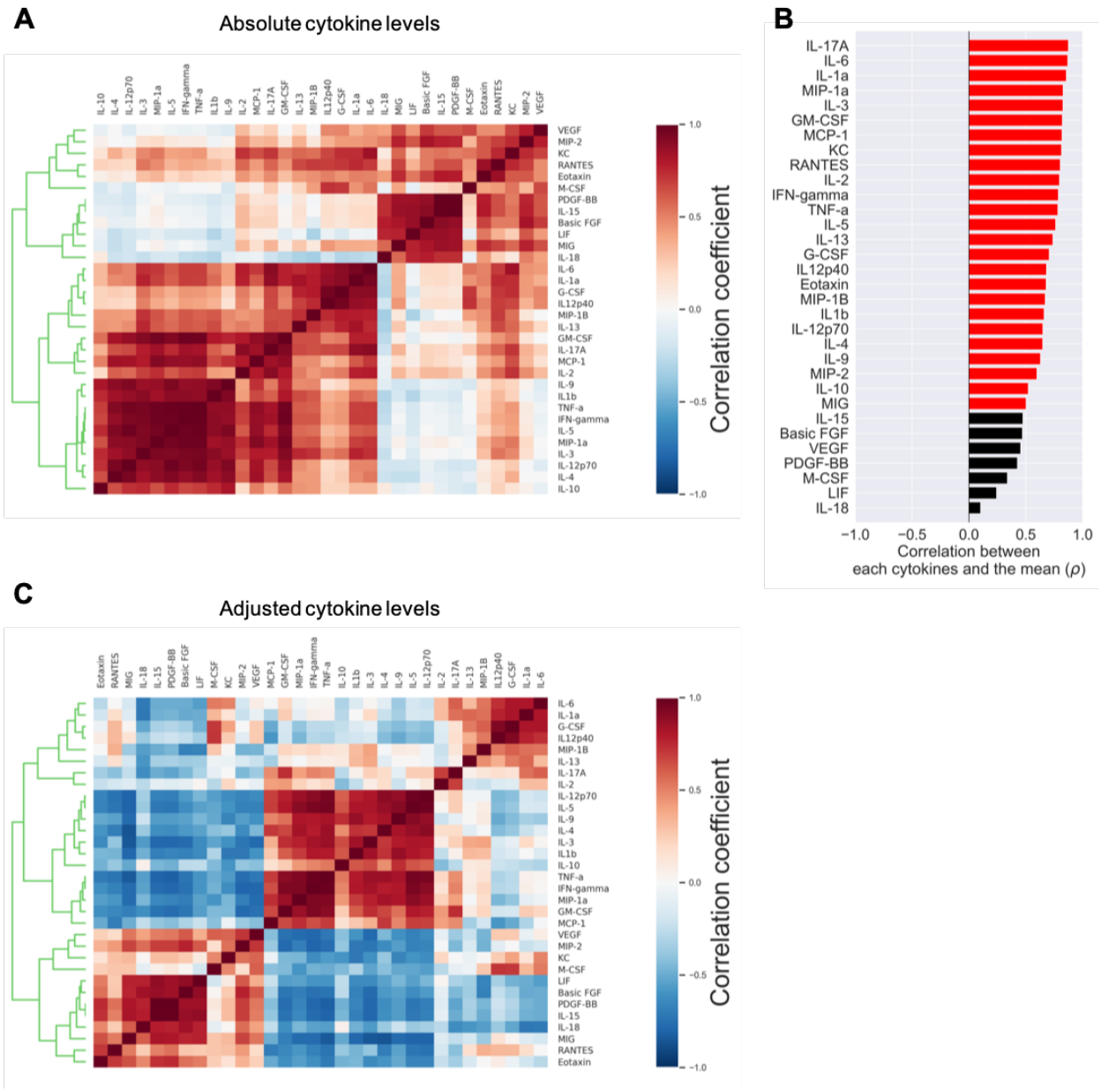

Figure 2.3. Cytokine levels in combined dataset of FVB/n and *Il10*$^{-/-}$ mice.

(A) Hierarchical clustering of Pairwise Pearson's correlations among absolute cytokine levels. **(B)** Correlation between individual cytokine level and mean concentration of all cytokines for each sample. **(C)** Hierarchical clustering among adjusted cytokine levels

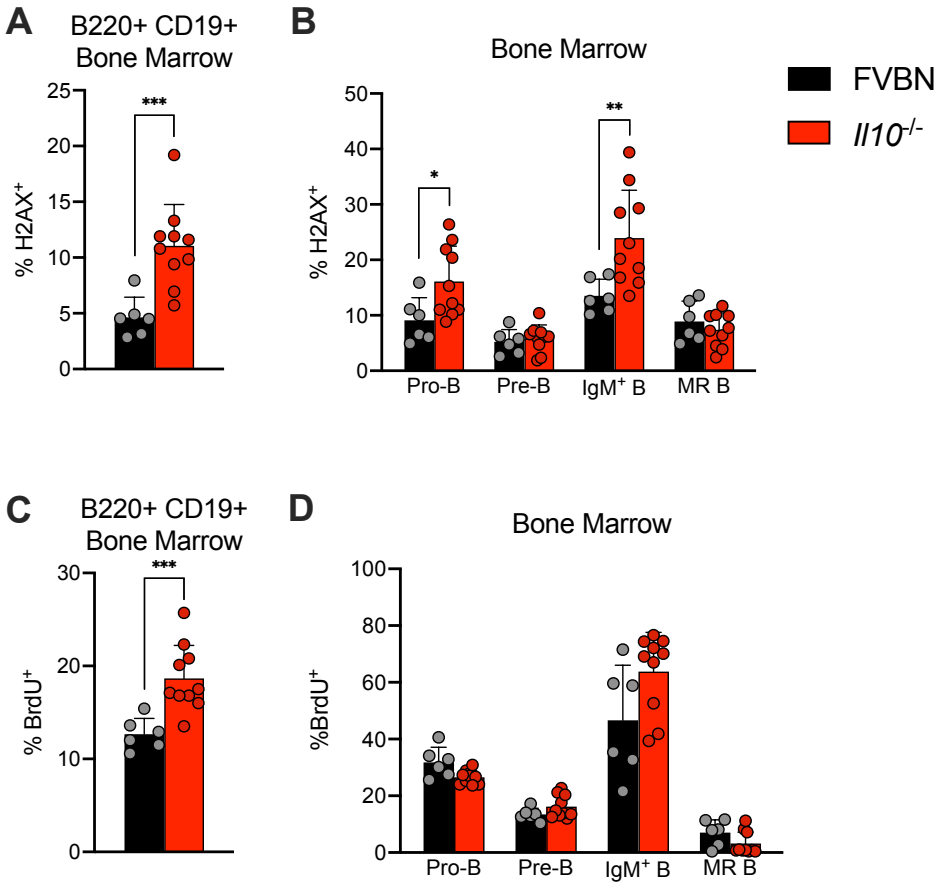

Figure 2.4. Bone marrow B cells in *Il10*$^{-/-}$ mice have increased DNA damage and proliferation.

Analysis of 8-12 week-old FVB/n and *Il10*$^{-/-}$ mice. Percent of H2AX+ cells among **(A)** Total bone marrow B cells and **(B)** Bone marrow B cell subsets. Percent of BrdU+ cells among **(C)** Total bone marrow B cells and **(D)** Bone marrow B cell subsets. Bar graph data show mean ± SD. *p ≤ 0.05, **p ≤ 0.01, ***p ≤ 0.001, ****p ≤ 0.001.

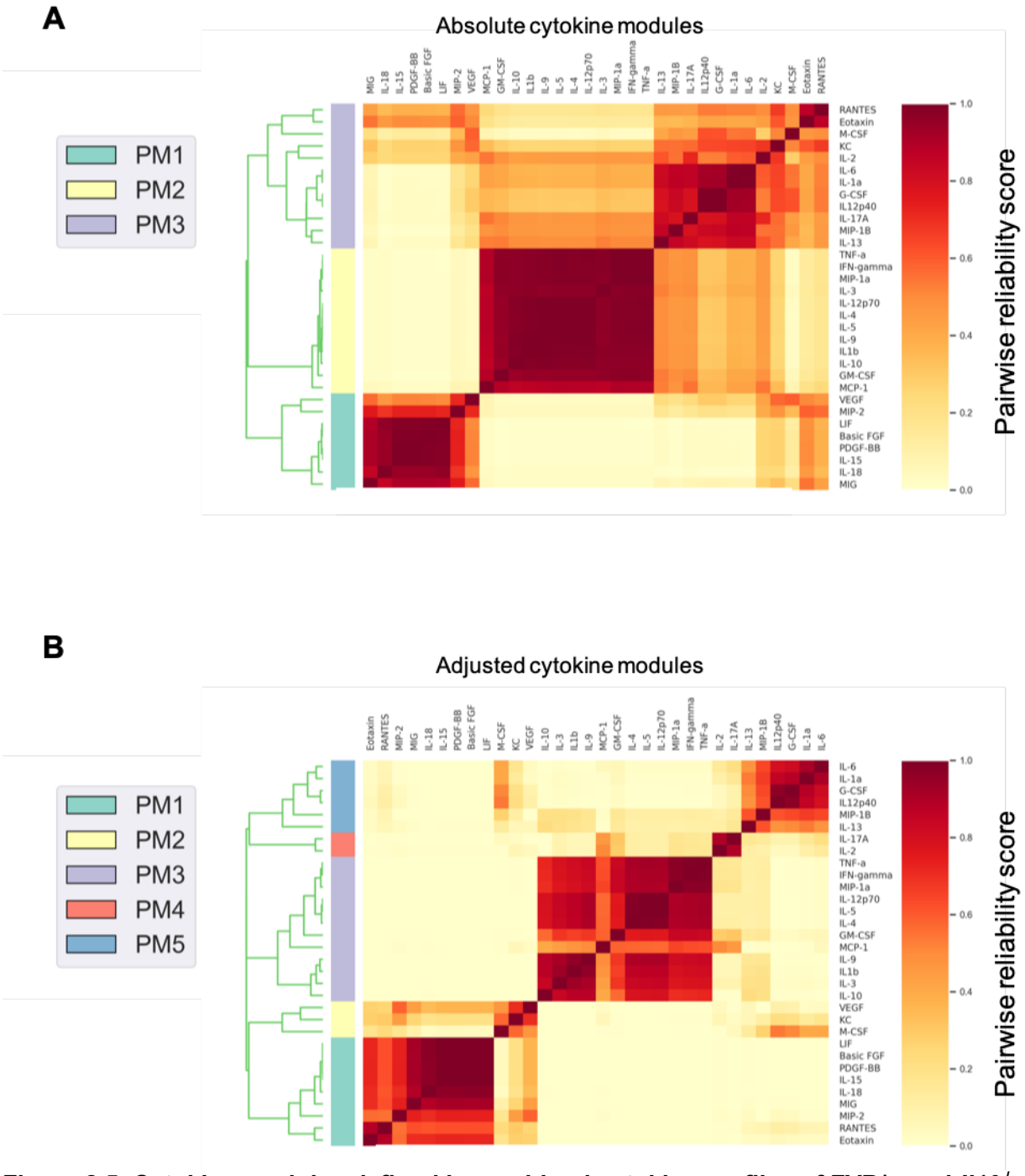

Figure 2.5. Cytokine modules defined in combined cytokine profiles of FVB/n and *Il10*$^{-/-}$ mice.

Heatmap of cytokine modules displaying pairwise reliability scores of **(A)** Absolute and **(B)** Adjusted cytokines over 1,000 random samplings of subjects. The optimal number of clusters was determined by the Tibshirani gap statistic method.

2.5 TABLES

Table 2.1. Univariate analysis comparing cytokine profiles of 6 FVB/n controls and 10 *Il10*$^{-/-}$ mice.

Cytokine	FVB/n Median (pg/ml)	*Il10*$^{-/-}$ Median (pg/ml)	Nominal p-value	Corrected p-value	Fold Change (relative to control)
IL-1a	11.19	50.06	7.094E-07	**2.270E-05**	4.48
IL12p40	710.07	2953.65	3.705E-06	**0.0001**	4.16
G-CSF	119.80	5738.25	4.653E-06	**0.0001**	47.90
IL-6	12.21	131.50	0.0002	**0.0056**	10.77
MIP-1B	8.14	37.47	0.0003	**0.0098**	4.60
IL-17A	20.71	46.49	0.0011	**0.0349**	2.24
M-CSF	5945.67	7082.69	0.0017	0.0545	1.19
IL-13	37.17	238.62	0.0039	0.1260	6.42
RANTES	64.04	180.56	0.0058	0.1861	2.82
IL-3	3.32	6.54	0.0381	1.2186	1.97
Eotaxin	568.11	812.23	0.0962	3.0783	1.43
KC	60.61	286.56	0.1035	3.3122	4.73
MIG	314.23	507.64	0.1903	6.0886	1.62
VEGF	103.58	112.79	0.1906	6.0987	1.09
GM-CSF	137.65	183.49	0.2481	7.9377	1.33
IL-2	34.25	48.70	0.2585	8.2715	1.42
IL1b	4.56	8.01	0.3035	9.7117	1.76
IL-10	10.28	22.86	0.3236	10.3552	2.22
PDGF-BB	2413.06	2494.89	0.3463	11.0805	1.03
TNFα	32.35	47.65	0.3571	11.4271	1.47
MIP-1a	8.07	8.92	0.3715	11.8874	1.11
MIP-2	13.52	23.12	0.4077	13.0463	1.71
LIF	357.17	327.99	0.4342	13.8933	0.92
IL-4	6.32	5.98	0.4403	14.0902	0.95
IL-5	18.62	26.32	0.4426	14.1636	1.41
IL-18	256.09	59.91	0.4564	14.6057	0.23
IFNγ	40.10	51.32	0.4734	15.1486	1.28
IL-15	2371.44	2851.94	0.4985	15.9534	1.20
IL-9	24.49	26.31	0.6781	21.7002	1.07
MCP-1	569.99	665.52	0.7017	22.4540	1.17
Basic FGF	160.09	159.87	0.8299	26.5580	1.00
IL-12p70	70.71	85.91	0.9682	30.9819	1.21

Table 2.2. Absolute plasma cytokine associations with immune cell phenotypes

Outcome	Module/Analyte	Coef	P-value	FWER	FDR
PBMonosCount	IL-17A	0.5843	1.31E-06	**4.19E-04**	3.55E-04
AbsMRCount	IL12p40	-3.4133	2.22E-06	**7.08E-04**	3.55E-04
AbsPreBCount	G-CSF	-13.2357	5.41E-06	**0.0017**	4.44E-04
AbsBCount	G-CSF	-18.4784	5.91E-06	**0.0019**	4.44E-04
AbsMRCount	G-CSF	-3.3445	6.93E-06	**0.0022**	4.44E-04
AbsBCount	IL12p40	-18.0805	1.71E-05	**0.0054**	9.03E-04
BMMonosCount	IL12p40	0.0551	1.99E-05	**0.0063**	9.03E-04
PBNeutsCount	IL-6	2.8140	2.48E-05	**0.0078**	9.03E-04
AbsPreBCount	IL12p40	-12.8124	2.54E-05	**0.0079**	9.03E-04
PBMonosCount	IL-1a	0.2734	9.53E-05	**0.0296**	0.0030
PBNeutsCount	G-CSF	1.9312	1.69E-04	0.0525	0.0049
PBMonosCount	IL12p40	0.2021	1.95E-04	0.0604	0.0052
BcellH2AX	G-CSF	2.9753	3.09E-04	0.0952	0.0076
PBNeutsCount	IL-1a	2.4503	4.36E-04	0.1339	0.0100
BMMonosCount	M-CSF	0.0494	6.31E-04	0.1932	0.0135
BcellH2AX	MIP-1B	2.8400	9.35E-04	0.2852	0.0187
AbsPreBCount	M-CSF	-11.2483	0.0011	0.3451	0.0213
PBMonosCount	G-CSF	0.1955	0.0012	0.3625	0.0213
PBMonosCount	IL-6	0.2699	0.0018	0.5339	0.0287
AbsBCount	M-CSF	-15.3550	0.0018	0.5408	0.0287
BcellH2AX	IL-1a	2.7387	0.0019	0.5662	0.0288
ProBH2AX	RANTES	4.0118	0.0021	0.6143	0.0298
ProBH2AX	MIP-1B	4.0022	0.0021	0.6380	0.0298
BMMonosCount	G-CSF	0.0462	0.0024	0.7112	0.0319
AbsPreBCount	MIP-1B	-10.7500	0.0026	0.7648	0.0321
PBNeutsCount	MIP-1B	1.3723	0.0026	0.7697	0.0321
AbsBCount	MIP-1B	-14.9896	0.0027	0.7964	0.0321
PBNeutsCount	IL-17A	4.5575	0.0031	0.8960	0.0349
ImmatureBH2AX	RANTES	5.0754	0.0044	1	0.0481
AbsMRCount	MIP-1B	-2.6249	0.0047	1	0.0491
PBMonosCount	RANTES	0.1708	0.0048	1	0.0491

Continued on next page

Outcome	Module/Analyte	Coef	P-value	FWER	FDR
AbsMRCount	M-CSF	-2.6147	0.0049	1	0.0491
BcellH2AX	IL12p40	2.5669	0.0051	1	0.0499
PBNeutsCount	IL12p40	1.6431	0.0062	1	0.0577
BMNeutsCount	IL12p40	0.2751	0.0063	1	0.0577
AbsMRCount	IL-1a	-2.5518	0.0067	1	0.0600
PBMonosCount	MIP-1B	0.1380	0.0083	1	0.0720
ImmatureBH2AX	IL-1a	4.7662	0.0096	1	0.0808
ImmatureBH2AX	G-CSF	4.7213	0.0106	1	0.0873
AbsBCount	IL-1a	-13.3418	0.0122	1	0.0950
BMMonosCount	Eotaxin	0.0408	0.0122	1	0.0950
AbsPreBCount	IL-1a	-9.4468	0.0134	1	0.1009
PBMonosCount	Eotaxin	0.1348	0.0136	1	0.1009
ImmatureBH2AX	IL-13	4.5640	0.0150	1	0.1091
BcellH2AX	IL-13	2.3073	0.0169	1	0.1199
AbsPreBCount	IL-6	-9.0828	0.0194	1	0.1328
BMMonosCount	IL-1a	0.0388	0.0195	1	0.1328
ProBH2AX	IL-1a	3.3243	0.0204	1	0.1358
AbsBCount	IL-6	-12.4547	0.0229	1	0.1466
BMMonosCount	MIP-1B	0.0381	0.0229	1	0.1466
BcellH2AX	IL-6	2.2181	0.0237	1	0.1485
ImmatureBH2AX	MIP-1B	4.3016	0.0251	1	0.1543
AbsMRCount	IL-6	-2.2033	0.0280	1	0.1647
AbsBCount	IL-13	-12.1021	0.0286	1	0.1647
ImmatureBH2AX	MIP-2	4.2265	0.0287	1	0.1647
AbsPreBCount	IL-13	-8.6373	0.0290	1	0.1647
ProBH2AX	G-CSF	3.1753	0.0293	1	0.1647
AbsMRCount	IL-13	-2.1842	0.0299	1	0.1649
PBMonosCount	M-CSF	0.1278	0.0312	1	0.1694
BcellH2AX	RANTES	2.1314	0.0320	1	0.1708
BMMonosCount	IL-6	0.0360	0.0346	1	0.1813
BMMonosCount	RANTES	0.0356	0.0377	1	0.1946
PBNeutsCount	IL-18	-1.3917	0.0415	1	0.2109
BMNeutsCount	IL-1a	0.2216	0.0434	1	0.2172

Continued on next page

Outcome	Module/Analyte	Coef	P-value	FWER	FDR
BMNeutsCount	G-CSF	0.2204	0.0449	1	0.2193
PBNeutsCount	IL-13	1.3635	0.0452	1	0.2193
ProBH2AX	IL-13	2.9514	0.0477	1	0.2269
ImmatureBH2AX	IL12p40	3.9099	0.0482	1	0.2269

Table 2.3. Adjusted plasma cytokine associations with immune cell phenotypes

Outcome	Module/Analyte	Coef	P-value	FWER	FDR
AbsBCount	G-CSF	-19.5885	1.11E-07	**3.57E-05**	1.8762E-05
AbsPreBCount	G-CSF	-13.9993	1.17E-07	**3.74E-05**	1.8762E-05
AbsMRCount	IL12p40	-3.4911	4.92E-07	**1.57E-04**	5.2507E-05
AbsMRCount	G-CSF	-3.4634	8.67E-07	**2.75E-04**	6.9397E-05
AbsBCount	IL12p40	-18.6473	3.59E-06	**0.0011**	2.30E-04
AbsPreBCount	IL12p40	-13.1377	7.96E-06	**0.0025**	4.25E-04
BMMonosCount	IL12p40	0.0546	2.90E-05	**0.0091**	0.0012
PBMonosCount	MCP-1	-0.2265	3.10E-05	**0.0097**	0.0012
PBNeutsCount	G-CSF	1.9439	1.09E-04	**0.0341**	0.0039
PBNeutsCount	IL-1a	2.4353	1.84E-04	0.0573	0.0059
BcellH2AX	IL-1a	2.9229	4.87E-04	0.1510	0.0142
AbsMRCount	IL-1a	-2.8526	0.0012	0.3588	0.0310
BcellH2AX	G-CSF	2.7655	0.0016	0.4870	0.0389
BMNeutsCount	IL12p40	0.2955	0.0022	0.6754	0.0477
PBNeutsCount	MIP-1B	1.3384	0.0022	0.6841	0.0477
AbsBCount	IL-1a	-15.0445	0.0026	0.7785	0.0510
PBNeutsCount	IL12p40	1.8573	0.0033	1	0.0619
BMNeutsCount	IL-1a	0.2862	0.0037	1	0.0619
AbsPreBCount	IL-1a	-10.5099	0.0037	1	0.0619
BMMonosCount	M-CSF	0.0445	0.0042	1	0.0679
PBMonosCount	IL12p40	0.1948	0.0051	1	0.0716
AbsPreBCount	M-CSF	-10.2560	0.0052	1	0.0716
AbsPreBCount	MIP-1B	-10.2373	0.0053	1	0.0716
AbsBCount	MIP-1B	-14.3072	0.0054	1	0.0716
AbsPreBCount	IL-6	-10.1129	0.0062	1	0.0779
BcellH2AX	MIP-1B	2.5268	0.0063	1	0.0779
BMMonosCount	G-CSF	0.0430	0.0067	1	0.0792
AbsBCount	M-CSF	-13.9636	0.0073	1	0.0836
AbsBCount	IL-6	-13.7374	0.0089	1	0.0978
BMMonosCount	MCP-1	-0.0411	0.0113	1	0.1209
AbsMRCount	MIP-1B	-2.3959	0.0136	1	0.1403

Continued on next page

Outcome	Module/Analyte	Coef	P-value	FWER	FDR
BMNeutsCount	IL-6	0.2509	0.0170	1	0.1703
AbsMRCount	M-CSF	-2.3229	0.0182	1	0.1761
BMMonosCount	IL-1a	0.0383	0.0218	1	0.1960
PBNeutsCount	IL-6	1.5024	0.0219	1	0.1960
BMMonosCount	IL-12p70	-0.0382	0.0220	1	0.1960
AbsMRCount	IL-6	-2.2376	0.0249	1	0.2100
PBNeutsCount	IL-18	-1.4807	0.0249	1	0.2100
PBNeutsCount	LIF	-1.1018	0.0265	1	0.2177
BcellH2AX	IL12p40	2.1665	0.0284	1	0.2260
AbsMRCount	MCP-1	2.1936	0.0290	1	0.2260
BMMonosCount	IL-5	-0.0366	0.0312	1	0.2380
BMMonosCount	IL-9	-0.0353	0.0394	1	0.2889
BMNeutsCount	G-CSF	0.2248	0.0397	1	0.2889
BMNeutsCount	MIP-2	-0.2233	0.0414	1	0.2941
BMMonosCount	Eotaxin	0.0350	0.0423	1	0.2941
PBMonosCount	IL-2	-0.1402	0.0446	1	0.3037
PBMonosCount	G-CSF	0.1488	0.0467	1	0.3112

Table 2.4. Absolute plasma module associations with immune cell phenotypes

Outcome	Module/Analyte	Coef	P-value	FWER	FDR
PBMonosCount	PM3	0.2428	7.2166E-05	**0.0022**	0.0022
PBNeutsCount	PM3	2.0589	0.0018	**0.0511**	0.0264
BMMonosCount	PM3	0.0430	0.0067	0.1864	0.0513
AbsPreBCount	PM3	-10.0407	0.0068	0.1864	0.0513
AbsBCount	PM3	-13.7786	0.0086	0.2228	0.0514
BcellH2AX	PM3	2.4232	0.0103	0.2586	0.0517
AbsMRCount	PM3	-2.4233	0.0121	0.2908	0.0519
ImmatureBH2AX	PM3	4.5961	0.0140	0.3225	0.0526
ProBH2AX	PM3	3.4070	0.0164	0.3603	0.0546
BMNeutsCount	PM3	0.1876	0.1003	1	0.3010
ProBH2AX	PM2	2.2825	0.1465	1	0.3997
ImmatureBH2AX	PM2	2.8602	0.1739	1	0.4348
PBNeutsCount	PM1	-0.8918	0.2592	1	0.5982
PBNeutsCount	PM2	1.1437	0.2893	1	0.6198
ImmatureBH2AX	PM1	2.0863	0.3358	1	0.6716
PBMonosCount	PM2	0.1043	0.3774	1	0.7076
BcellH2AX	PM2	0.9246	0.4085	1	0.7143
BMNeutsCount	PM1	-0.0966	0.4286	1	0.7143
AbsMRCount	PM1	0.6597	0.5660	1	0.7844
AbsMRCount	PM2	-0.6352	0.5809	1	0.7844
ProBH2AX	PM1	0.9049	0.5877	1	0.7844
BcellH2AX	PM1	-0.5991	0.5974	1	0.7844
BMMonosCount	PM1	0.0101	0.6013	1	0.7844
BMNeutsCount	PM2	0.0571	0.6446	1	0.8057
AbsBCount	PM1	2.6975	0.6717	1	0.8060
AbsPreBCount	PM1	1.4573	0.7495	1	0.8433
PBMonosCount	PM1	0.0258	0.7763	1	0.8433
AbsBCount	PM2	-1.7260	0.7870	1	0.8433
AbsPreBCount	PM2	-0.8457	0.8533	1	0.8828
BMMonosCount	PM2	-0.0028	0.8870	1	0.8870

Table 2.5. Adjusted plasma module associations with immune cell phenotypes

Outcome	Module/Analyte	Coef	P-value	FWER	FDR
AbsBCount	PM5	-18.5633	4.62E-06	**2.31E-04**	9.53E-05
AbsPreBCount	PM5	-13.2290	5.56E-06	**2.72E-04**	9.53E-05
PBNeutsCount	PM5	2.0300	5.72E-06	**2.75E-04**	9.53E-05
AbsMRCount	PM5	-3.2836	1.68E-05	**7.91E-04**	2.10E-04
BcellH2AX	PM5	2.8579	8.17E-04	**0.0376**	0.00817
BMNeutsCount	PM5	0.2890	0.0032	0.1419	0.02629
BMMonosCount	PM5	0.0431	0.0065	0.2882	0.04678

CHAPTER 3: DECREASED LEVELS OF IL-10 ACCELERATE THE DEVELOPMENT OF B CELL DISEASE

3.1 INTRODUCTION

Given the association between IL-10 deficiency and increased risk of childhood B cell lymphoblastic leukemia[11,62,63] and B cell lymphoma[12] in humans, we sought to determine whether decreased levels of IL-10 contribute to the development of disease in a mouse model of B cell leukemia/lymphoma. The coordination between pre-existing genetic lesions and inflammatory cues can contribute to the development of pediatric B-ALL. Two well-supported mechanisms of inflammation-driven B leukemogenesis are (1) selection of B cell clones harboring initiating mutations that confer a competitive advantage in inflammatory milieus and (2) aberrant activation of RAG and AID endonucleases, resulting in mutagenesis of Ig and non-Ig genes. These pathways have been observed in disease models that have relied on the induction of specific inflammatory conditions including aging-induced inflammation[53] and TLR stimulation[8,64]. Interestingly, we have observed increased B cell suppression and DNA damage in *Il10*$^{-/-}$ mice with inflammation. Therefore, we propose that inflammation in *Il10*$^{-/-}$ mice, rather than a direct loss of IL-10 signaling, can contribute to the development of B cell malignancies in a disease model.

Infections and inflammation are capable of driving the selection of B cell progenitors with pre-existing oncogenic lesions, which may lead to leukemia development. Whereas normal B cell progenitors are suppressed by aging-associated inflammation, B cells with oncogenic lesions such as *BCR-ABL*, *NRAS*^{V12}, and *Myc*, are resistant to the suppressive effects of the aged-inflammatory environment[53]. The mutated population of B cells can undergo an expansion in compartment size over time, suggesting that they may eventually develop into B-ALL. Whether similar inflammatory responses are capable of driving the selection of in pre-leukemic clones in young mice is unclear. In the *Pax5*$^{+/-}$ model of B-ALL, exposing young mice to infectious pathogens results in B cell suppression and permits the acquisition of somatic mutations in *Jak3*[52]. Interestingly, several pro-inflammatory cytokines that drive aging inflammation are also elevated

during spontaneous inflammatory responses in young *Il10*$^{-/-}$ mice. It is therefore feasible that inflammation in young *Il10*$^{-/-}$ mice may favor the selection of B cells with oncogenic mutations and lead to subsequent leukemic development.

Another mechanism of pathogenesis that is related to chronic inflammation is increased tissue damage caused by activated neutrophils. Other groups have established that *Il10*$^{-/-}$ mice with colitis have extensive DNA damage in peripheral blood lymphocytes in comparison to *Il10*$^{-/-}$ mice without colitis or wild-type controls[18]. No previous studies have reported whether the DNA damage in *Il10*$^{-/-}$mice extends to the B cell compartment of the bone marrow. Of note, the TLR4 agonist LPS in combination with withdrawal of IL-7 from B cell culture conditions is able to induce DNA damage in B cells by increasing the activity of the RAG and AID enzymes[8], which are involved in VDJ recombination and somatic hypermutation (SHM). Thus, selection of pre-leukemic B cell clones and RAG/AID-mediated mutagenesis could represent processes that contribute to B cell leukemogenesis.

3.2 RESULTS

3.2.i IL-10 deficiency disrupts B cell properties in pre-leukemic mice

To investigate the interactions between inflammation and B cell properties in a mouse model of B cell leukemia/lymphoma, we crossed *Il10*$^{-/-}$ mice to *Cdkn2a*$^{-/-}$ mice to generate *Il10*$^{-/-}$ *Cdkn2a*$^{-/-}$ mice. *Cdkn2a* codes for the p16Ink4a and p19Arf (p14ARF in humans) tumor suppressor proteins, which are key regulators of the cell cycle. *CDKN2A* loss is found in 1/3 of ALL[65] and when the homolog of this gene is deleted in mice, B-ALL is induced with a penetrance of 40%[23]. We hypothesized that the loss of IL-10 in *Cdkn2a*$^{-/-}$ mice would have a similar effect on inducing B cell loss and DNA damage as *Il10* loss in mice with wild-type *Cdkn2a*. Although no aberrations in B cell proliferation have been reported in *Cdkn2a*$^{-/-}$ mice, it is possible that the combination of *Il10* and *Cdkn2a* deletions may coordinate to increase B cell

proliferation to a level that exceeds what we have observed in Il10-/- mice. We demonstrated that pre-B cells in *Il10*$^{-/-}$ *Cdkn2a*$^{-/-}$ mice are less abundant than they are in control *Cdkn2a*$^{-/-}$ mice (**Figure 3.1A**). The absence of IL-10 also increased the percent of DNA damage and proliferation in B cells relative to *Cdkn2a*-/- mice (**Figure 3.1B**). FVB/n and *Il10*$^{-/-}$ mice were not included in this experiment, therefore we were unable to evaluate whether *Cdkn2a* loss coordinated with *Il10* loss to further impact B cells. However, it is worth noting that the fold change between *Il10*$^{-/-}$ and control mouse B cell numbers, DNA damage, and proliferation was similar across different experiments. Therefore, the loss of IL-10 has similar effects on B cells in *Cdkn2a* wild-type mice and in the *Cdkn2a*$^{-/-}$ mouse model of B cell leukemia/lymphoma.

3.2.ii IL-6 and IL-17 are associated with B cell DNA damage in pre-leukemic Il10$^{-/-}$ *mice*

To confirm the association between inflammation and altered B cell properties in the context of *Cdkn2a* deletion, we measured cytokine concentrations in the blood of *Cdkn2a*$^{-/-}$ and *Il10*$^{-/-}$ *Cdkn2a*$^{-/-}$ mice. We used the approach described in Chapter 2 to determine whether associations were present between individual cytokines or cytokine modules and B cell outcomes. Linear regression of single cytokines showed an inverse correlation between pre-B cell numbers and the levels of G-CSF, IL-6, and IL-17 (**Tables 3.1 and 3.2**). In our previous analysis of cytokine associations in *Il10*$^{-/-}$ mice, G-CSF had a similar negative correlation with pre-B cell number. This result suggests that the relationship between G-CSF and pre-B cells persists in the presence of pre-leukemic mutations. IL-6 and IL-17 on the other hand, were only correlated with low pre-B cell numbers in *Il10*$^{-/-}$ mice on the *Cdkn2a*$^{-/-}$ background. This result could demonstrate that either *Cdkn2a* loss alters the pattern of cytokine expression in *Il10*$^{-/-}$ mice or that *Cdkn2a*$^{-/-}$ pre-B cells are more responsive to changes in IL-6 and IL-17 than pre-B cells from *Cdkn2a* wild-type mice. Alternatively, our initial study in *Cdkn2a* wild-type mice may have been underpowered to detect differences in IL-6 and IL-17 due to the modest number of

evaluated mice and variability. Overall, G-CSF was consistently associated with low pre-B cell numbers in *Il10*$^{-/-}$ mice regardless of whether *Cdkn2a* was deleted.

We also tested whether the cytokines in plasma 5 module (PM5) from Chapter 2 retained an association with B cell DNA damage in *Il10*$^{-/-}$ *Cdkn2a*$^{-/-}$ mice. These cytokines included IL-1α, IL-6, IL-12p40, IL-13, G-CSF, and MIP-1β. Of the cytokines in PM5, only IL-6 was independently associated with B cell DNA damage by linear regression (**Table 3.1**). We also observed an association between IL-17 levels and B cell DNA damage. We expected that modular analysis of cytokines may reveal significant correlations between a group of cytokines and B cell DNA damage, but did not find any such associations that withstood multiple hypothesis testing (data not shown). These results demonstrate that although IL-6 is related to B cell DNA damage across non-pre-leukemic and pre-leukemic *Il10*$^{-/-}$ datasets, IL-17 is only associated with DNA damage in B cells in pre-leukemic *Il10*$^{-/-}$ *Ckdn2a*$^{-/-}$ mice. Our data identify IL-6 and IL-17 as potential mediators of B cell DNA damage in *Il10*$^{-/-}$ mice, which is consistent with the characterization of these cytokines as ALL risk factors in human newborns[66].

3.2.iii IL-10 deficiency does not alter B cell number, DNA damage, or proliferation in the absence of monocyte inflammation

To gain insight into the mechanism of B cell deficiency and DNA damage in *Il10*$^{-/-}$ *Ckdn2a*$^{-/-}$ mice, we addressed the dependency of these B cell properties on inflammation. 8-12 week old *Il10*$^{-/-}$ *Ckdn2a*$^{-/-}$ mice with variable levels of inflammation were chosen and their bone marrow B cells were compared to *Cdkn2a*$^{-/-}$ mice. Each *Il10*$^{-/-}$ mouse had an elevated count of peripheral blood monocytes or neutrophils relative to the average count of these populations in the control *Cdkn2a*$^{-/-}$ group. Cytokine levels were strongly associated with myeloid cell counts in the peripheral blood (**Tables 3.1 and 3.2**), therefore we used monocyte and neutrophil counts as markers of inflammation. *Il10*$^{-/-}$ *Cdkn2a*$^{-/-}$ mice with neutrophil or monocyte counts > 2 standard deviations above the average were classified as having elevated neutrophils

(neutrophilia) or elevated monocytes (monocytosis). Decreased numbers of bone marrow B cells were only observed in *Il10*$^{-/-}$ mice with neutrophilia (**Figure 3.2A**) and monoyctosis (**Figure 3.2B**), however there was no significant correlation between B cell count and the number of myeloid cells in the blood. We next sought to compare B cell development, DNA damage, and proliferation between *Il10*$^{-/-}$ mice with and without elevated myeloid cell counts. Because 5 out of 6 *Il10*$^{-/-}$ *Cdkn2a*$^{-/-}$ mice had neutrophilia, we were unable to draw comparisons of B cell properties between mice with normal and elevated neutrophil levels. For this reason, blood monocyte count was the primary measure of inflammation in this experiment. As expected, *Il10*$^{-/-}$ *Cdkn2a*$^{-/-}$ mice with monocytosis had impaired B cell development starting at the pre-B cell stage (**Figure 3.2C**) and increased DNA damage (**Figure 3.2D**) and proliferation (**Figure 3.2E**) in mature Lin^{+} B cells relative to *Cdkn2a*$^{-/-}$ mice. Interestingly, *Il10*$^{-/-}$ *Cdkn2a*$^{-/-}$ mice with normal monocyte levels had no detectable abnormalities in these B cell properties in comparison to *Cdkn2a*$^{-/-}$ mice. These results established that IL-10 deficiency in the absence of substantial monocyte-related inflammation is not sufficient to alter B cell abundance, DNA damage, or proliferation.

3.2.iv Loss of IL-10 production in non-hematopoietic cells drives inflammation

To better understand how the absence of IL-10 production induces inflammation and B cell deficiency in *Il10*$^{-/-}$ mice, we used a mouse model of *ETV6-RUNX1* ALL. *ETV6-RUNX1* is the most common chromosomal translocation in pediatric ALL and encodes the TEL-AML1 (TA) oncogenic protein. TA can coordinate with infectious exposures to promote ALL development[8,9]. In the *Cdkn2a*$^{-/-}$ mouse model, expression of an EGFP-labeled TA transgene increases the risk of B-ALL from 26% to 50% and allows for detection of pre-leukemic cells by flow cytometry[23]. We first used TA *Cdkn2a*$^{-/-}$ mice to identify how pre-leukemic B cells respond to IL-10 deficiency in different cellular compartments. To this end, we generated chimeric mice by transplanting pre-leukemic TA *Cdkn2a*$^{-/-}$ bone marrow from *Il10*$^{+/+}$ or *Il10*$^{-/-}$ donor mice into irradiated *Il10*$^{+/+}$ or

Il10$^{-/-}$ recipient mice (**Figure 3.3A**). The resulting four groups of mice (*Il10*$^{+/+}$ → *Il10*$^{+/+}$, *Il10*$^{-/-}$ → *Il10*$^{+/+}$, *Il10*$^{+/+}$ → *Il10*$^{-/-}$, *Il10*$^{-/-}$→ *Il10*$^{-/-}$) were bled on a monthly basis to track the growth dynamics of myeloid cells and pre-leukemic TA expressing B cells over time.

Since IL-10 is produced by hematopoietic and non-hematopoietic cells[13], it is possible for IL-10 deficiency in either of these cellular compartments to disrupt myeloid and B cell homeostasis. If a loss of IL-10 production in hematopoietic cells drives myeloid expansion, then we would expect the transplantation of *Il10*$^{-/-}$ donor marrow to induce higher myeloid counts in recipient mice than the transplantation of *Il10*$^{+/+}$ donor marrow. If, on the other hand, a non-hematopoietic *Il10* deficiency is sufficient to induce inflammation, then all *Il10*$^{-/-}$ recipients should have elevated myeloid counts, regardless of donor strain. An additional possibility is that *Il10* deficiency in both hematopoietic and non-hematopoietic cells contributes to inflammation. In this case, we would expect *Il10*$^{-/-}$ recipients of *Il10*$^{-/-}$ donor cells to have the highest level of myeloid expansion in comparison to any of the other three transplantation conditions.

Differences in the white blood cell counts were apparent as early as 5 weeks post-transplantation. Based on studies that have demonstrated the importance of lymphoid-derived IL-10 suppressing immune cell activation[67–69], we expected a loss of IL-10 in hematopoietic donor cells to induce an inflammatory response in FVB/n recipients. Surprisingly, the loss of IL-10 in hematopoietic donor cells had the opposite effect, which was suppression of granulocytes in FVB/n recipients (**Figure 3.3B**). Therefore, the loss of IL-10 production in hematopoietic cells was not sufficient to induce an inflammatory response in *Il10*$^{+/+}$ recipients. Instead, both groups of *Il10*$^{-/-}$ recipients had an increased percent of granulocytes along with a decreased percent of TA(EGFP+) granulocytes in the peripheral blood compared to FVB/n recipients (**Figure 3.3B**). Additionally, *Il10*$^{-/-}$ recipients had decreased lymphocyte percentages relative to FVB/n recipients (**Figure 3.3C**). We hypothesized that pre-leukemic lymphocytes in *Il10*$^{-/-}$ recipients may be resistant to inflammation-mediated suppression, however these mice had

a decreased percent of TA(EGFP+) lymphocytes (**Figure 3.3C**). These data show that a B-cell extrinsic loss of IL-10 in the non-hematopoietic compartment drives myeloid expansion, and possibly inflammation, in *Il10*$^{-/-}$ mice.

3.2.v Decreased levels of IL-10 accelerate B cell neoplasms in TEL-AML1 Cdkn2a$^{-/-}$ *mice*

Children born with low levels of IL-10 were found to have a 25-fold increased risk of developing ALL[11]. Whether this association reflects causality had not been previously tested. To determine whether low levels of IL-10 promote the development of B-cell leukemia/lymphoma, we followed a cohort of TA *Cdkn2a*$^{-/-}$ mice with wild-type IL-10 (*Il10*$^{+/+}$ TA *Cdkn2a*$^{-/-}$) for the development of disease alongside a cohort of mice with either decreased IL-10 expression (*Il10*$^{+/-}$ TA *Cdkn2a*$^{-/-}$) or absent IL-10 expression (*Il10*$^{-/-}$ TA *Cdkn2a*$^{-/-}$). We did not observe a significant difference in the incidence of either solid tumors or leukemia/lymphomas among our survival cohorts (**Table 3.3**). Time to illness analysis revealed that a complete loss of IL-10 in the TA *Cdkn2a*$^{-/-}$ model significantly decreased cancer free survival (**Figure 3.4A**) and leukemia/lymphoma free survival (**Figure 3.4B**) relative to *Il10*$^{+/+}$ controls. The median time to leukemia/lymphoma in *Il10*$^{-/-}$ TA *Cdkn2a*$^{-/-}$ mice was 140 vs. 220 days for *Il10*$^{+/+}$ TA *Cdkn2a*$^{-/-}$ mice (**Table 3.4**). For *Il10*$^{+/-}$ TA *Cdkn2a*$^{-/-}$ mice, the median time to leukemia/lymphoma was intermediate at 174 days, supporting a dose-dependent relationship between decreased levels of IL-10 and early onset of leukemia/lymphoma. Moreover, the latency of leukemia/lymphoma in *Il10*$^{+/-}$ TA *Cdkn2a*$^{-/-}$ mice was significantly shorter than that of the control *Il10*$^{+/+}$ TA *Cdkn2a*$^{-/-}$ survival cohort (Mann-Whitney *U*-test p=0.0107). These data demonstrate that low levels of IL-10 increase the aggressiveness of leukemia/lymphoma development in the TA *Cdkn2a*$^{-/-}$ model by accelerating time to illness.

3.2.vi IL-10 loss increases frequency of C>G and C>T mutations in B cell neoplasms

We next sought to determine whether the increased levels of B cell lesions observed in pre-leukemic *Il10*$^{-/-}$ mice corresponded to an increased mutational burden or altered mutational pattern in *Il10*$^{-/-}$ B-cell leukemia/lymphomas. To this end, we used whole exome sequencing to characterize the number and type of mutations in B-cell leukemia/lymphomas from 9 *Il10*$^{+/+}$ TA *Cdkn2a*$^{-/-}$ mice and 8 *Il10*$^{-/-}$ TA *Cdkn2a*$^{-/-}$ mice. Total and nonsynonymous single nucleotide variants (SNVs) were similar in number between *Il10*$^{+/+}$ and *Il10*$^{-/-}$ B cell leukemia/lymphomas (**Figure 3.4C**). The total number of C>G and C>T mutations was increased in *Il10*$^{-/-}$ samples (**Figure 3.4D**), although we did not find evidence for enrichment of inflammation-related COSMIC mutational signatures. Notably, C>T mutations are elevated in mouse tumors with IL-10 deletions[70]. SNVs related to human cancer were found in a number of genes (**Table 3.5**), with synonymous *Hoxa9* mutations in 63% of *Il10*$^{-/-}$ B cell leukemia/lymphomas (5 of 8). Similar synonymous mutations in HOX9A been found in several lymphoid neoplasm cell lines with a high pathogenicity score[71]. Although in the past, synonymous changes have been considered nonpathogenic, recent data suggests that these mutations have the potential to cause pathogenic effects[72]. We also observed mutations in *Jak3*, *Cdkn1a*, and *Dnm2*, which have human orthologs that are mutated in human leukemias[73–76]. The *Jak3*^{V670A} mutation was present in 3 of 17 B cell leukemia/lymphomas and is a homolog of human *JAK3*^{V674A}. Other canonical cancer SNVs were identified in our cohort, however there was little overlap in SNVs among samples. These results are consistent with sequencing data from human and mouse B-ALLs which provide evidence for a highly heterogeneous mutational landscape[7,9,58,77]. Overall, our results demonstrate that although IL-10 is dispensable for B cell lymphopoiesis, the myeloid inflammation that results from impaired IL-10 production in non-hematopoietic cells may lead to B cell loss and early DNA damage. Furthermore, decreased levels of IL-10 cause acceleration of lymphoid malignancies with increased C>G and C>T mutations in the TA *Ckdn2a*$^{-/-}$ model of B cell leukemia/lymphoma.

3.3 DISCUSSION

Our previous study, in which *Cdkn2a*$^{-/-}$ mice were genetically engineered to express TA in hematopoietic cells, revealed that following irradiation, TA positive B cells outcompeted TA negative cells[23]. We also found that irradiation also led to an early onset of B-ALL[23]. Thus, our initial expectation was that TA positive B cell numbers should increase in response to genotoxic stress associated with systemic inflammation in *Il10*$^{-/-}$ mice. The fact that transplanted TA positive B cells did not have a selective growth advantage in the blood of *Il10*$^{-/-}$ recipient mice is not consistent with this prediction. These observations raise the possibility that inflammation in *Il10*$^{-/-}$ mice may not be a sufficient source of genotoxic stress to favor the early selection of TA expressing cells. Analysis of cytokines and TA positive B cells in the bone marrow niche would be an interesting future direction that would address whether local changes in inflammatory environment select for pre-leukemic B cells.

Our survival data demonstrate that decreased levels of IL-10 contributed to the development of B cell leukemia/lymphomas (including both immature and mature neoplasms, Figure 3.5). This observation supports epidemiology studies that show an association between decreased IL-10 expression or signaling and the development of pediatric B-ALL[11] and DLBCL[12]. Rather than solely being a risk factor for childhood ALL, IL-10 deficiency was shown here to have an impact on leukemia/lymphoma development in a model of ALL. Our data supports that IL-10 deficiency indirectly disrupts B cell development, DNA damage, and proliferation through a monocyte-related inflammatory response. Whether monocytic inflammation is necessary to accelerate leukemia/lymphoma in *Il10*$^{-/-}$ mice is a question that requires further investigation. A future direction of particular interest is to delineate the impact of different inflammatory cell subsets on B cell DNA damage and disease in *Il10*$^{-/-}$ mice and neonates born with a predisposition for aberrant inflammatory responses. Given that SNPs that are associated with low IL-10 production are predictive of low overall survival and relapse[62,63], IL-10 therapy may be a suitable option for a subset of patients with aggressive disease. A PEGylated form of IL-10 (PEG-IL10) is currently in

phase 2 clinical trials for adult solid tumors and it may be beneficial to consider the possibility that high-risk pediatric B-ALL could be a new indication for this drug.

We had previously noted that our TA model developed both immature and mature B cell diseases in the presence of IL-10, but the most prevalent disease was B-ALL. Based on human data linking IL-10 deficiency to elevated ALL risk, we expected IL-10 loss in the TA *Cdkn2a*$^{-/-}$ model to increase the incidence of B-ALL. However, in the current study, the majority of *Il10*$^{-/-}$ TA *Cdkn2a*$^{-/-}$ mice developed myeloid hyperplasia due to inflammatory changes, including inflammatory bowel disease. The onset of these inflammatory changes occurred between 1-2 months of age, a timeframe that precedes leukemia/lymphoma development in the TA *Cdkn2a*$^{-/-}$ model. Similar numbers of mice were generated for each survival cohort therefore, the number of mice ultimately at risk for B cell disease was lower in *Il10*$^{-/-}$ TA *Cdkn2a*$^{-/-}$ mice than in controls. That being said, both immature and mature B cell disease were observed in all survival cohorts. It should be noted that a small subset of cases could not be diagnosed after histopathological review. Although the number of cases was too limited to reach as definitive conclusion, we observed a trend toward an increased proportion of mature B cell lymphomas and a decreased proportion of immature B cell leukemias in *Il10*$^{-/-}$ TA *Cdkn2a*$^{-/-}$ mice (Figure 3.5). The opposite was true for *Il10*$^{+/+}$ TA *Cdkn2a*$^{-/-}$ mice. Both pro-B cells and IgM+ immature B cells displayed increased DNA damage in in pre-leukemic *Il10*$^{-/-}$ *Cdkn2a*$^{-/-}$ mice relative to *Cdkn2a*$^{-/-}$ controls, suggesting the potential for immature or mature B cell disease to develop. However, the increase in DNA damage was greater in the IgM+ B cell population, which also had a proliferative advantage in *Il10*$^{-/-}$ *Cdkn2a*$^{-/-}$ mice. These factors could explain why IgM+ and Ig Kappa+ B cell lymphomas were more common in *Il10*$^{-/-}$ TA *Cdkn2a*$^{-/-}$ mice.

Differences between the pattern of IL-10 deficiency in the human and mouse studies could also explain a shift in the incidence of immature and mature B cell disease. In our mouse study, decreased IL-10 expression was achieved through a constitutive knockout of one or both alleles of the *Il10* gene. This resulted in decreased IL-10 expression throughout the lifetime of the mice,

as opposed to the decreased IL-10 expression that was detected at birth in the human cohort. We do not know whether low IL-10 levels were sustained in humans after birth; however genetic analysis of the IL-10 locus did not reveal any mutations that were associated with a prolonged decrease in IL-10 production (unpublished observation, Adam de Smith). In order to model a temporal decrease of IL-10 at birth, mice could be treated with an IL-10 blocking antibody or engineered to have a conditional knockout of *Il10*.

Another difference between the human and mouse studies was the number of genetic subtypes that were included in analysis. Multiple genetic subtypes of ALL developed in children born with low levels of IL-10, however only TA expressing mice were examined in the current study. Based on the data in Chang, et al., we did not expect decreased levels of IL-10 to coordinate with any particular initiating genetic lesion. However, there was a limited number of human ALLs with subtype data, which could have reduced the statistical power to detect an effect of a particular genetic lesion on ALL risk in the context of low IL-10 levels. A useful future direction would be to test whether low birth levels of IL-10 have the same impact on ALL risk for children born with different initiating genetic lesions.

3.4 FIGURES

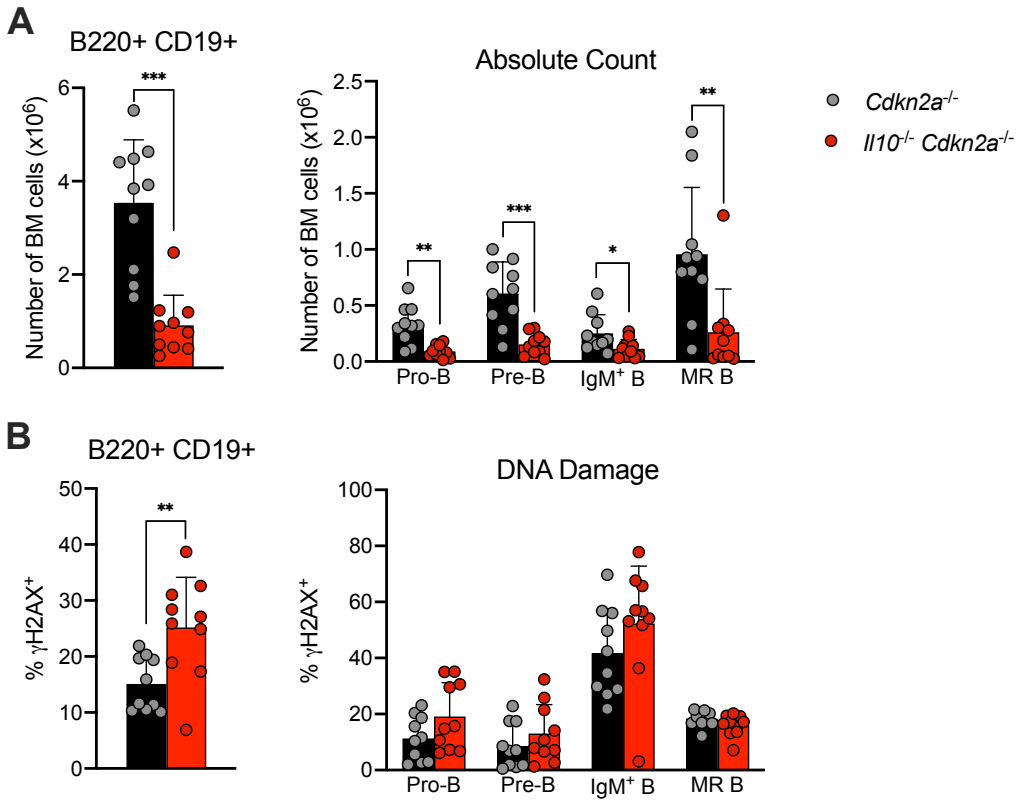

Figure 3.1. Bone marrow B cells in pre-leukemic *Il10*$^{-/-}$ *Cdkn2a*$^{-/-}$ mice are reduced and have elevated levels of DNA damage.

Analysis of 8-12 week-old *Cdkn2a*$^{-/-}$ and *Il10*$^{-/-}$ *Cdkn2a*$^{-/-}$ mice. Absolute bone marrow count of **(A)** Total B220+ CD19+ B cells and Bone marrow B cell subsets. Percent of H2AX+ cells among **(B)** Total bone marrow B cells and Bone marrow B cell subsets. Bar graph data show mean ± SD. Mann-Whitney *U*-test. *p ≤ 0.05, **p ≤ 0.01, ***p ≤ 0.001, ****p ≤ 0.001.

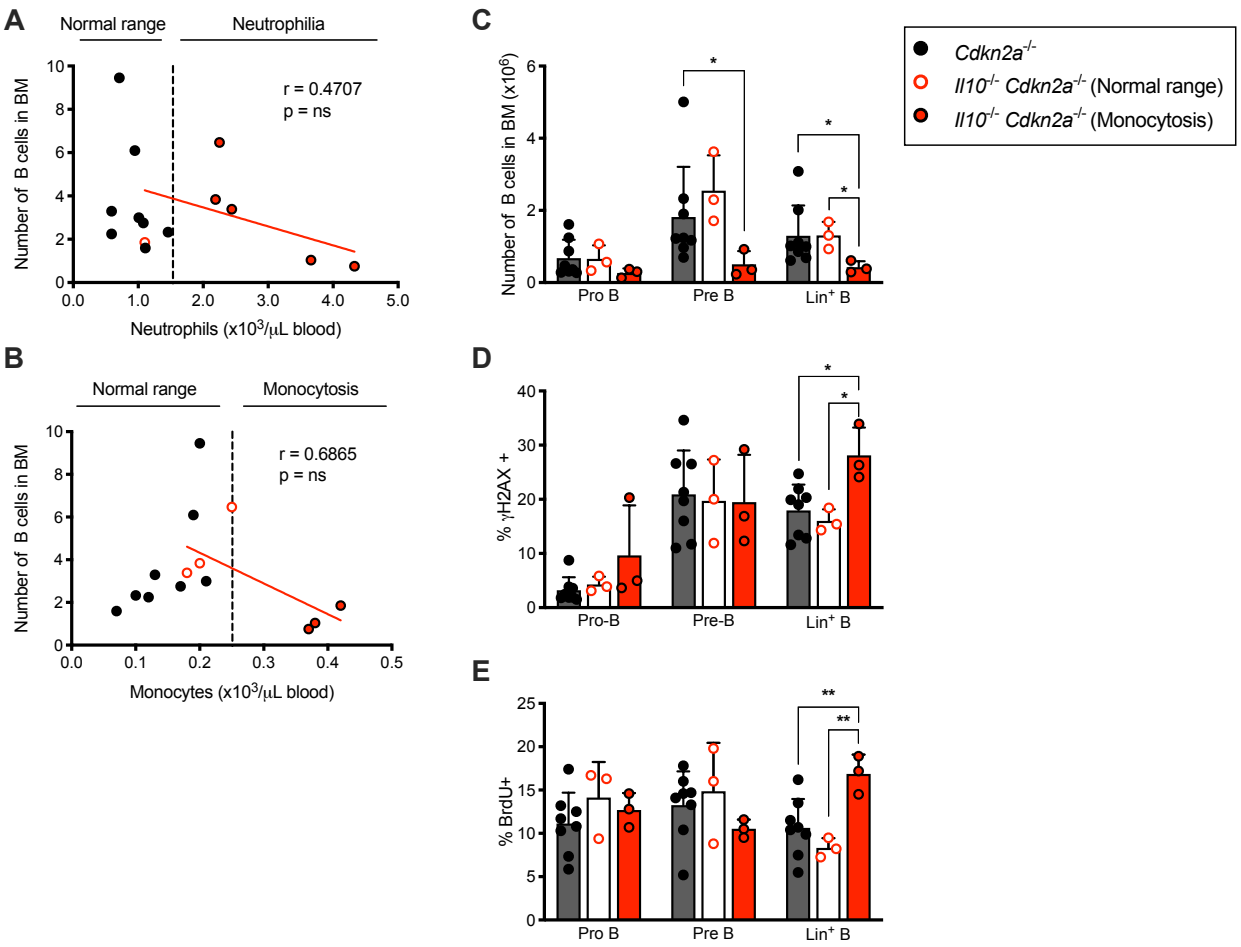

Figure 3.2. IL-10 is disposable for B cell homeostasis in the absence of elevated peripheral blood monocytes.

(A) Correlation between number of B cells in the bone marrow and peripheral blood count of neutrophils or **(B)** monocytes. Pearson correlation test excluding *Il10* wild-type *Cdkn2a*$^{-/-}$ mice. (**C**) Number, **(D)** percent γH2AX, and **(E)** percent BrdU of pro-B cells (B220^{+} CD19^{+} CD43^{+}), pre-B cells (B220^{+} CD19^{+} CD43^{-}), Lin^{+} B cells (B220^{+} CD19^{+} Lin^{+}) in the bone marrow. Lineage cocktail (IgM, TER119, NK1.1, CD3ε, TCRαβ, TCRλδ, Gr1, Ly6C) Bar graph data show mean ± SD. Mann-Whitney *U*-test. *p ≤ 0.05, **p ≤ 0.01.

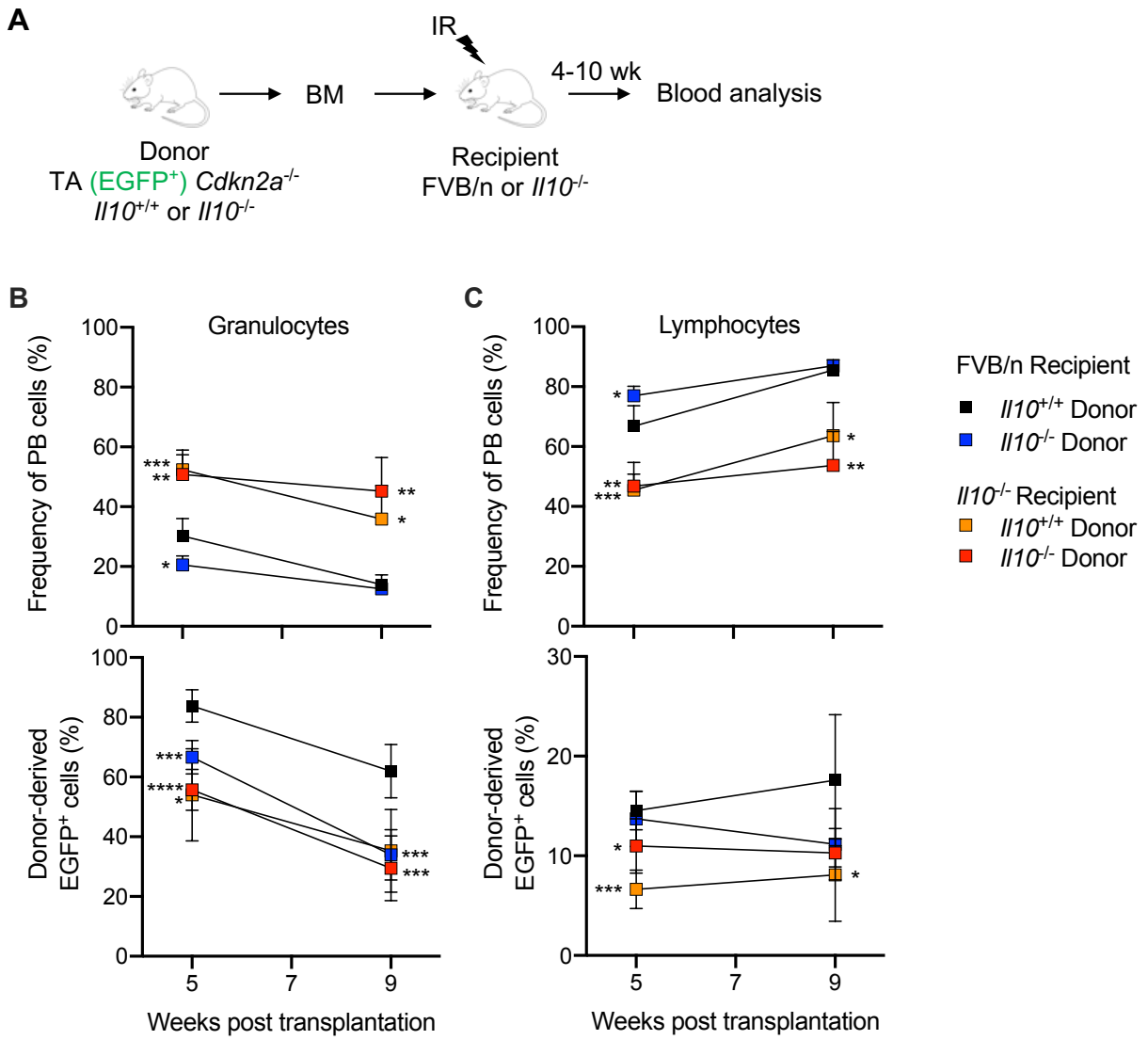

Figure 3.3. IL-10 loss in non-hematopoietic cells is necessary for induction of inflammatory response.

(A) Schematic diagram of bone marrow transplantation and tracking of peripheral blood cells in sublethally irradiated recipient mice (n=5 *Il10*$^{+/+}$ → *Il10*$^{+/+}$, n=4 *Il10*$^{-/-}$ → *Il10*$^{+/+}$, n=5 *Il10*$^{+/+}$ → *Il10*$^{-/-}$, n=5 *Il10*$^{-/-}$ → *Il10*$^{-/-}$). **(B)** Frequency of total and TA+(EGFP+) granulocytes and **(C)** lymphocytes at 5- and 9-weeks post-transplantation. Symbols and error bars show mean ± SD. Mann-Whitney *U*-test. *p ≤ 0.05, **p ≤ 0.01, ***p ≤ 0.001, ****p ≤ 0.001.

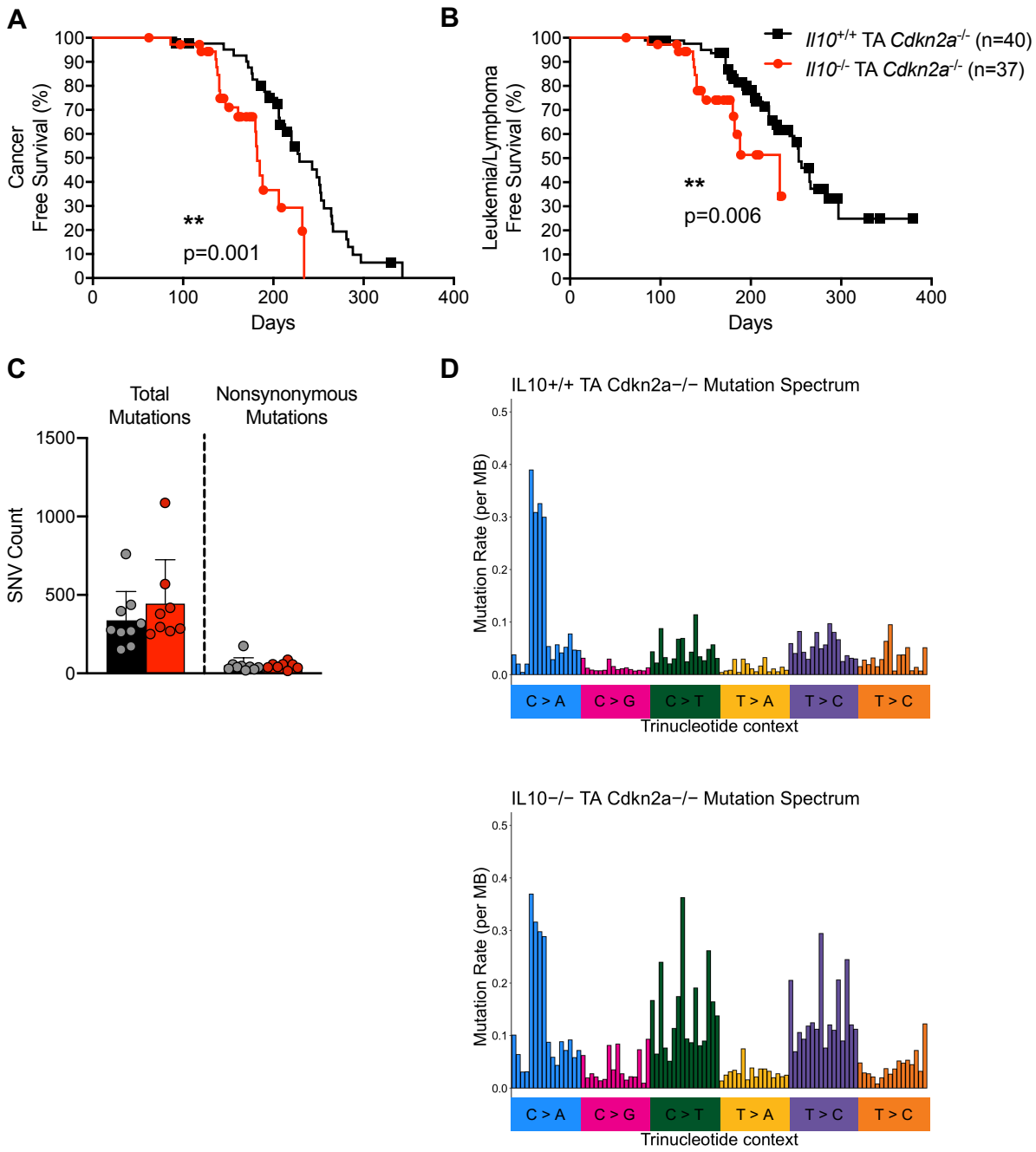

Figure 3.4. Decreased levels of IL-10 accelerate development of B-cell disease in TA *Cdkn2a*$^{-/-}$ model.

(A) Survival curves of cancer and **(B)** leukemia/lymphoma development in *Il10*$^{+/+}$ TA *Cdkn2a*$^{-/-}$ mice and *Il10*$^{-/-}$ TA *Cdkn2a*$^{-/-}$ mice. **(C)** Number of total or nonsynonymous single nucleotide variants (SNVs) in B cell leukemia/lymphomas from exome sequencing of 9 *Il10*$^{+/+}$ TA *Cdkn2a*$^{-/-}$ mice and 8 *Il10*$^{-/-}$ TA *Cdkn2a*$^{-/-}$ mice. **(D)** Mutation spectrum representing context of 96 possible trinucleotide contexts in sequenced *Il10*$^{+/+}$ TA *Cdkn2a*$^{-/-}$ and *Il10*$^{-/-}$ TA *Cdkn2a*$^{-/-}$ B cell leukemia/lymphomas. Gehan-Breslow-Wilcoxon test was applied to survival curves.

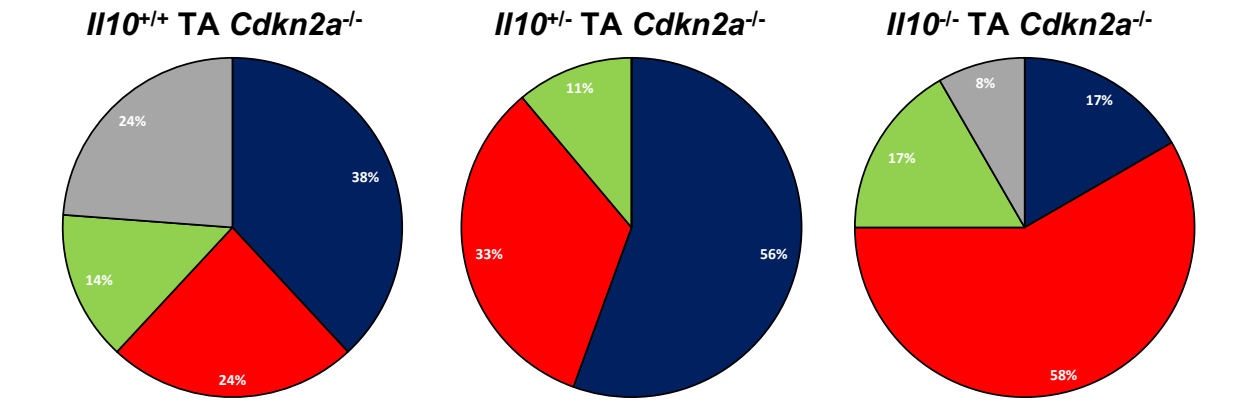

	Il10$^{+/+}$ TA *Cdkn2a*$^{-/-}$ (n=21)	*Il10*$^{+/-}$ TA *Cdkn2a*$^{-/-}$ (n=9)	*Il10*$^{-/-}$ TA *Cdkn2a*$^{-/-}$ (n=12)
	N (% total)		
Immature B cell	8 (38%)	5 (56%)	2 (17%)
Mature B cell	5 (24%)	3 (33%)	7 (58%)
Non-B cell	3 (14%)	1 (11%)	2 (17%)
Undetermined Lineage	5 (24%)	0 (0%)	1 (8%)

Figure 3.5. Lineage characterization of leukemia/lymphomas in survival cohorts of TA *Cdkn2a*$^{-/-}$ mice with wild-type, heterozygous, or null *Il10*.

Pie charts displaying the percent of leukemia/lymphomas characterized as Immature B cell leukemias, Mature B cell lymphomas, non-B cell leukemia/lymphoma, and undermined lineage. Table displays total number and percent of leukemia/lymphoma lineages belonging to each genotype.

3.5 TABLES

Table 3.1. Absolute plasma cytokine associations with immune phenotypes (pre-leukemic dataset)

Outcome	Module/Analyte	Coef	P-value	FWER	FDR
AbsPreBCount	IL-17A	-0.671343	4.82E-08	**9.25E-06**	7.88E-06
PBNeutsCount	IL-10	1.802837	8.21E-08	**1.57E-05**	7.88E-06
AbsBCount	MIP-1a	-1.281207	1.83E-07	**3.48E-05**	1.17E-05
AbsBCount	IL-6	-1.259533	5.67E-07	**0.000107**	2.41E-05
AbsBCount	IL-17A	-1.25749	6.27E-07	**0.000118**	2.41E-05
PBMonosCount	IL-10	0.147138	8.53E-07	**0.000159**	2.73E-05
AbsBCount	G-CSF	-1.224673	2.75E-06	**0.000511**	7.53E-05
BcellH2AX	IL-17A	0.060934	1.15E-05	**0.002133**	0.000257
AbsPreBCount	IL-6	-0.609466	1.3E-05	**0.002385**	0.000257
PBNeutsCount	MIP-1a	1.028502	1.34E-05	**0.002448**	0.000257
PBMonosCount	MIP-1a	0.086086	1.55E-05	**0.002814**	0.00027
AbsPreBCount	MIP-1a	-0.590058	4.34E-05	**0.007852**	0.000694
AbsPreBCount	G-CSF	-0.579227	7.9E-05	**0.014214**	0.001136
BcellH2AX	IL-6	0.057657	8.28E-05	**0.014825**	0.001136
PBMonosCount	RANTES	0.097701	9.71E-05	**0.017287**	0.001243
AbsMRCount	MIP-1a	-0.376393	0.000435	0.076952	0.005217
PBNeutsCount	IL-6	0.979095	0.000465	0.081815	0.00525
AbsBCount	IL-9	-1.03955	0.000589	0.103099	0.006284
PBNeutsCount	IL-17A	0.991938	0.000818	0.142266	0.008262
AbsMRCount	MCP-1	-0.362075	0.000965	0.166918	0.009263
BcellH2AX	G-CSF	0.05166	0.001111	0.191084	0.009835
PBNeutsCount	RANTES	1.062669	0.001127	0.192696	0.009835
AbsMRCount	G-CSF	-0.35737	0.001227	0.208593	0.010243
AbsBCount	MCP-1	-0.99844	0.001283	0.216799	0.010263
PBMonosCount	IL-6	0.078258	0.0014	0.235171	0.01064
PBNeutsCount	KC	0.882394	0.001441	0.240624	0.01064
AbsMRCount	IL-6	-0.353136	0.001511	0.250783	0.010743
AbsPreBCount	IL-9	-0.507366	0.001607	0.265225	0.010812
AbsBCount	IL12p40	-0.984529	0.001633	0.26783	0.010812
AbsBCount	TNF-a	-0.981647	0.001715	0.279492	0.010974

Continued on next page

Outcome	Module/Analyte	Coef	P-value	FWER	FDR
PBNeutsCount	IL-1a	1.545251	0.002447	0.396453	0.015157
AbsBCount	IL-12p70	-0.956596	0.002575	0.414505	0.015447
AbsBCount	IFN-gamma	-0.945676	0.003046	0.487297	0.01772
AbsBCount	RANTES	-0.940866	0.003274	0.520582	0.018489
AbsBCount	IL1b	-0.919147	0.004485	0.708586	0.02397
PBNeutsCount	Eotaxin	0.858479	0.004494	0.708586	0.02397
PBMonosCount	G-CSF	0.069702	0.004855	0.757417	0.025195
PBMonosCount	IL-17A	0.07508	0.005108	0.791767	0.025286
AbsMRCount	IFN-gamma	-0.324673	0.005136	0.791767	0.025286
PBMonosCount	MIP-1B	0.079624	0.005453	0.834247	0.025648
PBMonosCount	KC	0.068183	0.005571	0.84678	0.025648
PBNeutsCount	G-CSF	0.821619	0.00561	0.847176	0.025648
AbsPreBCount	RANTES	-0.461297	0.006147	0.922055	0.027447
PBMonosCount	MIG	0.066348	0.00659	0.98188	0.028262
AbsPreBCount	IL12p40	-0.458007	0.006682	0.989004	0.028262
AbsPreBCount	TNF-a	-0.457483	0.006771	0.995345	0.028262
BcellH2AX	IL-1a	0.045507	0.006947	1	0.02838
AbsMRCount	IL12p40	-0.315852	0.007121	1	0.028483
PBNeutsCount	MIP-1B	0.923548	0.007692	1	0.030138
AbsPreBCount	IL-1a	-0.438829	0.010582	1	0.040633
BcellH2AX	IL-9	0.043202	0.011973	1	0.045076
AbsMRCount	IL-9	-0.295558	0.013991	1	0.051374
AbsMRCount	IL-12p70	-0.29512	0.014181	1	0.051374
AbsPreBCount	IL1b	-0.42468	0.014453	1	0.05139
PBMonosCount	IL-18	0.069569	0.016001	1	0.05503
AbsBCount	IL-1a	-0.815176	0.016051	1	0.05503
AbsPreBCount	MCP-1	-0.417554	0.016777	1	0.056511
AbsMRCount	IL-17A	-0.287729	0.017707	1	0.058616
AbsPreBCount	IFN-gamma	-0.411488	0.018971	1	0.061736
PBMonosCount	IL-1a	0.108553	0.021268	1	0.068056

Continued on next page

Outcome	Module/Analyte	Coef	P-value	FWER	FDR
PBNeutsCount	MCP-1	0.680833	0.022925	1	0.072157
AbsMRCount	MIP-1B	-0.277399	0.023713	1	0.073433
AbsMRCount	TNF-a	-0.276484	0.02431	1	0.074088
PBNeutsCount	MIG	0.685101	0.027471	1	0.082413
PBMonosCount	IL12p40	0.060765	0.028785	1	0.085027
AbsMRCount	IL1b	-0.267095	0.031121	1	0.090534
PBNeutsCount	IL-12p70	0.808751	0.032375	1	0.092775
AbsPreBCount	IL-12p70	-0.378063	0.035211	1	0.098005
AbsBCount	MIP-1B	-0.734283	0.035221	1	0.098005
PBMonosCount	MCP-1	0.053758	0.036447	1	0.099969
PBNeutsCount	IL-18	0.738662	0.039875	1	0.10783
PBNeutsCount	GM-CSF	0.624582	0.041866	1	0.111642
PBNeutsCount	IFN-gamma	0.639359	0.043425	1	0.114214
AbsPreBCount	IL-3	-0.36259	0.045492	1	0.118033
PBNeutsCount	IL1b	0.639253	0.046253	1	0.118407

Table 3.2. Adjusted plasma cytokine associations with immune phenotypes (pre-leukemic dataset)

Outcome	Module/Analyte	Coef	P-value	FWER	FDR
BcellH2AX	IL-17A	0.047908	0.003658	0.702388	0.332997
AbsPreBCount	IL-17A	-0.47513	0.004256	0.812966	0.332997
AbsMRCount	Basic FGF	0.323874	0.005295	1	0.332997
BcellH2AX	IL-6	0.045513	0.006937	1	0.332997
AbsBCount	MIP-1a	-0.793214	0.020174	1	0.616739
AbsMRCount	LIF	0.281834	0.02097	1	0.616739
BcellH2AX	IL-4	-0.040005	0.023154	1	0.616739
AbsBCount	IL-6	-0.752354	0.029931	1	0.616739
PBMonosCoun	IL-10	0.098114	0.031705	1	0.616739
AbsPreBCount	IL-6	-0.381448	0.033213	1	0.616739
AbsBCount	IL-17A	-0.733918	0.035334	1	0.616739
PBMonosCoun	IL-13	-0.056372	0.039132	1	0.617357
AbsBCount	Basic FGF	0.711039	0.043003	1	0.617357
PBNeutsCount	IL-10	1.105219	0.046111	1	0.617357

Table 3.3. Disease outcomes in *Il10*$^{+/+}$, *Il10*$^{+/-}$, and *Il10*$^{-/-}$ mice on the TA *Ckdn2a*$^{-/-}$ background

	TA *Cdkn2a* $^{-/-}$ (n=40)	*Il10* $^{+/-}$ TA *Cdkn2a* $^{-/-}$ (n=31)	*Il10* $^{-/-}$ TA *Cdkn2a* $^{-/-}$ (n=37)
	N (% total)		
Cancer	30 (75%)	21 (68%)	17 (46%)
Leukemia/Lymphoma	21 (53%)	9 (29%)	12 (32%)
Solid tumor	11 (28%)	13 (42%)	6 (16%)
Not Cancer	10 (25%)	10 (32%)	20 (54%)
Unknown	6 (15%)	4 (13%)	1 (3%)
Myeloid hyperplasia or Inflammation	0 (0%)	2 (6%)	18 (49%)
Tissue Unavailable	4 (10%)	4 (13%)	1 (3%)

Table 3.4. Median cancer latency of *Il10*$^{+/+}$, *Il10*$^{+/-}$, and *Il10*$^{-/-}$ mice on the TA *Ckdn2a*$^{-/-}$ background

	Il10 $^{+/+}$ **TA *Cdkn2a*** $^{-/-}$ **(n=40)**	***Il10*** $^{+/-}$ **TA *Cdkn2a*** $^{-/-}$ **(n=31)**	***Il10*** $^{-/-}$ **TA *Cdkn2a*** $^{-/-}$ **(n=37)**
	Median latency (days)		
Cancer	229	203	182
Leukemia/Lymphoma	253	Undefined	232
Solid tumor	281	275	234

Table 3.5. List of COSMIC database genes with SNVs from whole-exome sequencing of B cell leukemia/lymphomas from *Il10*$^{+/+}$ TA *Ckdkn2a*$^{-/-}$ and *Il10*$^{-/-}$ TA *Ckdkn2a*$^{-/-}$

Gene	Total SNV count	*Il10* $^{+/+}$ TA *Ckdn2a* $^{-/-}$	*Il10* $^{-/-}$ TA *Ckdn2a* $^{-/-}$
Hoxa9	7	2	5
Jak3	3	2	1
Cdkn1a	3	3	0
Dnm2	3	3	0
Trrap	2	1	1
Alk	2	2	0
Ptpn11	2	2	0
Cblb	1	0	1
Cdh10	1	0	1
Ciita	1	0	1
Ddx10	1	0	1
Erc1	1	0	1
Isx	1	0	1
Jak2	1	0	1
Kmt2d	1	0	1
Maml2	1	0	1
Mllt3	1	0	1
Myh11	1	0	1
Ncor2	1	0	1
Pbx1	1	0	1
Polg	1	0	1
Sep9	1	0	1
Setd2	1	0	1
Six2	1	0	1
Xpo1	1	0	1
Aff4	1	1	0
Aspscr1	1	1	0
Atr	1	1	0
Bcl11b	1	1	0
Btk	1	1	0
Cbl	1	1	0
Chic2	1	1	0
Cic	1	1	0
Csmd3	1	1	0
Ctnna2	1	1	0

Gene	Total SNV count	*Il10* $^{+/+}$ TA *Ckdn2a* $^{-/-}$	*Il10* $^{-/-}$ TA *Ckdn2a* $^{-/-}$
Ddr2	1	1	0
Ddx3x	1	1	0
Epha7	1	1	0
Erbb2	1	1	0
Flna	1	1	0
Flt4	1	1	0
Ikbkb	1	1	0
Il7r	1	1	0
Kit	1	1	0
Lats2	1	1	0
Met	1	1	0
Mn1	1	1	0
Msh6	1	1	0
Nf1	1	1	0
Pax3	1	1	0
Pax5	1	1	0
Pax7	1	1	0
Phf6	1	1	0
Pten	1	1	0
Rap1gds1	1	1	0
Runx1t1	1	1	0
Stat5b	1	1	0
Tbx3	1	1	0
Ubr5	1	1	0
Ywhae	1	1	0
Zfhx3	1	1	0

CHAPTER 4: ALTERING THE INFLAMMATORY MILIEU INFLUENCES B CELL DNA DAMAGE AND THE DEVELOPMENT OF B CELL NEOPLASMS

4.1 INTRODUCTION

Pro-inflammatory cytokines are major regulators of blood cell function that can contribute to the development of hematopoietic malignancies[78]. ALL risk is associated with IL-10 deficiency[11] and high levels of IL-6, IL-17, and IL-18 at birth[66]. After the development of disease, elevated levels of TNFα, IL-1β, IL-12, and GM-CSF distinguish the cytokine profile of bone marrow supernatant of pediatric ALL patients from healthy donors[1]. The inflammatory state in neonates predisposed to ALL and children with ALL has similar features as innate immune responses mediated through myeloid cell activation. Although myeloid cells are conventionally the main population that is activated and mobilized in innate immune response, genetic lesions can allow provide B cells with the capacity to respond favorably to pro-inflammatory cytokines. Under particular inflammatory conditions, TEL-AML1 expression in B cell progenitors can induce co-expression of myeloid cell genes[79], confer a competitive advantage over normal cells[22,23,79], and increase reactive species-induced DNA damage[80]. Pro-inflammatory cytokines therefore have the potential to regulate the transformation of specific B cell clones during the development of disease. The mechanism by which pro-inflammatory cytokine production becomes dysregulated and contributes to childhood leukemia is largely unknown.

In *Il10*$^{-/-}$ mice, the increased presence of H. pylori contributes to myeloid cell expansion and dysregulation of splenic B cell differentiation[24]. Microbial species can also play a role in B cell mutagenesis and have been proposed to impact ALL risk. Within the lamina propria, VDJ recombination and receptor editing of pro-B and pre-B cells are stimulated by microbial signals in the gut[81]. The impact of gut microbes on B cell progenitors that reside in more distal sites of lymphoid development, such as the bone marrow, is less well understood. Others have demonstrated that microbial signals can indirectly induce hematopoietic progenitor expansion by

stimulating myeloid cell production of IL-1β, IL-6, and TNF-α[82]. We were particularly interested in addressing whether microbial signals in *Il10*$^{-/-}$ mice may increase the level of DNA damage in B cell progenitors in the bone marrow. Based on our observation that DNA damage in bone marrow B cells was associated with an IBD related cytokine signature in *Il10*$^{-/-}$ mice, we hypothesized that increased B cell DNA damage in *Il10*$^{-/-}$ mice was mediated through the gut microbiome. We aimed to address this question by using antibiotics to alter the gut microbiome of *Il10*$^{-/-}$ mice. Longitudinal analysis of the infection history within our SPF animal facility provided additional insight into how parasite-microbe interactions may influence the development of disease in mouse models of childhood leukemia.

4.2 RESULTS

4.2.i Antibiotic-mediated suppression of the inflammatory milieu promotes recovery of B cell development and diminishes B cell DNA damage

Others have found that the colonization of the gut with specific bacterial species is required for myeloid and B cell expansion in *Il10*$^{-/-}$ mice. Notably, treatment of *Il10*$^{-/-}$ mice with antibiotics that target helicobacter species limits the expansion of myeloid and marginal zone B cells[24]. Given the strong association between the cytokines that are elevated in *Il10*$^{-/-}$ mice on the FVB/n background and IBD, we reasoned that microbial dysbiosis may be an underlying cause of inflammation, bone marrow B cell deficiency, and elevated B cell DNA damage.

Given the probability that the microbial milieu was contributing to B cell DNA damage in *Il10*$^{-/-}$ mice, we investigated the effect of antibiotics on inflammation and B cell properties in pre-leukemic mice. To this end, we administered a 4-week regimen of antibiotics that target Helicobacter species or a placebo treatment to *Cdkn2a*$^{-/-}$ or *Il10*$^{-/-}$ *Cdkn2a*$^{-/-}$ mice (**Figure 4.1A**). Cytokine concentration in the peripheral blood was monitored before and after treatment by using a multiplex Luminex assay. Strikingly, antibiotic treatment reduced the concentration of several

cytokines that were associated with B cell deficiency and B cell DNA damage in *Il10*$^{-/-}$ *Cdkn2a*$^{-/-}$ mice including G-CSF, IL-6, and IL-17 (**Figure 4.1B**). This effect was also observed in antibiotic-treated *Cdkn2a*$^{-/-}$ mice with wild-type IL-10, which had statistically significant decreases in G-CSF and IL-6 relative to placebo-treated controls. We next assessed the impact of antibiotics on the frequency of immune cells and the extent of DNA damage in B cells residing in the bone marrow. As expected, IL-10 loss in placebo-treated mice resulted in an increased frequency of peripheral blood CD11b^{+} myeloid cells (data not shown). The expansion of myeloid cells within the bone marrow compartment of *Il10*$^{-/-}$ *Cdkn2a*$^{-/-}$ mice was attenuated by antibiotics (**Figure 4.1C**). Antibiotic treatment also partially abrogated the decrease in B cell number (**Figure 4.1D**) and remarkably reversed the increased B cell DNA damage (**Figure 4.1E**) that was observed in placebo-treated *Il10*$^{-/-}$ *Cdkn2a*$^{-/-}$ mice. These results are consistent with the hypothesis that microbial dysbiosis disrupts B cell development and contributes to B cell DNA damage in pre-leukemic *Il10*$^{-/-}$ mice.

4.2.ii Pinworm outbreak supports a role of Th2 immunity in B-ALL

Given that, in the context of decreased IL-10 levels, antibiotics achieved a partial restoration of B cell numbers and reduced B cell DNA damage, it follows that modifications to the commensal gut microbiome that suppress aberrant inflammation may protect against leukemia. Although infectious exposures are sufficient for B-ALL induction in Sca-1 *ETV6-RUNX1* mice[9], it has yet to be determined whether resolving infections in *ETV6-RUNX1* positive mice can protect against B-ALL. Over the course of several years, we noted a shift in the latency of leukemia/lymphoma in TA *Cdkn2a*$^{-/-}$ mice as compared with *Cdkn2a*$^{-/-}$ mice that lacked TA. Although these mice were continuously housed within the same room of our SPF facility, we were aware that pathogens were identified from time to time in our facility, and we hypothesized such a variation in milieu might explain our observation of a change in disease latency. Our approach to address this hypothesis was to compare our survival analyses of leukemia/lymphoma incidence

and latency in TA *Cdkn2a*$^{-/-}$ and *Cdkn2a*$^{-/-}$ mice housed in our SPF facility from 2009-2017, along with review of sentinel mouse infection records.

In separate experiments conducted in the 2009-2017 timeframe, we followed the survival of TA *Cdkn2a*$^{-/-}$ and *Cdkn2a*$^{-/-}$ mice in our SPF facility (**Figure 4.2A**). From 2009-2011, we noted differences in disease development between these two strains. Specifically, TA *Cdkn2a*$^{-/-}$ mice had an increased incidence and decreased latency of leukemia/lymphoma in comparison to *Cdkn2a*$^{-/-}$ mice (**Figure 4.2B**). Our interpretation of this result was that TA coordinated with *Cdkn2a* deletion to generate lymphoid leukemia/lymphoma. To our surprise, from 2015-2017, TA appeared to no longer impact the latency of B-ALL in the *Cdkn2a*$^{-/-}$ model, as demonstrated by two independent experiments showing overlap (**Figure 4.2C**) or minimal separation (**Figure 4.2D**) between the TA *Cdkn2a*$^{-/-}$ and *Cdkn2a*$^{-/-}$ survival curves. Work from other investigators suggested that in some settings TA requires the presence of infectious exposures to initiate ALL in mice[9]. We therefore suspected that the effect of TA on driving leukemia/lymphoma during 2009-2011 might be explained by a pathogen in our SPF facility that was eliminated by 2015, when the effect of TA was no longer observed. Review of sentinel health records spanning 2009-2017 revealed that in 2013 the pinworm *Aspiculuris* was detected by fecal float, leading to the treatment of all cages in the room with Fenbendazole (**Figure 4.2A**). Given the low sensitivity of the fecal float test relative to PCR, it is possible that pinworm infection was widespread within the room and present in non-sentinel cages from 2009-2011. These data suggest that pinworm infection was an important factor in the effect of TA on the acceleration of leukemia/lymphoma development in *Cdkn2a*$^{-/-}$ mice.

To determine whether intentional pinworm infection could restore the leukemogenic effect of TA in the *Cdkn2a*$^{-/-}$ model, we exposed mice to pinworm shortly after weaning (**Figure 4.2A**). This was accomplished by transferring 4-week-old *Cdkn2a*$^{-/-}$ and TA *Cdkn2a*$^{-/-}$ mice from our fenbendazole-treated SPF facility to a conventional facility where they were housed with bedding from pinworm-infected mice. This experiment confirmed that, in the context of pinworm infection,

TA *Cdkn2a*$^{-/-}$ mice develop leukemia/lymphoma earlier and with a higher incidence than *Cdkn2a*$^{-/-}$ mice (**Figure 4.2E**). Our observations were consistent with the hypothesis that treatment of infections can protect against leukemia/lymphoma by limiting the coordination between TA and infectious stimuli.

Further, we assessed whether the effect of pinworm could be attributed to enhanced leukemia development in TA *Cdkn2a*$^{-/-}$ mice or suppressed leukemia development in *Cdkn2a*$^{-/-}$ mice. Mice infected with pinworm have increased activation of B cells and Tregs that mediate Th2-directed suppression of Th1 and Th17 immune responses[83]. It is therefore feasible for pinworm infection to drive lymphoma development through B cell stimulation or to protect against cancer by suppressing chronic inflammation. A limited number of studies have demonstrated that CpG, a TLR9 agonist, can suppress the development of B-ALL in mice[64,84,85]. However, no studies to date have reported whether pinworm or other infectious stimuli can have a similar protective effect in B-ALL. Several studies, on the other hand, support the predominate theory that TA coordinates with infectious exposures to drive leukemogenesis, therefore we suspected that pinworm exposed TA *Cdkn2a*$^{-/-}$ mice might have had an increased incidence and decreased latency of leukemia/lymphoma development relative to pinworm-free mice in our fenbendazole-treated SPF facility.

Our intentional pinworm-exposure experiment did not include SPF-facility control mice, therefore we used historical data to compare the development of leukemia/lymphoma in pinworm infected vs. SPF conditions. Specifically, we combined data from the cohorts of pinworm-exposed TA *Cdkn2a*$^{-/-}$ and *Cdkn2a*$^{-/-}$ mice from 2018-2019 (**Figure 4.2E**) with the cohorts of genotype-matched mice housed in our SPF facility during the pinworm outbreak (**Figure 4.2B**). We also combined the datasets of TA *Cdkn2a*$^{-/-}$ and *Cdkn2a*$^{-/-}$ mice from independent experiments of post-Fenbendazole survival studies conducted in the pinworm-eradicated SPF facility from 2015-2017 (**Figures 4.2C and D**). Cancer and leukemia/lymphoma development were analyzed in the combined datasets. As expected, pinworm exposure caused TA *Cdkn2a*$^{-/-}$ mice to develop cancer

faster than SPF-housed TA *Cdkn2a*$^{-/-}$ mice (Gehan-Breslow-Wilcoxon p=0.013, **Figure 4.3A and Table 4.2**) and increased cancer incidence from 76% to 93% (Chi-square p=0.01, **Table 4.1**). The median latency to cancer was 202 days in pinworm exposed TA *Cdkn2a*$^{-/-}$ mice and 248 days in SPF-housed TA *Cdkn2a*$^{-/-}$ mice. In regards to *Cdkn2a*$^{-/-}$ mice, pinworm exposure had the opposite effect of slowing cancer development (median cancer free survival for pinworm *Cdkn2a*$^{-/-}$ vs SPF *Cdkn2a*$^{-/-}$ 259 vs 218 days, Gehan-Breslow-Wilcoxon p=0.033, **Figure 4.3B**). When all 4 curves were overlaid, the most apparent difference was observed between pinworm exposed TA *Cdkn2a*$^{-/-}$ and *Cdkn2a*$^{-/-}$ mice. Of note, although we observed changes in time to disease, there was no observed impact of pinworm on cancer *incidence* in *Cdkn2a*$^{-/-}$ mice, whether or not they expressed TA. These results identified pinworm as a specific infectious exposure that may have a dual capacity for protecting against or promoting cancer depending on the presence or absence of TA.

We then aimed to determine whether pinworm exposure had a similar bi-directional effect specifically on leukemia/lymphoma development in TA *Cdkn2a*$^{-/-}$ and *Cdkn2a*$^{-/-}$ mice. Contrary to our expectation, pinworm exposure did not impact the *incidence* of leukemia/lymphoma in TA *Cdkn2a*$^{-/-}$ mice. In fact, the 52% incidence of leukemia/lymphoma in pinworm-exposed TA *Cdkn2a*$^{-/-}$ mice was strikingly similar to the 51% incidence in pinworm-free SPF TA *Cdkn2a*$^{-/-}$ mice (**Table 4.1**). Survival curves provided further support for the lack of a leukemogenic effect of pinworm in TA *Cdkn2a*$^{-/-}$ mice (**Figure 4.3D**). The pinworm-exposed *Cdkn2a*$^{-/-}$ curve was shifted slightly to the right of the SPF *Cdkn2a*$^{-/-}$ cohort (**Figure 4.3E**). The median survival for pinworm-exposed *Cdkn2a*$^{-/-}$ mice increased to 365 days from the 305 day median survival for SPF-housed *Cdkn2a*$^{-/-}$ mice (**Table 4.2**), but this difference did not reach statistical significance. Although pinworm exposure only yielded a modest impact on leukemia/lymphoma development in TA *Cdkn2a*$^{-/-}$ and *Cdkn2a*$^{-/-}$ mice, the cumulative bi-directional effect of pinworm resulted in a significant difference between these two mouse strains that was not observed under SPF

conditions (**Figure 4.3F**). Overall our results suggest that, in the absence of TA, pinworm slows the development leukemia/lymphoma.

4.3 DISCUSSION

Our data demonstrate that low IL-10 levels indirectly promote the production of myeloid-associated pro-inflammatory cytokines and drive bone marrow B cell DNA damage by perpetuating a state of microbial dysbiosis. These results provide additional support for the hypothesis that early disruptions in microbiome development can increase the risk of ALL by predisposing children to aberrant responses to infection. Events that restrict early microbial exposures in newborns, such as elective cesarean birth and limited breastfeeding, are associated with an increased risk of childhood ALL[86–88]. In contrast, IL-10 deficiency, also associated with increased ALL risk, is known to elevate levels of particular bacterial species in the intestine[89,90]. It is possible that these seemingly divergent effects might in fact both increase ALL risk by disrupting the normal composition of the intestinal microbiome. As microbial composition can influence the type and severity of childhood infections[91,92], a valuable future direction would be to delineate which microbial communities may be associated with childhood leukemia by sequencing bacteria in fecal samples from human neonates or pre-leukemic mice. Moreover, prenatal and postnatal antibiotic treatment can drastically impact the infant microbiome[93]. Therefore, analysis of maternal and childhood antibiotic treatment records could provide key insight into the relationship between microbial dysbiosis and ALL risk.

Upregulation of TLR signaling is a key pathway by which microbial dysbiosis promotes lymphoid malignancies. *H. pylori*-derived LPS promotes gastric tumors and Mucosa-associated lymphoid tissue (MALT) lymphomas by stimulating proliferation and AID-associated mutagenesis of gastric epithelial cells and mature B cells. Given that TLR4 signaling can be negatively regulated by IL-10[94], it is possible that the loss of IL-10 may serve as an indirect source of TLR4 activation that contributes to B-ALL initiation in mice. Evidence from prior

animal studies on B-ALL pathogenesis suggests that TLR4 stimulation may require additional environmental cues in order to transform immature B cells[95–97]. Decreased IL-7 signaling is an example of one possible environmental cue that could play a critical role in the infectious etiology of B-ALL. Others have reported that IL-7 withdrawal, when combined with LPS stimulation, can trigger the concurrent activation of RAG and AID enzymes, leading to *in vitro* mutagenesis of TA B cells and *in vivo* initiation B-ALL in mice[8]. Additionally, IL-10 loss results in drastic upregulation of G-CSF, a potent inhibitor of stromal cell-derived IL-7. Based on these findings, it is interesting to consider that IL-10 deficiency may promote the development of pediatric B-ALL by influencing multiple B cell pathways, including those that involve TLR4 and IL-7 signaling.

Others have shown that TLRs can suppress the growth of pre-leukemic B cells and delay leukemogenesis[64]. Notably, studies showing a protective role of TLR agonists in B-ALL were conducted in the absence of chronic inflammation. Furthermore, IL-10 is a major downstream target of several TLRs[98–102]. Therefore, it is likely that TLRs play a dual role, either protective or pathogenic, in B-ALL development depending on the presence of coordinating environmental cues. An interesting future direction would be to dissect how TLR ligands in the presence and absence of inflammation impact mutagenesis and survival signaling pathways in immature B cells.

Our results also demonstrate that pinworm exposure slightly delays the development of leukemia/lymphoma in *Cdkn2a*$^{-/-}$ mice. Pinworm-microbiome interactions can be effective in driving the production of IL-10 and other Th2 cytokines[103,104]. Therefore, interventions that elicit similar Th2 or immunosuppressive responses may benefit children born with a high risk of developing B-ALL. Notably, the incidence of leukemia/lymphoma was not decreased by pinworm, which was unexpected considering the historical context of increased B-ALL incidence in the developed world[105–107]. This may reflect a different window of disease susceptibility between our mouse model and humans. Several reports have described a peak in the incidence

of childhood ALL between the ages of two and five[108]. This finding led to the idea that children are most vulnerable to ALL during a window of susceptibility that ranges from *in utero* development to the early years of life. Although the molecular characteristics of B-ALL in *Cdkn2a*$^{-/-}$ mice closely resemble that of human B-ALL, the timing of B-ALL onset coincides with murine adulthood and does not reflect an early-life window of susceptibility[23,109]. For this reason, pinworm exposure may have different protective outcomes in humans and mice depending on the timing of mutagenic events relative to the window of susceptibility. In regard to our survival study, it is possible that pinworm shifts the timing of mutagenic events so that they are delayed, but still able to occur within the window of susceptibility. This could explain why pinworm exposure increased the latency of leukemia/lymphoma in *Cdkn2a*$^{-/-}$ mice, without decreasing its incidence. If the window of susceptibility to ALL is more restricted in humans than in *Cdkn2a*$^{-/-}$ mice, it is possible that a pinworm-induced mutagenic delay in humans may cause the window of susceptibility to be completely missed, thereby decreasing the risk of ALL. Future analysis in humans, and in refined mouse models of B-ALL that more closely match the timing of human disease, will be required to delineate how the timing and type of early childhood parasite-microbiota interactions may influence ALL incidence.

The mutational status of pre-leukemic cells may also influence the effect of pinworm exposure on leukemia/lymphoma development. Interestingly, the protective effect of pinworm on suppressing leukemia/lymphoma in *Cdkn2a*$^{-/-}$ mice did not apply to TA positive *Cdkn2a*$^{-/-}$ mice, suggesting that TA blocks pinworm-mediated protection. This may reflect the previously described ability of TA to increase the responsiveness of pre-leukemic B cells to environmental exposures[8,9,23,110], thereby lowering the threshold for an inflammatory response to promote B-ALL. Despite the influence of pinworm infection on the acquisition of normal gut microbiota and Th2 immunity, hosts are still susceptible to infection and inflammation from other sources[111]. It is possible that normal levels of immune stimulation in the context of infection may be sufficient to elicit a proliferative or mutagenic response in TA+ B cell clones. Alternatively,

pre-leukemic TA+ B cells may be resistant to pinworm-mediated immunosuppression. It is well established that TA can coordinate with radiation, chemicals, and infectious exposures to drive lymphoid malignancies[8,9,23,110], however the potential for TA, or another initiating lesion, to interfere with protective exposures has not been fully explored. Thus, future studies are warranted to investigate the antagonistic effect of TA expression on pinworm-mediated protection in leukemia/lymphoma. Treatments that simulate the downstream effects of pinworm exposure on microbe-immune cell interactions may be an ideal intervention for neonates with a high-risk of developing ALL. Collectively, our data demonstrate that the Th2 immune response could be a suppressor of leukemia/lymphoma development. In the absence of IL-10, a key regulator of Th2 immunity, microbial dysbiosis may trigger an innate immune response that is associated with B cell DNA damage and leukemogenesis. Conversely, exposing TA negative mice to pinworm, a well-established stimulator of Th2 immunity, protects against leukemia/lymphoma. Fostering the development of Th2 immunity, particularly in children born with low IL-10 levels, may be an important approach in the prevention and treatment of childhood ALL.

4.4 FIGURES

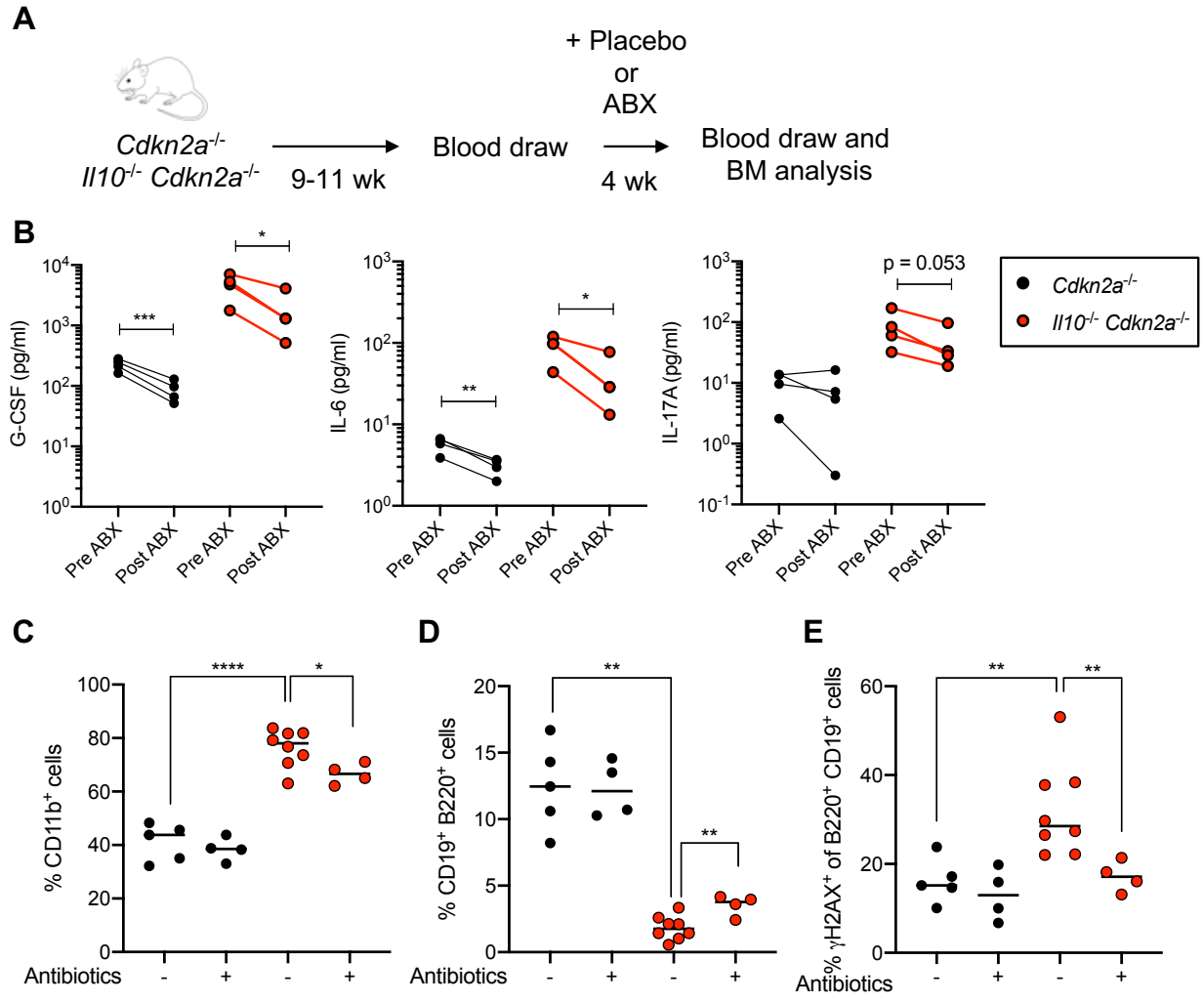

Figure 4.1. Antibiotic treatment response rescues *Il10*$^{-/-}$ *Ckdn2a*$^{-/-}$ B cells from impaired development and DNA damage.

(A) Schematic diagram of antibiotic treatment and tracking of peripheral blood and bone marrow cells in adult mice. **(B)** Concentration of cytokines in *Il10*$^{-/-}$ *Cdkn2a*$^{-/-}$ mice and controls. Lines connect values from the same mouse sampled before and after antibiotic treatment (ABX). Two-tailed paired *t*-test. **(C)** Flow analysis of percent CD11b^{+} cells and CD19^{+} B220^{+} cells of bone marrow, and percent γH2AX^{+} of CD19+ B220+ cells in *Cdkn2a*$^{-/-}$ and *Il10*$^{-/-}$ *Cdkn2a*$^{-/-}$ mice treatment with placebo (-) or antibiotics (+) for 4 weeks. Bar shows mean, Mann-Whitney *U*-test. *p ≤ 0.05, **p ≤ 0.01.

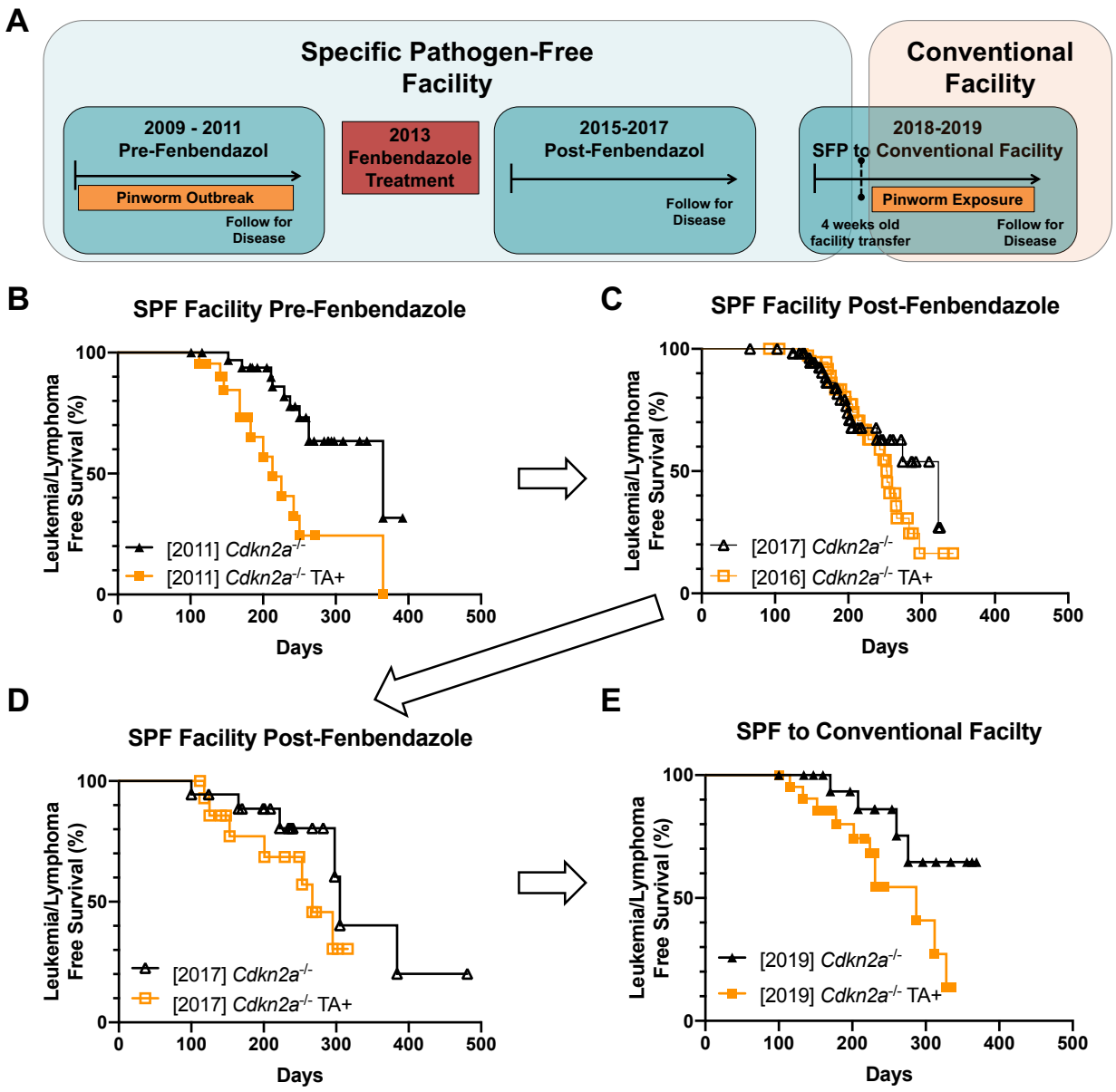

Figure 4.2. TA Cdkn2a-/- and Cdkn2a-/- differ in leukemia/lymphoma development in the presence of pinworm.

(A) Timeline of individual survival studies following *Cdkn2a*$^{-/-}$ and TA *Ckdn2a*$^{-/-}$ mice in SPF and Conventional facilities relative to the 2013 fenbendazole treatment. **(B)** Representative survival curves of leukemia/lymphoma development in *Cdkn2a*$^{-/-}$ (n=34) and TA *Cdkn2a*$^{-/-}$ (n=22) mice housed in an SPF facility during a pinworm outbreak prior to fenbendazole treatment (p=0.001). Arrows follow chronological order of survival studies. The year in brackets corresponds to the euthanasia date of the last mouse to develop illness in each cohort. **(C-D)** Survival curves from two independent experiments of mice housed in an SPF facility after pinworm was eradicated with fenbendazole treatment. 2016-2017: *Cdkn2a*$^{-/-}$ (n=58) and TA *Cdkn2a*$^{-/-}$ (n=40) (p=0.236); 2017: *Cdkn2a*$^{-/-}$ (n=18) and TA *Cdkn2a*$^{-/-}$ (n=15) (p=0.941). **(E)** Survival curve from one experiment in which *Cdkn2a*$^{-/-}$ (n=20) and TA *Cdkn2a*$^{-/-}$ (n=22) mice were housed in an SPF facility for 4 weeks, then transferred to a conventional facility for exposure to pinworm bedding (p=0.058). Gehan-Breslow-Wilcoxon test was applied to survival curves.

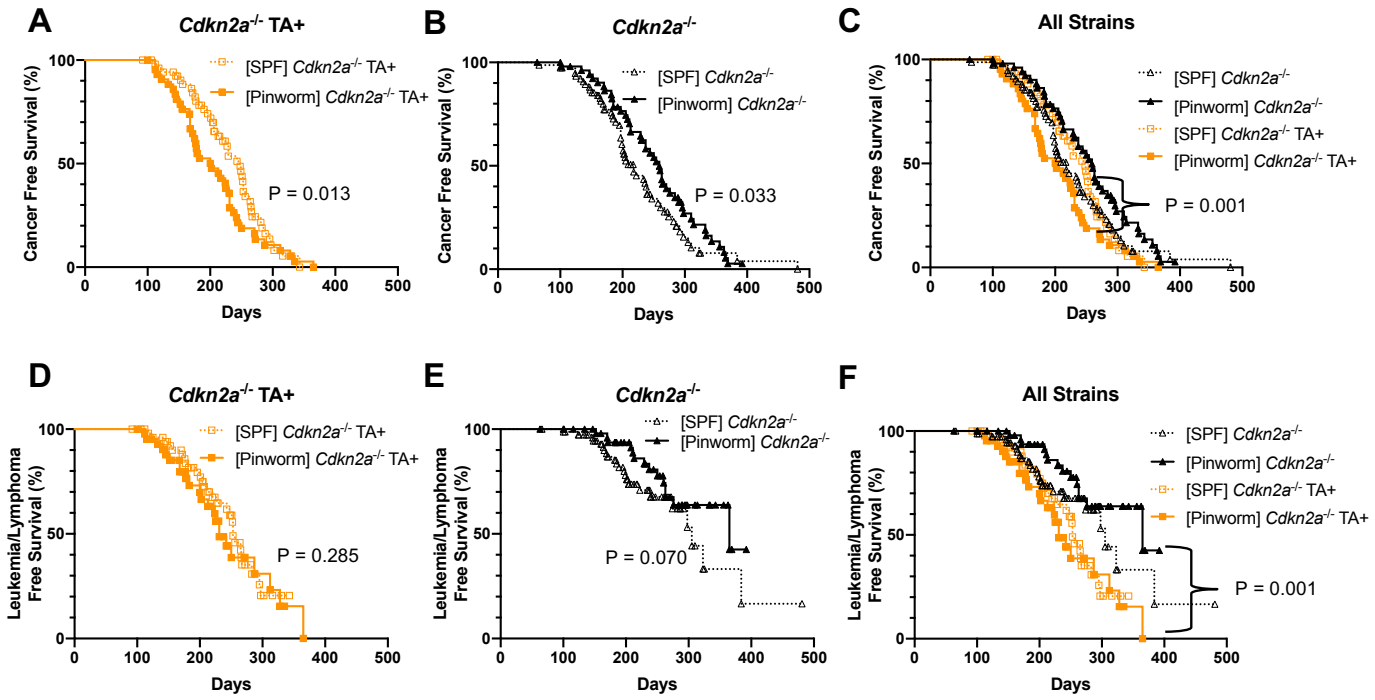

Figure 4.3. The capacity of pinworm to protect against or promote cancer in *Cdkn2a*$^{-/-}$ mice depends on TEL-AML1 status.

Cumulative survival curves showing combined data from cohorts in Figures 4B-E. Cancer free survival for SPF and pinworm-exposed **(A)** *Cdkn2a*$^{-/-}$ TA+ mice, **(B)** *Cdkn2a*$^{-/-}$ mice, and **(C)** all strains. Leukemia/lymphoma free survival for SPF and pinworm-exposed **(D)** *Cdkn2a*$^{-/-}$ TA+ mice, **(E)** *Cdkn2a*$^{-/-}$ mice, and **(F)** all strains. SPF TA *Cdkn2a*$^{-/-}$ mice (n=55, filled orange squares), pinworm-exposed TA *Cdkn2a*$^{-/-}$mice (n=44, open orange squares), SPF *Cdkn2a*$^{-/-}$mice (n=76, filled black triangles), pinworm-exposed *Cdkn2a*$^{-/-}$mice (n=54, open black triangles. Gehan-Breslow-Wilcoxon test was applied to survival curves.

4.5 TABLES

Table 4.1. Disease outcomes in *Ckdn2a*$^{-/-}$ and TA *Ckdn2a*$^{-/-}$ mice housed in a SPF facility or pinworm-infected conventional facility

	SFP *Cdkn2a*$^{-/-}$ (N=76)	SFP TA Cdkn2a$^{-/-}$ (N=55)	Pinworm *Cdkn2a*$^{-/-}$ (N=54)	Pinworm TA *Cdkn2a*$^{-/-}$ (N=44)
	N (% total)			
Cancer	56 (74%)	42 (76%)	44 (81%)	41 (93%)
Leukemia/Lymphoma	23 (30%)	28 (51%)	14 (26%)	23 (52%)

Table 4.2. Median cancer latency of *Ckdn2a*$^{-/-}$ and TA *Ckdn2a*$^{-/-}$ mice housed in a SPF facility or pinworm-infected conventional facility

	SFP *Cdkn2a* $^{-/-}$ (N=96)	SFP TA Cdkn2a$^{-/-}$ (N=68)	Pinworm *Cdkn2a* $^{-/-}$ (N=56)	Pinworm TA *Cdkn2a* $^{-/-}$ (N=44)
	Median latency (days)			
Cancer	218	248	259	202
Leukemia/Lymphoma	305	253	365	231

CHAPTER 5: CONCLUDING REMARKS

CONTRIBUTIONS TO THE FIELD OF B-ALL ETIOLOGY

Research conducted over the past century has suggested that pediatric B-ALL may be a preventable cancer. In recent years, numerous studies have provided evidence that immune dysfunction can drive ALL by coordinating with underlying genetic abnormalities[5]. These results led to proposals that vaccinations, probiotics, and synbiotics could prevent some cases of B-ALL by supporting the development of the neonatal immune system[5,59]. A challenge that the field now faces is to determine what type of immune responses should be promoted and which individuals have a high enough risk to be treated for prevention. This dissertation makes three insightful contributions to the above question by (1) identifying parasitic infection as protective against B-ALL, (2) providing evidence for IL-10 deficiency as a B-ALL risk factor, and (3) presenting a mechanism that describes how the microbial dysbiosis may serve as a convergence point for infectious stimuli in B-ALL pathogenesis.

5.1 PROTECTIVE EFFECT OF PARASITIC INFECTIONS IN B CELL LEUKEMIA/LYMPHOMA

Although the protective role of early childhood infections is a fundamental principle of the delayed infection hypothesis, no studies to date have demonstrated a causal role for infections in protection against B-ALL. Others have shown that treatment with synthetic CPG, a TLR9 agonist, can delay leukemogenesis in the Eμ-ret mouse model of B-ALL[64]. However, evidence supporting a role of infections in impairing the progression of leukemia was lacking. By demonstrating that pinworm infection slows the latency of leukemia/lymphoma in *Cdkn2a*$^{-/-}$ mice, our study is the first to demonstrate that pathogenic infections can have an inhibitory effect in leukemogenesis.

A remaining question is why pinworm infection demonstrated a protective effect, whereas other infectious exposures have been reported to promote B-ALL in mice. There is a

substantial gap of knowledge regarding the type of infections or inflammatory responses that impact B-ALL. Several epidemiology groups have noted a lack of evidence implicating a particular infectious pathogen in childhood leukemia development, and have instead suggested that impaired Th2 immunity or excessive Th1/Th17 responses may promote the development of childhood hematological malignancies. Our observation that pinworm exposure delays the latency of leukemia/lymphoma provides additional support for the protective role of Th2 immunity in childhood leukemia. Th2 immune responses to helminth infection have long been associated with suppression of autoimmunity and allergic disease. In fact, several studies have reported that pinworm infections often stimulate an IL-10 associated Th2 response in host mice[112]. A limitation of the current study was that we did not measure which cytokines were produced in response to pinworm-exposure. Future investigations could benefit from confirming that pinworm infection in our conventional facility stimulates a Th2 response in *Cdkn2a*$^{-/-}$ mice. Additional insight could be gained by determining whether other infectious pathogens that stimulate Th2 immune responses also have the capacity to delay leukemogenesis in the *Cdkn2a*$^{-/-}$ mouse model.

This work also provided new insight on the interaction between pinworm exposure and genetic lesions during the development of leukemia/lymphoma. Although pinworm exposure delayed leukemia/lymphoma development in *Cdkn2a*$^{-/-}$ mice, we did not detect a protective effect in *Cdkn2a*$^{-/-}$ mice that expressed TEL-AML1. This novel finding suggests that the benefit of using infectious exposures to suppress leukemia may be limited to children who lack specific genetic lesions. The implication of this result for preventive therapy development is that early immune stimulation alone may be insufficient to protect against leukemia in a subset of children. Therefore, developing combinational therapies that target both immune system development and genetic mutations could be a valuable future endeavor.

5.2 IL-10 DEFICIENCY DRIVES B CELL LEUKEMIA/LYMPHOMA

In addition to demonstrating a protective effect of Th2-associated infectious exposures, we showed that the absence of IL-10, a key regulator of Th2 response, accelerates the development of leukemia/lymphoma in TA+ *Cdkn2a*$^{-/-}$ mice. This finding builds upon the observation that low levels of IL-10 in neonates is associated with an increased risk of childhood ALL[11]. Of note, there was a surprising inconsistency between the epidemiological and mouse studies. In the human study, the risk of developing ALL was increased by low IL-10 levels. In mice, we found that leukemia/lymphoma latency, but not risk, was impacted by decreased IL-10. A possible explanation for this observation is that the relatively high incidence of leukemia/lymphoma in the TA+ *Cdkn2a*$^{-/-}$ model may limit the detection of changes in disease incidence. Therefore, a different mouse model with a lower incidence of leukemia/lymphoma may be better suited for future studies aimed at addressing whether low levels of IL-10, or other immune system manipulations, have an impact on the risk of developing ALL.

In addition to supporting a causal role of low IL-10 levels in B cell leukemia/lymphoma development, we characterized a set of pro-inflammatory cytokines, including G-CSF, IL-6, and IL-17, that are associated with DNA damage in bone marrow precursor B cells. Our finding that B cell γH2AX levels were not elevated in the absence of myeloid inflammation highlighted the potential role of inflammation in inducing B cell DNA damage in *Il10*$^{-/-}$ mice. Notably, inflammation in *Il10*$^{-/-}$ mice was also associated with a severe B cell suppression. This raises the possibility that the decrease in B-cells and the increase in double-strand breaks have a yet undelineated connection in their causality. This interpretation is supported by *in vitro* studies which showed the importance of IL-7 withdrawal and TGF-β, well-established inhibitors of B cell growth, in inducing DNA damage in human B cells[5,8]. Whether an *in vivo* innate inflammatory response acts through a common mechanism of DNA mutagenesis has yet to be determined. Future work should focus on identifying which inflammatory cytokines in *Il10*$^{-/-}$ mice are

necessary for inducing B cell DNA damage and leukemogenesis. This work may ultimately aid in compiling a panel of cells and cytokines that can be measured at birth and during early childhood infections to predict ALL risk.

5.3 MECHANISM FOR MICROBIAL-INDUCED INFLAMMATION IN CHILDHOOD B CELL MALIGNANCIES

Numerous epidemiological studies from past decades have supported there being a role of insufficient microbial exposures in promoting childhood leukemia[5,59]. A few recent studies have revealed that newborns delivered through cesarean section or breastfed either not at all or for only a short period of time have a significantly increased risk of developing leukemia during childhood[86–88,113]. Little is known about how the composition of the neonatal microbiome effects B cell transformation in distal microenvironments such as the bone marrow. However, evidence exists that gut bacteria can induce VDJ recombination in B cells within the lamina propria[81]. We used antibiotics to demonstrate that suppressing microbial dysbiosis in *Il10*$^{-/-}$ mice can reduce DNA damage in bone marrow B cells. Although we did not assess the impact of antibiotics on leukemia/lymphoma development, we found that pinworm exposure and wild-type IL-10 expression, both of which promote microbial homeostasis, protect against B cell disease in mice. These data are the first to provide evidence that microbial dysbiosis can contribute to B cell DNA damage in the bone marrow. Overall, these data support a mechanism in which low IL-10 levels promote the development childhood of B cell leukemia/lymphoma by disrupting the control of pathogenic inflammation by the gut microbiome (**Figure 5.1**). Helminth infections that induce microbial-mediated immunosuppression via IL-10, may have the opposite effect of protecting against leukemia.

5.4 FIGURES

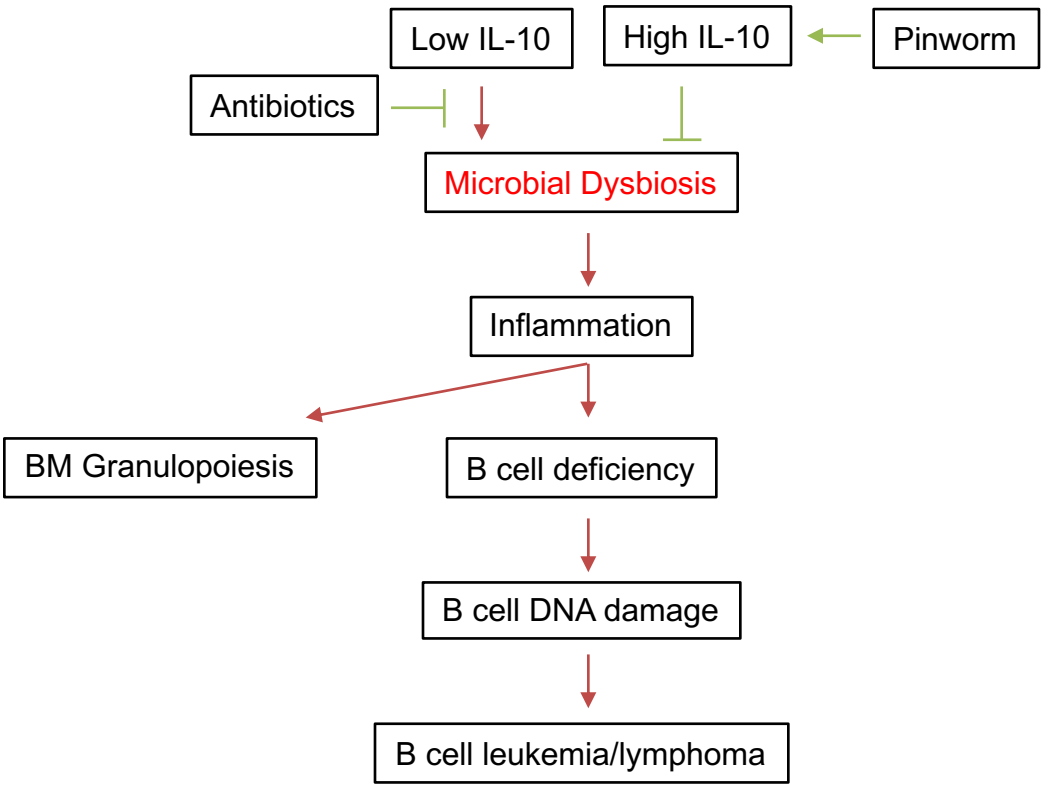

Figure 5.1. Model for the role of microbial dysbiosis in childhood B cell leukemia/lymphoma.

IL-10 deficiency induces microbial dysbiosis in the gut, resulting in inflammation with distal effects of granulopoieis, B cell deficiency, and B cell DNA damage in the bone marrow. The inflammation-associated acquisition of genetic lesions in bone marrow pro-B and IgM+ B cells leads to the development of B cell leukemia/lymphoma. Antibiotics may counteract the impact of low IL-10 by restoring bacterial homeostasis in the gut. Pinworm also counteracts microbial dysbiosis by increasing the production of Th2 related cytokines, such as IL-10.

CHAPTER 6: MATERIALS AND METHODS

Mice

B6.129P2-*Il10*^{tm1Cgn}/J mice (referred to in the text as *Il10*$^{-/-}$ mice, MGI: 1857199 Jackson Laboratory: 002251) were purchased from The Jackson Laboratory and then crossed >10 generations into the FVB/n strain background. Control FVB/n mice were bred in house. Cre^{+} TA^{+} *Cdkn2a*$^{-/-}$ mice have been previously described and were maintained on the FVB/n strain background. B6.129 *Il10*$^{-/-}$ mice had been crossed to Cre^{+} TA^{+} *Cdkn2a*$^{-/-}$ mice on the FVB/n background for 4 generations. All experiments were performed following institutional review and approval by the UCSF Institutional Animal Care and Use Committee.

Cytokine Analyses

For peripheral blood plasma, whole blood was obtained through submandibular bleeding, collected in EDTA-coated tubes (Becton Dickinson), and centrifuged for 10 minutes at 1,600 x g at 4°C to remove blood cells. Complete blood count analyses were performed using a Hemavet haematology system (Drew Scientific). The supernatant was assayed in duplicate. A total of 32 cytokines were measured (Table 1) using 9-plex (IL-15, IL-18, Basic FGF, LIF, M-CSF, MIG, MIP-2, PDGF-BB, and VEGF) and 23-plex (IL-1a, IL1b, IL-2, IL-3, IL-4, IL-5, IL-6, IL-9, IL-10, IL12p40, IL-12p70, IL-13, IL-17A, Eotaxin, G-CSF, GM-CSF, IFN-r, KC, MCP-1, MIP-1a, MIP-1B, RANTES, and TNF-a) luminex bead-based assays (Bio-Rad). Protein content of each extract was determined with the Bradford Assay (Bio-Rad). Cytokine measurements for each duplicate were averaged and normalized to protein concentrations.

Isolation of immune cells

For bone marrow cells, the four long bones (two femur and two tibiae) of the same mice were flushed with FACS buffer (Hank's balanced salt solution $Ca^{2+/}Mg^{2+}$ free, 2% heat-inactivated fetal bovine serum, 2.5% cell dissociation buffer, penicillin/streptomycin). Spleens and mesenteric lymph

nodes were physically dissociated in FACS buffer. Cell suspensions were filtered through a 70μm strainer. Mononuclear cells and granulocytes were collected after centrifugation of filtered suspensions on Histopaque 1119 (Sigma #11191). Whole peripheral blood was collected in EDTA tubes and incubated in ACK red blood cell lysis buffer immediately or after plasma depletion.

Cell staining and flow cytometry

Cell viability was measured before flow cytometry using Trypan Blue and tracked during flow cytometry using DAPI or Ghost dye Violet 450 viability dye. After viability staining, cells were blocked in FcBlock or Rat IgG for 10 minutes in the dark on ice. Without washing, primary surface staining antibodies were added for an additional 20 minutes. Cells stained with biotinylated surface antibodies were then stained with fluorochrome-labeled streptavidin for 20 minutes. For intracellular staining, EGFP signal was preserved by fixing cells in 4% Formaldehyde for 15 minutes at room temperature in the dark. Additional fixation and permeabilization was done using the BD Cytofix/Cytoperm kit per manufacturer's instructions. Cells from transplantation recipients were analyzed on a FACSCalibur (Becton Dickinson). All other flow cytometry analysis was acquired using a SP 6800 Spectral Analyzer (Sony Biotechnology). Antibody information, including clones and dilutions, is listed in listed in Table S2.

Apoptosis assay

After surface antibody staining, CellEvent Caspase-3/7 Green Detection Reagent (Invitrogen) was added to cells according to the manufacturer's instructions. DAPI was added to stain dead cells and the percentage of $DAPI^-$ CellEvent $Caspase\text{-}3/7^+$ cells was assessed by flow cytometry.

Proliferation assay

Mice were injected i.p. with 100μl (10mg/mL) BrdU and euthanized 1 hour later. Cells were first stained for surface markers and then processed according to the FITC BrdU Flow Staining Protocol (BD Pharmingen).

Transplantation

8-16 week-old FVB/n and *Il10*$^{-/-}$ recipient mice were sublethally irradiated with a split dose of irradiation (10Gy for FVB/n mice and 8-8.5Gy for *Il10*$^{-/-}$ mice) 4-5 hours apart from a Cs^{137} source (J.L. Shepherd). Irradiated recipients were injected retro-orbitally with 2 x 10^6 bone marrow cells from 5-6 week-old Cre^{+} TA^{+} Cdkn2a$^{-/-}$ or *Il10*$^{-/-}$ Cre^{+} TA^{+} Cdkn2a$^{-/-}$ mice. Transplant recipients were administered antibiotics following transplantation and analyzed for donor-derived $EGFP^{+}$ chimerism by regular bleeding.

Antibiotic treatment

Nutritionally complete pellets containing Amoxicillin, Clarithromycin, Metronidazole and Omeprazole (Bio-Serv) were provided to mice. These antibiotics are effective against a broad spectrum of Helicobacter strains.

Pathological Analyses

At the time of euthanasia, a gross necropsy was performed to identify potential sources of illness and selected tissues were placed into buffered formalin. If gross necropsy findings suggested a hematopoietic neoplasm, single cell suspensions of involved tissues were prepared when possible and cryopreserved in medium containing 10% DMSO. Formalin Fixed Paraffin Embedded (FFPE) tissues were stained with hematoxylin & eosin. Diagnoses were based upon gross necropsy and histopathology. Additional diagnostic information was obtained by immunophenotyping when necessary.

DNA extraction

The DNeasy and QIAamp DNA FFPE Tissue kits (Qiagen) were used to extract DNA from cryopreserved or FFPE samples from leukemic mice. DNA concentration and quality were determined by Nanodrop spectrophotometry and PicoGreen (Invitrogen).

Whole Exome Sequencing

DNA samples were submitted to MedGenome for mouse exome capture and sequencing. DNA sequencing libraries were prepared using the SureSelectXT Mouse All Exon Kit (Agilent) according to the manufacturer's instructions. Samples were sequenced with paired-end 100-bp reads on an Illumina HiSeq2500. The resulting reads in .bam files were aligned to the GRCm38/mm10 *M. musculus* genome reference using BWA. Genome Analysis Toolkit (GATK) was used to recalibrate base quality score and realign reads around insertions and deletions (indels). Alignment and coverage metrics were collected using Picard. SNVs were called using Mutect version 1.1.4, a somatic variant detection program. Each tumor was called against a panel of normal tails and spleens from this experiment. Calls were filtered against a database of known *M. Musculus* germline single-nucleotide polymorphisms. Results were further filtered to calls with a minimum read depth of 10 and a minimum mutant allele fraction of 10%. Variants were annotated using Annovar and mutations present in human cancers were identified using the COSMIC database.

Statistical Analysis

Pairwise statistical significance was evaluated by two-tailed Mann-Whitney *U*-test or Student's *t*-test. Correlations were calculated using the Spearman correlation. Survival analyses were performed using GraphPad Prism software. In previous survival analyses for *Cdkn2a*$^{-/-}$ mice, irradiation was associated with early disease development[23]. Given that the mice in the current

study are derivatives of *Cdkn2a*$^{-/-}$ mice, we chose to use the Gehan-Breslow-Wilcoxon test, which is the most sensitive and appropriate test for detecting early shifts in survival.

CHAPTER 7: REFERENCES

1. Roman E, Simpson J, Ansell P, et al. Childhood acute lymphoblastic leukemia and infections in the first year of life: a report from the United Kingdom Childhood Cancer Study. *Am J Epidemiol*. 2007;165(5):496-504. doi:10.1093/aje/kwk039

2. Gilham C, Peto J, Simpson J, et al. Day care in infancy and risk of childhood acute lymphoblastic leukaemia: findings from UK case-control study. *BMJ*. 2005;330(7503):1294. doi:10.1136/bmj.38428.521042.8F

3. Chang JS, Tsai C-R, Tsai Y-W, Wiemels JL. Medically diagnosed infections and risk of childhood leukaemia: a population-based case-control study. *Int J Epidemiol*. 2012;41(4):1050-1059. doi:10.1093/ije/dys113

4. Strachan DP. Hay fever, hygiene, and household size. *BMJ*. 1989;299(6710):1259-1260. doi:10.1136/bmj.299.6710.1259

5. Greaves M. A causal mechanism for childhood acute lymphoblastic leukaemia. *Nat Rev Cancer*. 2018;18(8):471-484. doi:10.1038/s41568-018-0015-6

6. Greaves M. Infection, immune responses and the aetiology of childhood leukaemia. *Nat Rev Cancer*. 2006;6(3):193-203. doi:10.1038/nrc1816

7. Papaemmanuil E, Rapado I, Li Y, et al. RAG-mediated recombination is the predominant driver of oncogenic rearrangement in ETV6-RUNX1 acute lymphoblastic leukemia. *Nat Genet*. 2014;46(2):116-125. doi:10.1038/ng.2874

8. Swaminathan S, Klemm L, Park E, et al. Mechanisms of clonal evolution in childhood acute lymphoblastic leukemia. *Nat Immunol*. 2015;16(7):766-774. doi:10.1038/ni.3160

9. Rodríguez-Hernández G, Hauer J, Martín-Lorenzo A, et al. Infection Exposure Promotes ETV6-RUNX1 Precursor B-cell Leukemia via Impaired H3K4 Demethylases. *Cancer Res*. 2017;77(16):4365-4377. doi:10.1158/0008-5472.CAN-17-0701

10. Couper KN, Blount DG, Riley EM. IL-10: The Master Regulator of Immunity to Infection. *J Immunol*. 2008;180(9):5771-5777. doi:10.4049/jimmunol.180.9.5771

11. Chang JS, Zhou M, Buffler P a, Chokkalingam AP, Metayer C, Wiemels JL. Profound deficit of IL10 at birth in children who develop childhood acute lymphoblastic leukemia. *Cancer Epidemiol Biomark Prev Publ Am Assoc Cancer Res Cosponsored Am Soc Prev Oncol*. 2011;20(8):1736-1740. doi:10.1158/1055-9965.EPI-11-0162

12. Neven B, Mamessier E, Bruneau J, et al. A Mendelian predisposition to B-cell lymphoma caused by IL-10R deficiency. *Blood*. 2013;122(23):3713-3722. doi:10.1182/blood-2013-06-508267

13. Moore KW, de Waal Malefyt R, Coffman RL, O'Garra A. Interleukin-10 and the Interleukin-10 Receptor. *Annu Rev Immunol*. 2001;19(1):683-765. doi:10.1146/annurev.immunol.19.1.683

14. Zhu L, Shi T, Zhong C, Wang Y, Chang M, Liu X. IL-10 and IL-10 Receptor Mutations in Very Early Onset Inflammatory Bowel Disease. *Gastroenterol Res*. 2017;10(2):65-69. doi:10.14740/gr740w

15. Kanneganti M, Mino-Kenudson M, Mizoguchi E. Animal Models of Colitis-Associated Carcinogenesis. *J Biomed Biotechnol*. 2011;2011. doi:10.1155/2011/342637

16. Almana Y, Mohammed R. Current concepts in pediatric inflammatory bowel disease; IL10/IL10R colitis as a model disease. *Int J Pediatr Adolesc Med*. 2019;6(1):1-5. doi:10.1016/j.ijpam.2019.02.002

17. Frick A, Khare V, Paul G, et al. Overt Increase of Oxidative Stress and DNA Damage in Murine and Human Colitis and Colitis-Associated Neoplasia. *Mol Cancer Res MCR*. 2018;16(4):634-642. doi:10.1158/1541-7786.MCR-17-0451

18. Westbrook AM, Wei B, Braun J, Schiestl RH. Intestinal inflammation induces genotoxicity to extraintestinal tissues and cell types in mice. *Int J Cancer*. 2011;129(8):1815-1825. doi:10.1002/ijc.26146

19. Veiby OP, Borge OJ, Mårtensson A, et al. Bidirectional Effect of Interleukin-10 on Early Murine B-Cell Development: Stimulation of flt3-Ligand Plus Interleukin-7–Dependent Generation of CD19− ProB Cells From Uncommitted Bone Marrow Progenitor Cells and Growth Inhibition of CD19+ ProB Cells. *Blood*. 1997;90(11):4321-4331.

20. Itoh K, Hirohata S. The role of IL-10 in human B cell activation, proliferation, and differentiation. *J Immunol*. 1995;154(9):4341-4350.

21. Clark MR, Mandal M, Ochiai K, Singh H. Orchestrating B cell lymphopoiesis through interplay of IL-7 receptor and pre-B cell receptor signalling. *Nat Rev Immunol*. 2014;14(2):69-80. doi:10.1038/nri3570

22. Ford AM, Palmi C, Bueno C, et al. The TEL-AML1 leukemia fusion gene dysregulates the TGF-beta pathway in early B lineage progenitor cells. *J Clin Invest*. 2009;119(4):826-836. doi:10.1172/JCI36428

23. Li M, Jones L, Gaillard C, et al. Initially disadvantaged, TEL-AML1 cells expand and initiate leukemia in response to irradiation and cooperating mutations. *Leukemia*. 2013;27(7):1570-1573. doi:10.1038/leu.2013.15

24. Ray A, Basu S, Gharaibeh RZ, et al. Gut Microbial Dysbiosis Due to Helicobacter Drives an Increase in Marginal Zone B Cells in the Absence of IL-10 Signaling in Macrophages. *J Immunol*. 2015;195(7):3071-3085. doi:10.4049/jimmunol.1500153

25. Redpath SA, Fonseca NM, Perona-Wright G. Protection and pathology during parasite infection: IL-10 strikes the balance. *Parasite Immunol*. 2014;36(6):233-252. doi:10.1111/pim.12113

26. Gomes-Santos AC, Moreira TG, Castro-Junior AB, et al. New Insights into the Immunological Changes in IL-10-Deficient Mice during the Course of Spontaneous Inflammation in the Gut Mucosa. Journal of Immunology Research. doi:10.1155/2012/560817

27. Brière F, Bridon JM, Servet C, Rousset F, Zurawski G, Banchereau J. IL-10 and IL-13 as B cell growth and differentiation factors. *Nouv Rev Fr Hematol*. 1993;35(3):233-235.

28. Heine G, Drozdenko G, Grün JR, Chang H-D, Radbruch A, Worm M. Autocrine IL-10 promotes human B-cell differentiation into IgM- or IgG-secreting plasmablasts. *Eur J Immunol*. 2014;44(6):1615-1621. doi:10.1002/eji.201343822

29. Berg DJ, Davidson N, Kühn R, et al. Enterocolitis and colon cancer in interleukin-10-deficient mice are associated with aberrant cytokine production and CD4(+) TH1-like responses. *J Clin Invest*. 1996;98(4):1010-1020.

30. Cain D, Kondo M, Chen H, Kelsoe G. Effects of Acute and Chronic Inflammation on B-Cell Development and Differentiation. *J Invest Dermatol*. 2009;129(2):266-277. doi:10.1038/jid.2008.286

31. Kühn R, Löhler J, Rennick D, Rajewsky K, Müller W. Interleukin-10-deficient mice develop chronic enterocolitis. *Cell*. 1993;75(2):263-274. doi:10.1016/0092-8674(93)80068-p

32. Bristol IJ, B.A., Mahler M, D.V.M., Leiter EH, Ph.D. Interleukin-10 gene targeted mutation. The Jackson Laboratory. Accessed January 1, 2020. https://www.jax.org/news-and-insights/1997/october/il10-tm1cgn-an-interleukin-10-gene-targeted-mutation

33. 002251 - B6.129P2-Il10<tm1Cgn>/J. Accessed January 1, 2020. https://www.jax.org/strain/002251

34. Cain DW, Snowden PB, Sempowski GD, Kelsoe G. Inflammation Triggers Emergency Granulopoiesis through a Density-Dependent Feedback Mechanism. Fessler MB, ed. *PLoS ONE*. 2011;6(5):e19957. doi:10.1371/journal.pone.0019957

35. Mosmann TR, Moore KW. The role of IL-10 in crossregulation of TH1 and TH2 responses. *Immunol Today*. 1991;12(3):A49-53. doi:10.1016/S0167-5699(05)80015-5

36. Laouini D, Alenius H, Bryce P, Oettgen H, Tsitsikov E, Geha RS. IL-10 is critical for Th2 responses in a murine model of allergic dermatitis. *J Clin Invest*. 2003;112(7):1058-1066. doi:10.1172/JCI200318246

37. Coomes SM, Kannan Y, Pelly VS, et al. CD4+ Th2 cells are directly regulated by IL-10 during allergic airway inflammation. *Mucosal Immunol*. 2017;10(1):150-161. doi:10.1038/mi.2016.47

38. Fiorentino DF, Zlotnik A, Vieira P, et al. IL-10 acts on the antigen-presenting cell to inhibit cytokine production by Th1 cells. *J Immunol*. 1991;146(10):3444-3451.

39. Fiorentino DF, Zlotnik A, Mosmann TR, Howard M, O'Garra A. IL-10 inhibits cytokine production by activated macrophages. *J Immunol*. 1991;147(11):3815-3822.

40. Kitching AR, Tipping PG, Timoshanko JR, Holdsworth SR. Endogenous interleukin-10 regulates Th1 responses that induce crescentic glomerulonephritis. *Kidney Int*. 2000;57(2):518-525. doi:10.1046/j.1523-1755.2000.00872.x

41. Dinarello CA. Historical Review of Cytokines. *Eur J Immunol*. 2007;37(Suppl 1):S34-S45. doi:10.1002/eji.200737772

42. Brubaker JO, Montaner LJ. Role of interleukin-13 in innate and adaptive immunity. *Cell Mol Biol Noisy--Gd Fr*. 2001;47(4):637-651.

43. Stockinger B, Veldhoen M, Martin B. Th17 T cells: Linking innate and adaptive immunity. *Semin Immunol*. 2007;19(6):353-361. doi:10.1016/j.smim.2007.10.008

44. Khader SA, Gaffen SL, Kolls JK. Th17 cells at the crossroads of innate and adaptive immunity against infectious diseases at the mucosa. *Mucosal Immunol*. 2009;2(5):403-411. doi:10.1038/mi.2009.100

45. Veldhoen M. Interleukin 17 is a chief orchestrator of immunity. *Nat Immunol*. 2017;18(6):612-621. doi:10.1038/ni.3742

46. Lee MY, Fevold KL, Dorshkind K, Fukunaga R, Nagata S, Rosse C. In vivo and in vitro suppression of primary B lymphocytopoiesis by tumor-derived and recombinant granulocyte colony-stimulating factor. *Blood*. 1993;82(7):2062-2068.

47. Day RB, Bhattacharya D, Nagasawa T, Link DC. Granulocyte colony-stimulating factor reprograms bone marrow stromal cells to actively suppress B lymphopoiesis in mice. *Blood*. 2015;125(20):3114-3117. doi:10.1182/blood-2015-02-629444

48. Winkler IG, Bendall LJ, Forristal CE, et al. B-lymphopoiesis is stopped by mobilizing doses of G-CSF and is rescued by overexpression of the anti-apoptotic protein Bcl2. *Haematologica*. 2013;98(3):325-333. doi:10.3324/haematol.2012.069260

49. Matsunaga T, Hirayama F, Yonemura Y, Murray R, Ogawa M. Negative regulation by interleukin-3 (IL-3) of mouse early B-cell progenitors and stem cells in culture: transduction of the negative signals by betac and betaIL-3 proteins of IL-3 receptor and absence of negative regulation by granulocyte-macrophage colony-stimulating factor. *Blood*. 1998;92(3):901-907.

50. Cohen L, Fiore-Gartland A, Randolph AG, et al. A Modular Cytokine Analysis Method Reveals Novel Associations With Clinical Phenotypes and Identifies Sets of Co-signaling Cytokines Across Influenza Natural Infection Cohorts and Healthy Controls. *Front Immunol*. 2019;10. doi:10.3389/fimmu.2019.01338

51. Greenbaum AM, Link DC. Mechanisms of G-CSF-mediated hematopoietic stem and progenitor mobilization. *Leukemia*. 2011;25(2):211-217. doi:10.1038/leu.2010.248

52. Martín-Lorenzo A, Auer F, Chan LN, et al. Loss of Pax5 Exploits Sca1-BCR-ABLp190 Susceptibility to Confer the Metabolic Shift Essential for pB-ALL. *Cancer Res*. 2018;78(10):2669-2679. doi:10.1158/0008-5472.CAN-17-3262

53. Henry CJ, Casás-Selves M, Kim J, et al. Aging-associated inflammation promotes selection for adaptive oncogenic events in B cell progenitors. *J Clin Invest*. 2015;125(12):4666-4680. doi:10.1172/JCI83024

54. Levy Y, Brouet JC. Interleukin-10 prevents spontaneous death of germinal center B cells by induction of the bcl-2 protein. *J Clin Invest*. 1994;93(1):424-428. doi:10.1172/JCI116977

55. Nagai Y, Garrett KP, Ohta S, et al. Toll-like receptors on hematopoietic progenitor cells stimulate innate immune system replenishment. *Immunity*. 2006;24(6):801-812. doi:10.1016/j.immuni.2006.04.008

56. Girschick HJ, Grammer AC, Nanki T, Mayo M, Lipsky PE. RAG1 and RAG2 expression by B cell subsets from human tonsil and peripheral blood. *J Immunol Baltim Md 1950*. 2001;166(1):377-386. doi:10.4049/jimmunol.166.1.377

57. Kuraoka M, Liao D, Yang K, et al. Activation-Induced Cytidine Deaminase Expression and Activity in the Absence of Germinal Centers: Insights into Hyper-IgM Syndrome. *J Immunol*. 2009;183(5):3237-3248. doi:10.4049/jimmunol.0901548

58. Martín-Lorenzo A, Hauer J, Vicente-Dueñas C, et al. Infection Exposure is a Causal Factor in B-cell Precursor Acute Lymphoblastic Leukemia as a Result of Pax5-Inherited Susceptibility. *Cancer Discov*. 2015;5(12):1328-1343. doi:10.1158/2159-8290.CD-15-0892

59. Wen Y, Jin R, Chen H. Interactions Between Gut Microbiota and Acute Childhood Leukemia. *Front Microbiol*. 2019;10. doi:10.3389/fmicb.2019.01300

60. Mumm JB, Emmerich J, Zhang X, et al. IL-10 Elicits IFNγ-Dependent Tumor Immune Surveillance. *Cancer Cell*. 2011;20(6):781-796. doi:10.1016/j.ccr.2011.11.003

61. Oft M. IL-10: master switch from tumor-promoting inflammation to antitumor immunity. *Cancer Immunol Res*. 2014;2(3):194-199. doi:10.1158/2326-6066.CIR-13-0214

62. Winkler B, Taschik J, Haubitz I, Eyrich M, Schlegel PG, Wiegering V. TGFβ and IL10 have an impact on risk group and prognosis in childhood ALL. *Pediatr Blood Cancer*. 2015;62(1):72-79. doi:10.1002/pbc.25142

63. Ghufran H, Riaz S, Mahmood N, et al. Polymorphism of Interleukin-10 (IL-10, -1082 G/A) and Interleukin-28B (IL-28B, C/T) In Pediatric Acute Lymphoblastic Leukemia (ALL). *Pak J Pharm Sci*. 2019;32(5(Supplementary)):2357-2361.

64. Fidanza M, Seif AE, DeMicco A, et al. Inhibition of precursor B cell malignancy progression by toll-like receptor ligand-induced immune responses. *Leukemia*. 2016;30(10):2116-2119. doi:10.1038/leu.2016.152

65. Mullighan CG, Goorha S, Radtke I, et al. Genome-wide analysis of genetic alterations in acute lymphoblastic leukaemia. *Nature*. 2007;446(7137):758-764. doi:10.1038/nature05690

66. Søegaard SH, Rostgaard K, Skogstrand K, Wiemels JL, Schmiegelow K, Hjalgrim H. Neonatal Inflammatory Markers Are Associated with Childhood B-cell Precursor Acute Lymphoblastic Leukemia. *Cancer Res*. 2018;78(18):5458-5463. doi:10.1158/0008-5472.CAN-18-0831

67. Madan R, Demircik F, Surianarayanan S, et al. Nonredundant roles for B cell-derived IL-10 in immune counter-regulation. *J Immunol Baltim Md 1950*. 2009;183(4):2312-2320. doi:10.4049/jimmunol.0900185

68. Scapini P, Lamagna C, Hu Y, et al. B cell-derived IL-10 suppresses inflammatory disease in Lyn-deficient mice. *Proc Natl Acad Sci*. 2011;108(41):E823-E832. doi:10.1073/pnas.1107913108

69. Dennis KL, Saadalla A, Blatner NR, et al. T-cell Expression of IL10 Is Essential for Tumor Immune Surveillance in the Small Intestine. *Cancer Immunol Res*. 2015;3(7):806-814. doi:10.1158/2326-6066.CIR-14-0169

70. Sato Y, Takahashi S, Kinouchi Y, et al. IL-10 deficiency leads to somatic mutations in a model of IBD. *Carcinogenesis*. 2006;27(5):1068-1073. doi:10.1093/carcin/bgi327

71. Cosmic. HOXA9 Gene - COSMIC. Accessed March 17, 2020. https://cancer.sanger.ac.uk/cell_lines/gene/analysis?ln=HOXA9

72. Sun H, Yu G. New insights into the pathogenicity of non-synonymous variants through multi-level analysis. *Sci Rep*. 2019;9(1):1-11. doi:10.1038/s41598-018-38189-9

73. Mullighan CG, Zhang J, Harvey RC, et al. JAK mutations in high-risk childhood acute lymphoblastic leukemia. *Proc Natl Acad Sci*. 2009;106(23):9414-9418. doi:10.1073/pnas.0811761106

74. Ding L-W, Sun Q-Y, Tan K-T, et al. Mutational Landscape of Pediatric Acute Lymphoblastic Leukemia. *Cancer Res*. 2017;77(2):390-400. doi:10.1158/0008-5472.CAN-16-1303

75. Oshima K, Khiabanian H, da Silva-Almeida AC, et al. Mutational landscape, clonal evolution patterns, and role of RAS mutations in relapsed acute lymphoblastic leukemia. *Proc Natl Acad Sci U S A*. 2016;113(40):11306-11311. doi:10.1073/pnas.1608420113

76. Abbas T, Dutta A. p21 in cancer: intricate networks and multiple activities. *Nat Rev Cancer*. 2009;9(6):400-414. doi:10.1038/nrc2657

77. Lindqvist CM, Nordlund J, Ekman D, et al. The Mutational Landscape in Pediatric Acute Lymphoblastic Leukemia Deciphered by Whole Genome Sequencing. *Hum Mutat*. 2015;36(1):118-128. doi:10.1002/humu.22719

78. Mirantes C, Passegué E, Pietras EM. Pro-inflammatory cytokines: emerging players regulating HSC function in normal and diseased hematopoiesis. *Exp Cell Res*. 2014;329(2):248-254. doi:10.1016/j.yexcr.2014.08.017

79. Böiers C, Richardson SE, Laycock E, et al. A Human IPS Model Implicates Embryonic B-Myeloid Fate Restriction as Developmental Susceptibility to B Acute Lymphoblastic Leukemia-Associated ETV6-RUNX1. *Dev Cell*. 2018;44(3):362-377.e7. doi:10.1016/j.devcel.2017.12.005

80. Kantner H-P, Warsch W, Delogu A, et al. ETV6/RUNX1 Induces Reactive Oxygen Species and Drives the Accumulation of DNA Damage in B Cells. *Neoplasia*. 2013;15(11):1292-IN28. doi:10.1593/neo.131310

81. Wesemann DR, Portuguese AJ, Meyers RM, et al. Microbial colonization influences early B-lineage development in the gut lamina propria. *Nature*. 2013;501(7465):112-115. doi:10.1038/nature12496

82. Lee S, Kim H, You G, et al. Bone marrow CX3CR1+ mononuclear cells relay a systemic microbiota signal to control hematopoietic progenitors in mice. *Blood*. 2019;134(16):1312-1322. doi:10.1182/blood.2019000495

83. Elliott DE, Weinstock JV. Inflammatory bowel disease and the hygiene hypothesis: an argument for the role of helminths. In: Rook GAW, ed. *The Hygiene Hypothesis and Darwinian Medicine*. Progress in Inflammation Research. Birkhäuser; 2009:149-178. doi:10.1007/978-3-7643-8903-1_9

84. Seif AE, Barrett DM, Milone M, Brown VI, Grupp SA, Reid GSD. Long-term protection from syngeneic acute lymphoblastic leukemia by CpG ODN-mediated stimulation of innate and adaptive immune responses. *Blood*. 2009;114(12):2459-2466. doi:10.1182/blood-2009-02-203984

85. Jo S, Fotovati A, Duque-Afonso J, et al. Differential Depletion of Bone Marrow Resident B-ALL after Systemic Administration of Endosomal TLR Agonists. *Cancers*. 2020;12(1). doi:10.3390/cancers12010169

86. Marcotte EL, Thomopoulos TP, Infante-Rivard C, et al. Caesarean delivery and risk of childhood leukaemia: a pooled analysis from the Childhood Leukemia International Consortium (CLIC). *Lancet Haematol*. 2016;3(4):e176-185. doi:10.1016/S2352-3026(16)00002-8

87. Wang R, Wiemels JL, Metayer C, et al. Cesarean Section and Risk of Childhood Acute Lymphoblastic Leukemia in a Population-Based, Record-Linkage Study in California. *Am J Epidemiol*. 2017;185(2):96-105. doi:10.1093/aje/kww153

88. Amitay EL, Keinan-Boker L. Breastfeeding and Childhood Leukemia Incidence: A Meta-analysis and Systematic Review. *JAMA Pediatr*. 2015;169(6):e151025. doi:10.1001/jamapediatrics.2015.1025

89. Maharshak N, Packey CD, Ellermann M, et al. Altered enteric microbiota ecology in interleukin 10-deficient mice during development and progression of intestinal inflammation. *Gut Microbes*. 2013;4(4):316-324. doi:10.4161/gmic.25486

90. Yang I, Eibach D, Kops F, et al. Intestinal Microbiota Composition of Interleukin-10 Deficient C57BL/6J Mice and Susceptibility to Helicobacter hepaticus-Induced Colitis. *PLOS ONE*. 2013;8(8):e70783. doi:10.1371/journal.pone.0070783

91. Madan JC, Farzan SF, Hibberd PL, Karagas MR. Normal neonatal microbiome variation in relation to environmental factors, infection and allergy. *Curr Opin Pediatr*. 2012;24(6):753-759. doi:10.1097/MOP.0b013e32835a1ac8

92. Biesbroek G, Tsivtsivadze E, Sanders EAM, et al. Early Respiratory Microbiota Composition Determines Bacterial Succession Patterns and Respiratory Health in Children. *Am J Respir Crit Care Med*. 2014;190(11):1283-1292. doi:10.1164/rccm.201407-1240OC

93. Stiemsma LT, Michels KB. The Role of the Microbiome in the Developmental Origins of Health and Disease. *Pediatrics*. 2018;141(4). doi:10.1542/peds.2017-2437

94. Curtale G, Mirolo M, Renzi TA, Rossato M, Bazzoni F, Locati M. Negative regulation of Toll-like receptor 4 signaling by IL-10-dependent microRNA-146b. *Proc Natl Acad Sci U S A*. 2013;110(28):11499-11504. doi:10.1073/pnas.1219852110

95. Lehours P, Zheng Z, Skoglund A, Mégraud F, Engstrand L. Is There a Link between the Lipopolysaccharide of Helicobacter pylori Gastric MALT Lymphoma Associated Strains and Lymphoma Pathogenesis? *PLoS ONE*. 2009;4(10). doi:10.1371/journal.pone.0007297

96. Matsumoto Y, Marusawa H, Kinoshita K, et al. Helicobacter pylori infection triggers aberrant expression of activation-induced cytidine deaminase in gastric epithelium. *Nat Med*. 2007;13(4):470-476. doi:10.1038/nm1566

97. Stolte M, Bayerdörffer E, Morgner A, et al. Helicobacter and gastric MALT lymphoma. *Gut*. 2002;50(suppl 3):iii19-iii24. doi:10.1136/gut.50.suppl_3.iii19

98. Horwood NJ, Page TH, McDaid JP, et al. Bruton's tyrosine kinase is required for TLR2 and TLR4-induced TNF, but not IL-6, production. *J Immunol Baltim Md 1950*. 2006;176(6):3635-3641. doi:10.4049/jimmunol.176.6.3635

99. Samarasinghe R, Tailor P, Tamura T, Kaisho T, Akira S, Ozato K. Induction of an anti-inflammatory cytokine, IL-10, in dendritic cells after toll-like receptor signaling. *J Interferon Cytokine Res Off J Int Soc Interferon Cytokine Res*. 2006;26(12):893-900. doi:10.1089/jir.2006.26.893

100. Bai W, Liu H, Ji Q, et al. TLR3 regulates mycobacterial RNA-induced IL-10 production through the PI3K/AKT signaling pathway. *Cell Signal*. 2014;26(5):942-950. doi:10.1016/j.cellsig.2014.01.015

101. Re F, Strominger JL. IL-10 released by concomitant TLR2 stimulation blocks the induction of a subset of Th1 cytokines that are specifically induced by TLR4 or TLR3 in human dendritic cells. *J Immunol Baltim Md 1950*. 2004;173(12):7548-7555. doi:10.4049/jimmunol.173.12.7548

102. Sanin DE, Prendergast CT, Mountford AP. IL-10 Production in Macrophages Is Regulated by a TLR-Driven CREB-Mediated Mechanism That Is Linked to Genes Involved in Cell Metabolism. *J Immunol Author Choice*. 2015;195(3):1218-1232. doi:10.4049/jimmunol.1500146

103. Gale E a. M. A missing link in the hygiene hypothesis? *Diabetologia*. 2002;45(4):588-594. doi:10.1007/s00125-002-0801-1

104. Michels C, Goyal P, Nieuwenhuizen N, Brombacher F. Infection with Syphacia obvelata (Pinworm) Induces Protective Th2 Immune Responses and Influences Ovalbumin-Induced Allergic Reactions. *Infect Immun*. 2006;74(10):5926-5932. doi:10.1128/IAI.00207-06

105. McNeil DE, Coté TR, Clegg L, Mauer A. SEER update of incidence and trends in pediatric malignancies: acute lymphoblastic leukemia. *Med Pediatr Oncol*. 2002;39(6):554-557; discussion 552-553. doi:10.1002/mpo.10161

106. Barrington-Trimis JL, Cockburn M, Metayer C, Gauderman WJ, Wiemels J, McKean-Cowdin R. Trends in Childhood Leukemia Incidence Over Two Decades from 1992–2013. *Int J Cancer*. 2017;140(5):1000-1008. doi:10.1002/ijc.30487

107. Gurney JG, Severson RK, Davis S, Robison LL. Incidence of cancer in children in the United States. Sex-, race-, and 1-year age-specific rates by histologic type. *Cancer*. 1995;75(8):2186-2195. doi:10.1002/1097-0142(19950415)75:8<2186::aid-cncr2820750825>3.0.co;2-f

108. Swensen AR, Ross JA, Severson RK, Pollock BH, Robison LL. The age peak in childhood acute lymphoblastic leukemia. *Cancer*. 1997;79(10):2045-2051. doi:10.1002/(SICI)1097-0142(19970515)79:10<2045::AID-CNCR28>3.0.CO;2-T

109. Morse HC, Anver MR, Fredrickson TN, et al. Bethesda proposals for classification of lymphoid neoplasms in mice. *Blood*. 2002;100(1):246-258. doi:10.1182/blood.v100.1.246

110. Schindler JW, Van Buren D, Foudi A, et al. TEL-AML1 corrupts hematopoietic stem cells to persist in the bone marrow and initiate leukemia. *Cell Stem Cell*. 2009;5(1):43-53. doi:10.1016/j.stem.2009.04.019

111. Zaiss MM, Rapin A, Lebon L, et al. The Intestinal Microbiota Contributes to the Ability of Helminths to Modulate Allergic Inflammation. *Immunity*. 2015;43(5):998-1010. doi:10.1016/j.immuni.2015.09.012

112. McSorley HJ, Maizels RM. Helminth Infections and Host Immune Regulation. *Clin Microbiol Rev*. 2012;25(4):585-608. doi:10.1128/CMR.05040-11

113. Francis SS, Selvin S, Metayer C, et al. Mode of delivery and risk of childhood leukemia. *Cancer Epidemiol Biomark Prev Publ Am Assoc Cancer Res Cosponsored Am Soc Prev Oncol*. 2014;23(5):876-881. doi:10.1158/1055-9965.EPI-13-1098

Publishing Agreement

It is the policy of the University to encourage open access and broad distribution of all theses, dissertations, and manuscripts. The Graduate Division will facilitate the distribution of UCSF theses, dissertations, and manuscripts to the UCSF Library for open access and distribution. UCSF will make such theses, dissertations, and manuscripts accessible to the public and will take reasonable steps to preserve these works in perpetuity.

I hereby grant the non-exclusive, perpetual right to The Regents of the University of California to reproduce, publicly display, distribute, preserve, and publish copies of my thesis, dissertation, or manuscript in any form or media, now existing or later derived, including access online for teaching, research, and public service purposes.

DocuSigned by:
Briana Fitch
68D78AD3C4F04E4...
Author Signature

6/12/2020
Date